Preparation, Modification, and Characterization of Nanocellulose for Wastewater Treatment

Hizkeal Tsade Kara

A Dissertation Submitted to:

The Department of Applied Chemistry

School of Applied Natural Science

Presented in Partial Fulfillment of the Requirements for the Degree of Doctor of Philosophy in Materials Chemistry

Office of Graduate Studies

Adama Science and Technology University

September, 2021

Adama, Ethiopia

Preparation, Modification and Characterization of Nanocellulose for Wastewater Treatment

Hizkeal Tsade Kara

Supervisors:
Major Supervisor: Sisay Tadesse (PhD)
Co-Supervisor: Fedlu Kedir (PhD)

A Dissertation Submitted to:
The Department of Applied Chemistry
School of Applied Natural Science

Presented in Partial Fulfillment of the Requirements for the Degree of Doctor of Philosophy in Materials Chemistry

Office of Graduate Studies
Adama Science and Technology University

September, 2021
Adama, Ethiopia

APPROVAL OF BOARD OF EXAMINERS

We, the undersigned, members of the Board of Examiners of the final open defense by **Hizkeal Tsade Kara** have read and evaluated his dissertation entitled **"Preparation, Modification and Characterization of Nanocellulose for Wastewater Treatment"** and examined the candidate. This is, therefore, to certify that the dissertation has been accepted in partial fulfillment of the requirement of the **Degree of Doctor of Philosophy in Materials Chemistry.**

Supervisors	Signature	Date
Major Supervisor: Sisay Tadesse (PhD)		September 07, 2021
Co-Supervisor: Fedlu Kedir (PhD)		Sept 07, 2021
Chairperson Dr. Aschalew Tadesse		08/10/2021
Internal Examiner Dereje Tsegaye		07/09/21
External Examiner1 ABI TADDESSE		07-08-21
External Examiner2 Alemayehu Paulos (PhD)		07/09/21

Finally, approval and acceptance of the dissertation is contingent upon submission of its final copy to the Office of Postgraduate Studies (OPGS) through the candidate's Department Graduate Council (DGC) and School Graduate Committee (SGC).

Department Head	Signature	Date 08/10/2021
School Dean Tegene Desalegn Zeleke (PhD/C)	Signature	Date 08/10/2021
Postgraduate Dean Legesse Lemecha Obsu (Ph.D)	Signature	Date 08/10/21

Postgraduate Office Dean

i

DECLARATION

I hereby declare that this PhD Dissertation is my original work and has not been presented for a degree in any other university, and all sources of material used for this dissertation have been duly acknowledged.

Name: Hizkeal Tsade Kara

Signature:_____

Date:_____

This PhD dissertation has been submitted for examination with our approval as dissertation Supervisors.

Major Supervisor: Sisay Tadesse (PhD)

Signature: 

Date: September, 2021

Co-Supervisor: Fedlu Kedir (PhD)

Signature: 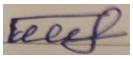

Date: September, 2021

APPROVAL OF SUPERVISORS

To: Applied Chemistry Department

Subject: Dissertation Submission

This is to certify that the dissertation entitled "**Preparation, Modification and Characterization of Nanocellulose for Wastewater Treatment**" submitted in partial fulfillment of the requirements for the degree of Doctor of Philosophy in Materials Chemistry, the Graduate program of the Department of Applied Chemistry and has been carried out by Hizkeal Tsade Kara, Id. No GSR/016/10, under our supervision. Therefore, we recommend that the student has fulfilled the requirements and hence hereby he/she can submit the dissertation to the department.

Sisay Tadesse (Ph.D)		_____
Name of major supervisor	Signature	Date
Fedlu Kedir (PhD)	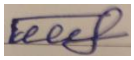	September, 2021
Name of co-supervisor	Signature	Date

ACKNOWLEDGEMENTS

I thank my supervisors, **Sisay Tadesse (PhD),** associate professor of physical chemistry at Hawassa University and **Fedlu Kedir (PhD),** associate professor of physical chemistry at Adama Science and Technology University, for their genuine guidance and encouragement from the very beginning of the selection of the dissertation title to dissertation final submission. I thank Ministry of Science and Higher Education (MoSHE) and Adama Science and Technology University for providing the research funding for effective realization of the dissertation work. Also I thank **Dr. Getachew Adam (PhD),** associate professor of physical chemistry at Addis Ababa Science and Technology University, in the Department of Industrial Chemistry, College of Applied Science, for his cooperation during the SEM characterization of the samples. My thanks also go to the Department of Applied Chemistry and Postgraduate office of **Adama Science and Technology University (ASTU)** for providing any facilites that supports the dissertation work. I thank all the postgraduate Applied Chemistry and Materials Science and Engineering Department academic and research assistant of **ASTU**, who cooperated in my dissertation work. I thank Mr. Guta Amanu, academic and research assistant in the Department of Applied Chemistry, Mr. Yeshaneh Admasu, Lecturer in the Department of Applied Biology, and Mr. Iticha Abdisa academic and research assistant in the Department of Applied Biology for their genuine cooperation during the dissertation experimental works.

Furthermore, I would also like to thank Chemistry Department of Arba Minch University (AMU) for their cooperation during the adsorption studies. I would like to express my appreciation to all my parents, especially my beloved wife Selamnesh Worku, for invaluable financial and moral support up to the end of this study. I thank **Dr. Ravikumar C. R.** associate professor at department of chemistry East West Institute of Technology, DST-SAIF Cochin analysis center, Bangalore-560091 Karnataka, India for his cooperation during the SEM-EDX characterization of the samples. Finally, I thank my friends who encouraged and helped me during my dissertation research work.

TABLE OF CONTENTS

LIST OF TABLES

TABLE **PAGE**

LIST OF FIGURES

FIGURE **PAGE**

LIST OF APPENDIX TABLES

APPENDIX TABLE **PAGE**

LIST OF APPENDIX FIGURES

APPENDIX FIGURE **PAGE**

LIST OF ACRONYMS AND ABBREVIATIONS

AAS	Atomic Absorption Spectroscopy
AAU	Addis Ababa University
AMU	Arba Minch University
ACS	American Chemical Society
APHA	American Public Health Association
ASTU	Adama Science and Technology University
BOD	Biochemical Oxygen Demand
BN	Bacterial Nanocellulose
CA	Citric Acitate
CFCN	Chemically Functionalized Cellulose Nanomaterial
CMC	Chemically Modified Cellulose
CMED	Carboxymethyl Cellulose Ethylenediamine
CMSB	Chemically Modified Cellulose Sugarcane Bagasse
CNMs	Cellulose Nanomaterials
CNCs	Cellulose Nanocrystals
CNFs	Cellulose Nanofibrils
COD	Chemical Oxygen Demand
CS@SSC	Carbon Sheet @Sea Sand Composite
CYCS/CNC	Crossliked Carboxylatedchitason/Carboxylated Nanocellulose
DCA	Deacetylated CA Nanofiber Membrane
DACNM	Dialdehyde Cellulose Nanomaterial
DMF	Dimethylformamide
DMSO	Dimethyl Sulfoxide
DR	Dubinin Radushkevich
DTA	Differential Thermogravimetric Analysis
EB	*Erythrina Brucei*
EC	Electrical Conductivity
ECNF	Electrospun Cellulose Nanofibers
EDX	Energy Dispersive Analysis of X-Ray

EDTA	Ethylenediaminetetraacetic Acid
EDTAD	Ethylenediaminetetraaceticdianhydride
EPA	Environmental Protection Agency
Fe_3O_4@TATS@ATA	Magnetic Triamine-triethoxysilane-aminoterephatic Acid
FTIR	Fourier Transform Infrared Spectroscopy
FCMC	Fibrous Carboxymethyl Cellulose
FWHM	Full Width at Half Maximum
IARC	International Agency for Research on Cancer
JMP	Joint Monitoring Program
LCB	Lignocellulosic Biomass
LIDI	Leather Industry Development Institute
MA	Maieic Anhydride
m-CS/PVA/CCNFs	Magnetic Hydrogel Beads
MA-CNM	Maieic Anhydride Modified Cellulose Nanomaterial
MF	*Millettia Ferruginea*
NC	Nanocellulose
NCC	Nanocrystalline Cellulose
NFC	Nanofibrilled Cellulose
NPS	Non-Point Source
NP	Nanoparticle
OM	Organic Matter
OC	Organic Carbon
PDA@DCA-COOH	Polydopamine (PDA) Coating Nanofibers
PE	Polyethylene
PFO	Pseudo-First-Order
PS	Point Source
PSO	Pseudo-Second-Order
PTEs	Potentially Toxic Elements
pHPZC	Point of Zero Charge
%R	Percent Removal
SA	Succinic Anhydride

S-CNM	Succinic Anhydride Modified Cellulose Nanomaterial
SEM	Scanning Electron Microscope
SERWW	Secondary Runoff Wastewater
TAPPI	Technical Association of Pulp and Paper Industry
TEMPO	2,2,6,6-tetramethylpiperidine-1-oxy
TGA	Thermogravimeter Analysis
TN	Total Notrogene
TNCC	Tannin Nanocellulose
TP	Total Phosphorus
UV-Vis	Ultraviolet Visible Spectroscopy
WHO	World Health Organization

Preparation, Modification, and Characterization of Nanocellulose for Wastewater Treatment

Hizkeal Tsade Kara*[1], Sisay Tadesse Anshebo[2], Fedlu Kedir Sabir[1]
[1]Department of Applied Chemistry, School of Applied Natural Science, Adama Science and Technology University, P.O.Box 1888, Adama, Ethiopia
[2]Department of Chemistry, College of Natural and Computational Science, Hawassa University, Hawassa, P.O. Box 05, Ethiopia

ABSTRACT

Currently, heavy metals and cationic dyes seriously affect the environment and threaten human health. Due to this reason, the removal of such pollutants is an important issue all over the world. Thus, the removal of Pb(II), Cd(II) and Cr(VI) ions and cationic methylene blue (MB) dye from wastewater (WW) was performed using pristine cellulose nanomaterials (CNM) and chemically modified cellulose nanomaterial (C-CNM) adsorbents. CNMs adsorbents were prepared by using sulfuric acid hydrolysis method from the stems of Erythrina brucei and Millettia ferruginea plants, and Eichhornia crssipes weed. These adsorbents were chemically modified by using oxidation and esterification methods. Both of the as-prepared and C-CNM adsorbents were characterized for functional groups, average crystallite size, surface morphologies, elemental analysis, and thermal stability by using fourier transform infrared (FT-IR) spectroscopy, x-ray diffraction (XRD), scanning electron microscope (SEM), energy dispersive x-ray (EDX), and thermogravimetric with difrential thermal analysis (TGA-DTA) techniques, respectively. The physicochemical analyses of the WW samples were performed within 24 hours after collection. Next, CNMs and C-CNMs adsorbents were applied for the removal of Cr(VI), Pb(II), Cd(II) ions, and cationic methylene blue (MB) dye from WW. The adsorption kinetic data confirmed to the pseudo-second-order (PSO) kinetic model, and the isotherm data fit well with the Freundlich and Langmuir isotherm models. The maximum adsorption capacity (q_{max}) of the CNMs adsorbent for Cr(VI), Pb(II), and Cd(II), ions in WW evaluated by batch adsorption experiments were 60.24, 91.74, and 75.76 $mgg^{-1,}$ respectively. Also maximum adsorption capacity (q_{max}) of the succinic anhydride cellulose nanomaterial (S-CNM), dialdehyde cellulose nanomaterial (DACNM), maleic anhydride cellulose nanomaterial (MA-CNM), and DACNM adsorbents for Cr(VI), Pb(II), Cd(II), and MB in WW were 156.25, 384.62, 215.52, and 90.91 mgg^{-1}, respectively. Furthermore, the results have showed that the adsorption capacities were affected by the presence of competing cations in the WW. The thermodynamic studies revealed that the adsorption process was spontaneous and feasible. Due to their high efficiencies, S-CNM, MA-CNM, and DACNM adsorbents were selected for the regeneration study and performed through desorption of Cr(VI), Cd(II), Pb(II), and MB dye cations, respectively, by treating it with 0.1 M HCl. The results have showed that all adsorbents were easily regenerated and re-used for the adsorption of Cr(VI), Pb(II), Cd(II), and MB cations from WW up to successive 13^{th} cycles with only less than 6% efficiency loss in each successive cycles.

Keywords: Wastewater treatment, Cellulose nanomaterial preparation, Surface modification, Heavy metal, Cationic MB dye, Adsorption isotherm, Adsorption kinetics.

1. INTRODUCTION

1.1. Background

Water is essential to every aspect in all living things [1-3], however, the water pollution with several toxic chemical contaminants is recently considered as the greatest stimulating issue all over the world and specially, in the developing countries like Ethiopia [4-6]. These chemical contaminants such as, toxic heavy metal ions, inorganic anions, micropollutants, organic pollutants including persistent organic pollutants and others are emanated from different sources including different industrial activities, urbanization, increased number of population, agricultural activities, etc [7-11]. They greatly affect the ecological balance and have caused harmful effects on flora and fauna [12,13]. Many of these pollutants have great tendency for bioaccumulation in the food chain as they are not biodegradable in nature [14].

Among these pollutants, the contamination of water with heavy metals is a severe cause of environmental and human health problems [15-17]. This is because, they are non-biodegradable and can be stored in living tissues, that lead to innumerable diseases and disorders due to their toxic and carcinogenic nature unlike to organic pollutants [18,19]. Some of the extreme toxic heavy metals found in water bodies are As, Pb, Hg, Cd, Cr, Cu, Ni, Ag, and Zn. The increased amounts of these heavy metals are introduced into the water bodies by different activities and cause to dangerous human health and environmental problems. For instance, the presence of high amount of Pb and Cd in the environment makes dangerous toxicity to the reproductive systems and that damages the brain, liver, acute and chronic diseases and kidney of human beings and aquatic living things [20,21].

Furthermore, based on the toxicological studies on nephrotoxicity, exposure to Pb(II) ions can be related to renal tubular necrosis, and exposure to Pb is directly related to the failure of glomeruli [22]. Chromium has a potential risk to the whole environment in general and wastewater in particular because of its non-biodegradability, carcinogenicity, persistence and bioaccumulation nature [23]. Also, different dyes cause to eyes injury, mental disability, sickness, vomiting, and methamoglobinemia [24,25].

Wastewater treatment strategies have several advantages over the entire world in general and in developing countries like Ethiopia in particular. This is because, the water pollutants arise from different activities causes serious environmental and health problems [25]. Currently, a number of technologies are available for the removal of pollutants from industrial wastewater effluents such as coagulation-flocculation, oxidation, membrane separation, ion exchange, electro-precipitation, evaporation, floatation and adsorption [26-30]. Among all available methods for the treatment of industrial wastewater effluents, adsorption is still the most widely used technique in wastewater treatment due to low capital cost, can remove most of all kinds of pollutant, and have high pollutants removal capacity [25]. However, the adsorbent materials selection is very necessary because of cost and separation of the adsorbent from the reaction media. This is because; some adsorbents were not suitable on a commercial scale due to the use of expensive chemicals and high temperatures, difficulty for adsorbent regeneration and generation of waste byproducts.

Several types of adsorbents have been used for the removal of various kinds of pollutants such as activated carbon, montmorillonite, zeolites, kaolin, microorganism, and agricultural wastes [31]. Among these, most industrial activities normally use activated carbon as an adsorbing reagent due to its high absorbency and specific surface area [28]. However, activated carbon obtained from the market is much expensive because of its high production cost for regeneration purposes [29]. Due to its abundant availability and broad range of applicability, lignocellulosic materials have attracted the attention of various researchers to utilize it for environmental application [25]. One of the promising applications of lignocellulosic material is as the adsorbent for wastewater treatment. Cellulose is the major components of lignocellulosic biomass and has improved merits of easily available, non-poisonous, renewable and has plenty of accessible hydroxyl functional groups which are very active for different chemical modification systems [32,33].

There were several natural bio-based materials used in wastewater treatment, among these cellulose is one of the natural bio-based materials. Cellulose $(C_6H_{10}O_5)_n$, is considered an inexhaustible natural macromolecular compound, has many excellent properties, such as renewability, biodegradability, biocompatibility, non-toxicity, extremely cheap, and so on,

which has received increasing interest from many researchers all over the world [34]. It consists of a linear homopolysaccharide composed of repeating β-D gluco-pyranosyl units joined by 1–4 glycosidic linkages in a variety of arrangements. Correspondingly, it is the most abundant biopolymer on Earth and regarded as a promising candidate due to its merits of green and sustainable chemistry [35]. Particularly, owing to its advantage of high number of hydroxyl groups in its structure, cellulose can be modified with other specific reactive groups such as carboxyl group, sulfo group and amine group [36], using esterification and oxidation method for removal of desired pollutants effectively.

In spite of its pronounced properties, the demerits of cellulose in wastewater treatment are its low hydrophilicity, physical and chemical stability, and removal capacity [37]. Due to this reason currently, the idea of the use of nanomaterials as adsorbents is increasing [38]. However, nanomaterials, such as Titania nanotube, carbon nanotube, and nano zerovalent iron are toxic and not suitable for pollutant removal [38]. These limitations were easily solved preparing nanomaterials by disintegrating cellulose materials into cellulose nanomaterials (CNMs) using different preparation methods [37]. The prepared CNMs show pronounced properties such as high surface area, small particle size, high mechanical strength, and chemical stability [38,39]. Depending on the preparation methods and source materials, CNMs can be classified into cellulose nanofibers (CNFs), cellulose nanocrystals (CNCs), and bacterial cellulose [40]. Different acid hydrolysis methods, such as sulfuric acid, hydrochloric acid, and hydrobromic acids are used for preparation of cellulose nanocrystallines (CNCs) [41]. Among these, sulfuric acid is the most widely used acid for the preparation of CNCs [42]. These is due to it produces half ester functional groups on the surfaces of the materials that is ready for adsorption processes. Therefore, in this study sulfuric acid hydrolysis method was used to prepare CNCs. Furthermore, the prepared CNCs are chemically modified by using different modifiers, such as periodate, succinic, and maleic anhydride to increase the specific surface area of CNCs. The prime purpose of chemically modifying CNMs using oxidation and esterification is to increase the surface areas of CNMs adsorbents [36].

Recently, the Technical Association of Pulp and Paper Industry (TAPPI, Japan) proposed standardization in terms and definitions for cellulose nanomaterials [43]. Cellulose

nanomaterials (CNMs) can be divided into two categories: nano-objects and nano-structured, which, at the same time, each category is divided into two subcategories: cellulose nanocrystals (CNCs) and cellulose nanofibers (CNFs) for nano-objects and cellulose microcrystals (CMCs) and cellulose microfibrils (CMFs) for nano-structured. As expected, the classification is based on the different methods and source materials [44]. Extraction of nanocellulose from the cellulosic biomass includes two major steps viz. pretreatment and removal of amorphous phase by appropriate methods [45]. Before the mechanical, chemical or enzymatic treatment, pretreatments such as alkali treatment and bleaching are required. The prime objective of pretreatment is to remove certain amount of lignin, hemicellulose, wax and oils which cover on the external surface of the fiber cell wall. Alkali treatment depolymerizes the native cellulose structure, defibrillates the external cellulose microfibrils and exposes short length crystallites. Furthermore, bleaching treatment is required in order to remove the cementing material completely from the fiber [46]. Although, many research articles have been published so far discussing the importance of cellulose-based adsorbents in wastewater pollution control, many of them are generally either adsorbate-specific for instance, metals [47-50], dyes [51-53], or adsorbent-specific for instance, cellulose nanomaterials [54] or nanocomposites [55].

Moreover, extensive research has been reported so far on cellulose-based adsorbents extracted from different biomaterials including microorganisms like algae, plant materials, date palm (*Phoenix Dactylifera L.*) [56], Cotton residue [57], banana peel [58], corn husk [59] and others. As per the knowledge of the author, there is a research gap on the nano-cellulose based adsorbent materials prepared from *Erythrina Brucei* (Korch, in Amharic, Walensu, in Afaan Oromo, Boro in Ganta) and *Millettia ferruginea (*Birbira in Amaharic, Sotellu in Afaan Oromo) plants and *Eichornia crassipes weeds*, in Amaharic Emboch, in Afaan Oromo, Gorora ferrida for wastewater (WW) treatment. Furthermore, it was prepared from the dried form of the stems of *Eichornia crassipes* weed. This material is the worst waste material negatively affecting the aquatic environment. Thus, using the worst waste material instead of beneficiary material for pollutant removal purpose is economically effective. For this purpose the dried form of the stem was used for CNMs preparation and applied for wastewater treatment. Therefore, the study was focused on wastewater treatment using cellulose

nanomaterials prepared from locally available stems of *Erythrina Brucei* and *Millettia ferruginea* plants and the stems of *Eichornia crassipes* weed as adsorbent.

1.2. Statement of the Problem

Currently, the contamination of water is a serious problem for more than 60% of the world human population [60]. This is due to the rapid growth of population, urbanization, development of industry, climate change, and others [61]. Toxic chemical contaminants enter into water system mostly through the direct discharge of untreated industrial WW effluents. Thus, the presence of these contaminants in water environment creates severe problems for human and water ecosystem through out the world [61].

Although, rapid industrial expansion in Ethiopia is viewed as an indicator of economic progress, they are greatly associated with environmental degradation, particularly due to the discharge of untreated wastewater effluents [62]. There are several industries found near Modjo town such as, leathers, textiles, metals, minerals, glass, beverages, etc [63]. Among these, especially, leather manufacturing is an industry with a long history in Ethiopia, which is the largest livestock producer in Africa and tenth largest in the world [64]. Tannery industry is the first most chromium containing wastewater effluent dischargers in Ethiopia. It is a relatively older industry that is located in Modjo town, Oromia region, with more than 80 years of involvement in processing leather [65]. Ethiopia is one of the leading countries that have the largest livestock populations in the Africa providing a strong raw material base for the leather industry. Its livestock population is estimated at 50 million cattle, 25 million sheep and 23 million goats. About 80% of all hides and skins entering the formal market come from rural areas where they are collected by private traders. The remaining 20% are derived from slaughtering facilities found in major town and cities. About 15.5 million pieces of sheep and goat skins and 1.2 million pieces of cattle hides are supplied to the tanneries per annum [66].

Nowaday, more than 27 tanneries present in Ethiopia that export semi-finished and finished leather products [67], and the rest few are under construction. The processing of leather is an export industry for Ethiopia, making up almost 6% of annual exports per year (around $127

million USD) [68]. Tanning involves the use of large quantities of water as well as inorganic and organic chemicals. Machines convert the putrescible raw hide and skin into what is known as non-putrescible and strong leather. During this process, sizable liquid, solid and gaseous wastes are generated. According to leather industry development (LIDI), tanneries in Ethiopia generate about 12,500 m^3 liquid waste and 150 tons of solid wastes per day [69]. Some tanneries in Ethiopia have primary and secondary treatment to manage their wastes, but not all tanneries treat the wastes properly due to the high costs involved. This problem has increased since many tanneries, in particular in near Addis Ababa, are now often located closer to or in cities due to the cities expansions. Ethiopia has a regulatory framework to reduce the environmental impact of tanning, but the laws are often not enforced properly.

Furthermore, one among other industries that containing methylene blue dye wastewater effluent dischargers in Ethiopia is textile manufacturing processes. The textile industry is primarily concerned with the design, production and distribution of yarn, cloth and clothing. The raw material may be natural or synthetic using products of the chemical industry. Firstly, the textile industry in Ethiopia was established around 1939 in relation with Italian colonialism era, in specific region of Dire-Dawa named Dire-Dawa textile mill. Since 2010, the Ethiopian government has positioned strength to advance, maintenance, and develop the textile industry, helping the national marketplace but primarily with the purpose of exporting and be economical at the worldwide market [70]. Our country Ethiopia has a possibility of construction a textile industry with governmental provision, proposing low-cost fabrication and raw material and with increasing young population enthusiastic for professions [71]. The industry is one of the largest employers in Ethiopia, with 35,000 direct employees (cotton farming (10%) and textile/garment manufacturing (90%)), excluding the 500,000 engaged in the informal hand-loom weaving sector [72,73].

Generally, the textile industry affects economic worldwide development; however, it is considered one of the major sources of environmental pollutants because of the discharge of large amount of effluents that contain non-biodegradable dyes. The textile industry consumes large quantities of water from the pretreatment to final products during various processing stages. Approximately, 100 to 200 L of water is consumed to finish 1 Kg of the final product.

The dyeing process is an intermediate stage, involving the addition of dyes to fibers, together with other chemicals for enhancing of the binding between dyes and fibers. In the final manufacturing process, traces of these dyes and chemicals are discharged as textile effluents. Some of the textile factories in Ethiopia towns including Alemgena Textile, Modjo Textile, Adama Textile, Yirgalem Addis Textile, Bahir Dar textile, Awassa Textile, Kombolcha, and Arbaminch Textile factories that were built near different Rivers and Lakes, where most of them dispose their solid and liquid wastes directly into this Rivers and Lakes. Because, these industries were uses large quantities of chemicals and huge quantities of wastewater to remove dirt, gravels, oils, and waxes from the products. These activities mostly release non-biodegradable toxic contaminants into the environment in general and water bodies in particular. Due to this reason different Rivers found near to these industries are mostly polluted by the untreated wastewater effluents emanated from different textile industries. This wastewater effluent contains different pollutants such as toxic heavy metals, organic pollutants, microorganisms, etc. The presence of these pollutants greatly affects the ecological balance and has causes harmful effects on flora and fauna [74,75]. In addition to these, it has severely affected by several pollutants/contaminants released from different industries [76]. Since water pollution is a major problem, therefore, a strict toxic chemical contaminants removal technology is urgently required. There is a need to remove such pollutants from WW using different removing techniques.

At present, a number of technologies are available for the removal of hazardous substances from industrial effluents such as biological treatments using aerobic and anaerobic microorganisms, advanced chemical oxidation, membrane separation, photo catalysis oxidation and adsorption [27-29]. Among all available methods for the treatment of industrial effluents, adsorption is still the most widely used method in wastewater treatment due to low capital cost, can remove most of all kinds of pollutants, and easy regeneration [25]. Several types of adsorbents have been used for the removal of various kinds of pollutants such as activated carbon, montmorillonite, zeolites, kaolin, microorganism, and agricultural wastes [77]. Mosly, activated carbon was used as adsorbent for wastewater treatment, however, due to its high cost, large chemical consumsion, and difficulty in regeneration after adsorption its usage was limited. In order to solve these problems there is need to search low-cost

adsorbents. Lignocellulosic materials have attracted the attention of various researchers to utilize it for environmental application, due to its abundant availability and broad range of applicability [28]. One of the promising applications of lignocellulosic material is as the adsorbent for wastewater treatment. Cellulose is one of the major components in lignocellulosic material. This natural polymer has been investigated as bio-sorbent in its raw, nano, and chemically modified form [25,28]. Different studies have been reported for the adsorptive removal of heavy metals and dyes utilizing cellulose and chitosan based adsorbents [25,78]. Extraction of cellulose in the form of nanocrystal has been extensively studied adsorption of heavy metals and dyes. The preparation of nanocrystalline cellulose (NCC) can be conducted by mechanical and chemical methods. Among this, chemical methods, such as, acid hydrolysis are used to prepare NCC due to it have high adsorption efficiency for toxic chemical contaminant than NFC prepared by mechanical method [77].

In addition to this, many research articles have been published so far on cellulose-based adsorbents extracted from different microorganisms like algae [79], date palm (*Phoenix Dactylifera L.*) [80], Cotton [57], banana peel [58], corn husk [59], etc. called green materials. However, to the best of the authors' knowledge there is a research gap for wastewater treatment using these low cost adsorbent materials. Furthermore, there is a dearth of research information regarding the preparation of CNMs from the stems of *Erythrina Brucei* and *Millettia ferruginea* plants, for wastewater treatment. Moreover, few studies have been reported [99,155-159] on CNMs prepared from the dried stems of *Eichornia crassipes* weed for wastewater treatment. Here using this weed for wastewater treatment, provides best knowledge of good resource utilization without any negative economic impact. In addition to this, the study would fill the research gap of environmentally benign, economically affordable, easy operation and regeneration or reuse as current condition of Ethiopia. Also, most of research studies reported in the review literature were synthetic solution only, but, there was research gap on real wastewater treatment. Generally, the statement of the problem describes, the research gap presented in adsorbent preparation methods, wastewater treatment techniques, and wastewater treatment materials.

1.3 General and Specific Objectives

1.3.1. General objective

- To prepare pristine and modified cellulose nanomaterials (CNMs) adsorbents and evaluate their adsorption capability for wastewater treatment.

1.3.2. Specific objectives

- To extract cellulose from the stems of indigenous plants *Erythrina Brucei* and *Millettia ferruginea* and that of *Eichornia crassipes* weeds.
- To prepare cellulose nanomaterials (CNMs) from the extracted cellulose using sulfuric acid hydrolysis method.
- To modify the prepared CNMs using sodium periodate, succinic, and maleic anhydride modifiers.
- To characterize the pristine and modified CNMs by using modern instrumental techniques such as FT-IR, XRD, SEM, EDX, and TGA-DTA.
- To investigate the effects of solution pH, adsorbent dose, contact time and Cr(VI), Cd(II), Pb(II), and MB dye cations initial concentration on the removal of pollutants by both pristine and chemically modified CNMs adsorbents.
- To elucidate the Cr(VI), Cd(II), Pb(II), and MB dye cations adsorption mechanisms of the CNMs adsorbents through adsorption isotherms and kinetics.
- To study the regenerability of the CNMs adsorbents for repeated use in pollutant removal.

1.4. Significance of the Study

Pollution of the aquatic environment especially due to the presence of heavy metals, dyes and inorganic anions becomes a worldwide problem, because they are indestructible and most of them have long-term adverse effects on flora and fauna [81, 83]. Some of the important issues preventing these long-term adverse effects from flora and fauna are of treating industrial wastewater efflunts using eco-friendly techniques [81]. Recently, different wastewater treatment technologies such as chemical precipitation, membrane filtration, electrodialysis, ion exchange, reverse osmosis with ultraviolet light and ozonation have been reported [82].

The main significance of this study is to generate, collect and analyze information and make this knowledge available for the development of CNMs production from the stems of indigenous plants of *Erythrina Brucei*, *Millettia ferruginea,* and *Eichornia crassipes* weed. These adsorbents were used for removing toxic heavy metals including Pb(II), Cd(II), Cr(VI) ions and cationic methylene blue (MB) from industrial wastewater effluents. Also, the removal of thses toxic chemical pollutants prefers development to the people having positive impact on the environment. This study can also be used as one means in tackling the problem of *Eichornia crassipes* weed which has created great danger on Ethiopian water bodies. It is also helpful for the major objectives of making the environment clean in general and wastewater effluents in particular. Furthermore, this result is of high significance to industry managers; city planners; and environmental regulators (e.g. EPA, Ethiopia) in their effort to upgrade or newly establish treatment plants. Additionally, this study provides information about the unique characteristics of CNMs due to their nanoscale size, fibril morphology and large surface area for adsorption application. Figure 1 shows the main significance of cellulose nanomaterial as adsorbents for Cr(VI), Cd(II), Pb(II), and MB cations from the perspectives of cellulosic nature, adsorption and its nanoscale size [84,85].

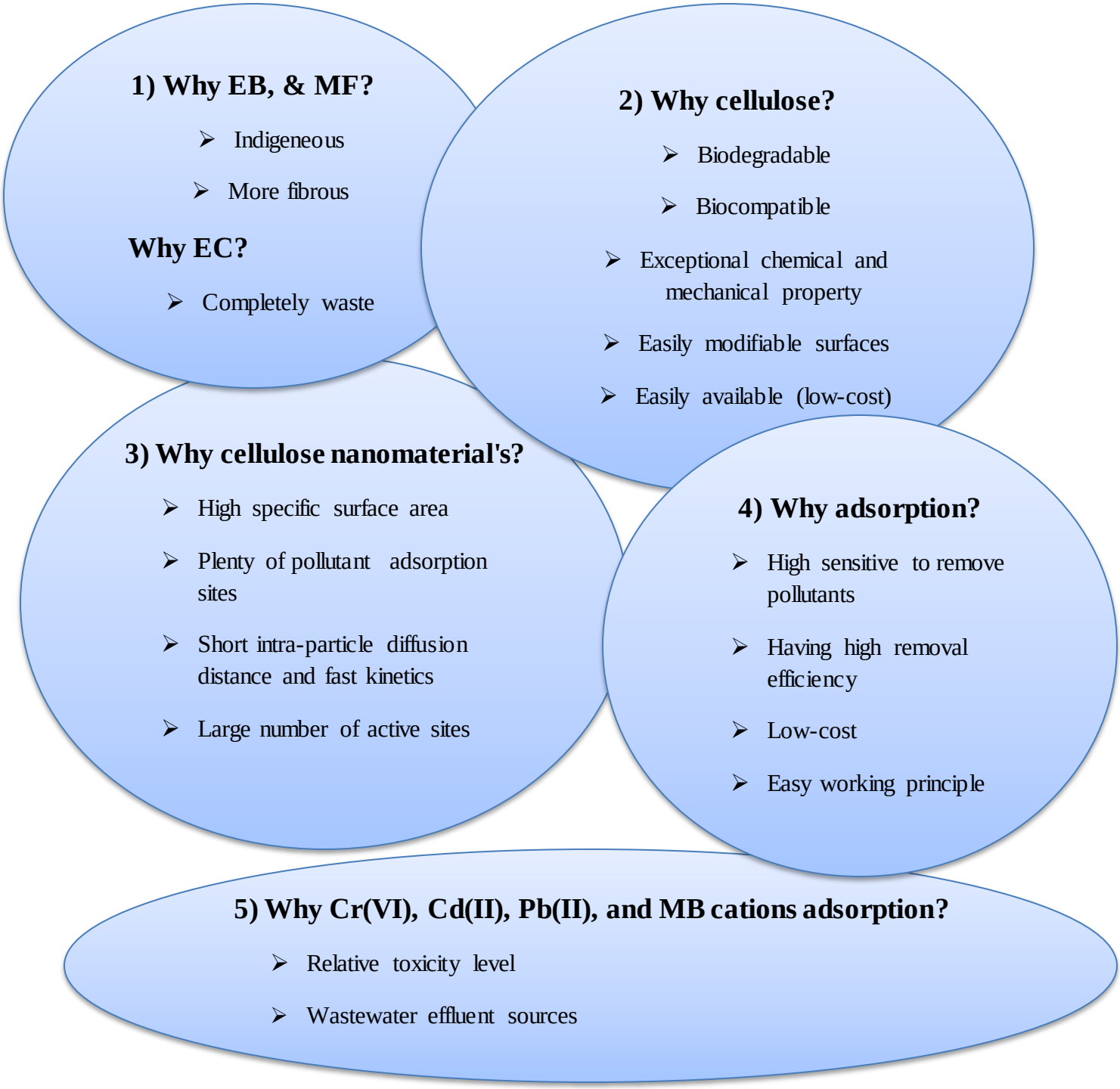

Figure 1. The main significance of cellulose nanomaterials as adsorbents for Cr(VI), Cd(II), Pb(II), and MB cations from the perspectives of cellulosic nature, adsorption and the nano scale size.

1.5. The Scope of the Study

Wastewater treatment technologies in developing countries like Ethiopia are paramount important due to the rapid increment of population, urbanization, industrialization and agricultural activities. This is because from wastewater effluents, different pollutants such as, toxic inorganic, organic, microorganism and other affect human and animal healths. Among these pollutants, heavy metals such as, Pb, Cd, Cr, As, Pd, and dyes have great impact for human health due to their non-biodegradable nature. Thus, the study was focused on wastewater treatment using pristine and modified CNMs as adsorbent due to cost, abundance (availablity), biodegradablity, compatiblity, environmentally friendly and easy regeneration by acid washing. In most reports activated carbon [28] was used instead of CNMs as adsorbent found problems including, cost, energy, and adsorbent materials recyclability. Thus, this study uses CNMs as adsorbent extracted from the stem of indigenous *Erythrina Brucei* and *Millettia ferruginea* plants and *Eichornia crassipes* weed to fill the current research gap and due to time, resources, money, materials and equipment's, constraint in our country Ethiopia. Adsorption technique was chosen in order to remove Pb(II), Cd(II), Cr(VI) ions and cationic methylene blue (MB) from real wastewater using CNMs adsorbent due to its high efficiency, cost effectiveness and easily recyclable nature. Different characterization techniques including atomic absorption spectroscopy (AAS), x-ray diffraction (XRD), scanning electron microscope (SEM), Fourier transform infrared (FTIR) spectroscopy, energy dispersive x-ray (EDX) spectroscopy, and thermogravimetric with differential thermal (TGA-DTA) was used to determine the adsorption, average crystalite size, surface morphology, functional groups and thermal stability of the CNMs adsorbents respectively. UV-Vis spectroscopy was used to determine the absorbance measurement of MB dye cations. Furthermore, the study included the modification of the prepared CNMs to increase the surface area. The pollutant uptake capacity was investigated in the study using adsorption isotherms and adsorption kinetics. Finally, the separation of the loaded adsorbents into free adsorbents and adsorbates was performed through desorption process and the regenerated adsorbents were re-used for 13^{th} successive cycles.

2. LITERATURE REVIEW

2.1. Sources of Water Pollution

Water pollution can be defined as any physical, biological, or chemical changes in water quality that adversely affect living organisms or make water unsuitable for desired uses. The main sources of water pollution are either point or non-point sources. Nonpoint source (NPS) pollution generally results from land runoff, precipitation, atmospheric deposition, and drainage systems. NPS pollution, unlike pollution from industrial and sewage treatment plants, comes from many diffuse sources. NPS pollution is caused by rainfall or snowmelt moving over and through the ground. As the runoff moves, it picks up and carries away natural and human-made pollutants, finally depositing them into lakes, rivers, wetlands, coastal waters and ground waters. Unlike NPS pollution, point source (PS) pollution release pollutants from discrete transportations, such as a discharge pipe, and are regulated by federal and state agencies. The main point source dischargers are different industrial activities, municipal solid and liquid wastes or oily wastes from garages and fuel stations [86]. Among these, different industrial activities release several wastewater effluents into the environment in general and aquatic bodies in particular.

The above stated wastewater effluents containing different inorganic and organic pollutants discharged into the water bodies, such as, rivers, lakes, drinking waters and adversely affect human and aquatic animals' health. The most serious water pollutants discharged from the different sources worldwide are both bacterial and viral, nitrates from fertilizer use, toxic heavy metals from contaminated soil, untreated industrial wastewater effluents and urban runoff, dyes from different textile processing untreated wastewater effluents, mineral oil discharges from illegal dumping, chlorinated solvent discharges from poorly managed waste disposal sites, acid rain, and a cocktail of poisons from working industrial and mineral sites [87]. Especially, the contamination of wastewater with toxic heavy metals and cationic methylene blue dye is a serious cause of both environmental and human health problems [88-90]. This was due to; unlike organic pollutants heavy metals and azo dyes are non-

biodegradable and can be accumulated in living tissues, causing various diseases and disorders, since they can be toxic and carcinogenic.

2.1.1. Heavy metals

The term "heavy metal" is entirely applied to a group of metals (and metal-like elements) with density greater than 5 g/cm³, atomic number above 20 and is toxic or poisonous at low concentrations [91]. Three kinds of heavy metals are of concern, including toxic metals (such as Hg, Cr, Pb, Zn, Cu, Ni, Cd, As, Co, Sn, etc.), precious metals (such as Pd, Pt, Ag, Au, Ru etc.) and radionuclides such as U, Th, Ra, Am, etc. [92]. The most common toxic heavy metals in wastewater include arsenic, lead, mercury, cadmium, chromium, copper, nickel, silver, and zinc. Heavy metals are natural components from the earth's crust. They cannot be destroyed or degraded. However, most of these heavy metals become toxic at high concentrations due to their ability to accumulate in living tissues. Removal of heavy metals from industrial wastewater is of primary importance. Cadmium, zinc, copper, nickel, lead, mercury and chromium are often detected in industrial wastewaters.

2.1.1.1. Chromium (Cr)

There are two stable oxidation states of chromium found in the environment, Cr(III) and Cr(VI) which have contrasting toxicities, mobility and bioavailability. Oxidation state Cr^{6+} chromium compounds were considered as powerful oxidants. Hexavalent chromium Cr(VI) compounds were used as pigments for Photography, and in pyrotechnics, dyes, paints, inks, and plastics. They could also be used for stainless steel production, textile dyes, wood preservation, leather tanning, and as anti-corrosion coatings. While Cr(III) is relatively innocuous and immobile, Cr(VI) moves readily through soils and aquatic environments and is a strong oxidizing agent capable of being absorbed through the skin. For normal carbohydrate and lipid metabolism, an essential element required is trivalent chromium, Cr(III). The largest source of contaminated effluent generation is the industrial activities, particularly electroplating, metal casting, and numerous product manufacturing processes; these activities can generate highly toxic metallic waste in wastewater, which can have a long-term negative

impact. The toxicity of each metal depends on the amount of chemical species available in the water, the absorbed dose, and exposure time [93].

Among these metals, some as potentially toxic elements (PTEs) and have raised social concerns. Some examples found in contaminated waters are copper (Cu), zinc (Zn), lead (Pb), cobalt (Co), chromium (Cr), arsenic (As), molybdenum (Mo) and manganese (Mn) [94]. Among these elements, Cr represents a high risk to the ecosystem and public health due to its carcinogenicity, persistence and bioaccumulation. In general, Cr is present as trivalent chromium (Cr(III)) and hexavalent chromium (Cr(VI)) in the natural environment. While Cr(III) is required as a trace element (low concentrations) to maintain human body metabolism, the Cr(VI) is considered as a toxic oxidation state of Chromium and has high solubility and mobility in aqueous systems, and it exists as oxyanions CrO_4^{2-}, $HCrO_4^-$ and $Cr_2O_7^{2-}$ [95]. This hexavalent chromium (Cr(VI)) is about 500 to 1000 times more toxic than its trivalent form, i.e., Cr(III), because of its high solubility and high mobility in almost the whole pH range of its solution [95]. The main sources for chrome contamination are: Hardware factory, Chrome tanning plant, Electroplating plant, Electropolishing plant, Tannery plant, among others, and the Cr(VI) concentration in wastewater produced are estimated to be between 0.1 and 200 $mg.L^{-1}$ [96]. According to World Health Organization (WHO), the long term exposure of Cr(VI) levels of over 0.1 mgL^{-1} causes respiratory problems, liver and kidney damage, and carcinogenicity. Thus, the chromium discharge limits in water are regulated on a national scale and often vary depending on the different type of industry or receiving water body (marine water, lake, river, sewer system). In Europe, the admissible concentration values of Cr(VI) as mgL^{-1} range from 0.05 to 2 according to the environmental policy of Norway and Poland (most precautionary value) and Netherlands [96].

2.1.1.2. Lead (Pb)

Among toxic heavy metals, a naturally occurring bluish-gray metal is known as Lead (Pb). Although it could be found in all parts of our environment most of it is in human activities including manufacturing, mining, and burning fossil fuels. Lead (Pb) has an atomic number of 82 and atomic mass of 207. It is the heaviest non-radioactive metal that naturally occurs in

substantial amounts in the earth's crust. Pb is the most common among the heavy metals and its most abundant isotope is ^{208}Pb. Lead is used in the production of batteries. It was probably the more common metal that is associated with heavy metal poisoning and toxicity. All the recent news about the presence of lead in kids' toys has helped create public awareness about the dangerous effects of lead [97].

Throughout the world in every year the industry produces about 2.5 million tons of lead mostly used for batteries. This metal forms complexes with Oxo-groups in enzymes to affect virtually all steps in the process of hemoglobin synthesis and porphyria metabolism. Toxic levels of lead in human have been associated with encephalopathy, seizures and mental retardation. The permissible limit (mgL^{-1}) for Pb(II) in wastewater, given by Environmental Protection Agency (EPA), is 0.05 mg/L [97]. In industrial wastewaters, lead ion concentrations approach 200–500 mgL^{-1}; this concentration is very high in relation to water quality standards, and lead ion concentration of wastewaters must be reduced to a level of 0.05–0.10 mg/L before discharging to water ways or sewage systems [97].

Human exposure to lead and its compounds occurs mostly in lead related occupations with various sources like leaded gasoline, industrial processes such as smelting of lead and its combustion, pottery, boat building, lead based painting, lead containing pipes, battery recycling, grids, arm industry, pigments, printing of books, etc. Though its widespread use has discontinued in many countries of the world, it is still used in many industries like car repair, battery manufacturing and recycling, refining, smelting, etc. Lead is a highly poisonous metal affecting almost every organ in the body. Of all the organs, the nervous system is the mostly affected target in lead toxicity, both in children and adults. The toxicity in children is however of a greater impact than in adults. This is because their tissues, internal as well as external, are softer than in adults [97].

Long-term exposure of adults can result in decreased performance in some tests of cognitive performance that measure functions of the nervous system. Infants and young children are especially sensitive to even low levels of lead, which may contribute to behavioural problems, learning deficits and lowered intelligence quotient [98]. Long-time exposure to lead has been

reported to cause anaemia, along with an increase in blood pressure, and that mainly in old and middle aged people [99]. Severe damage to the brain and kidneys, both in adults and children, were found to be linked to exposure to heavy lead levels resulting in death [100]. In pregnant women, high exposure to lead may cause miscarriage. Chronic lead exposure was found to reduce fertility in males [101]. Blood disorders and damage to the nervous system have a high occurrence in lead toxicity. Therefore, the removal of Pb(II) ions from wastewater is the most important aspect in recent times.

2.1.1.3. Cadmium (Cd)

Cadmium (Cd) is a silvery-white, soft, ductile chemical metal with atomic number 48, mass number 112.4 and belonging to the group IIB element in d block and period 5. It was discovered by German chemist F.S trohmeyer in 1817 as a constituent of smithsonite ($ZnCO_3$) from zinc ore. Cadmium is considered as a toxic metal and is hazardous to both human and wild life [102]. It acts as a mitogen and promotes cancer in a number of tissues. It also stimulates cell proliferation, inhibit DNA repair and inhibit apoptosis. On the one hand it induces the cell death which leads to tissue damage in kidney. This metal does not corrode easily and called novel metal and has many uses including: batteries, metal coatings, pigments and plastics.

Many different forms of exposure to cadmium have been shown over the past century, with cadmium being present in the environment as a result of many human activities [103]. The constant sources of cadmium contamination are related to its application in industry as a corrosive reagent, as well as its use as a stabilizer in PVC products, color pigments, and Ni-Cd batteries [104]. In areas with contaminated soils, house dust is a potential route for cadmium exposure [105]. Anthropogenic sources of Cd in the environment derive from copper and nickel smelting and refining, fossil fuel combustion, and the use of phosphate fertilizers. Cadmium is also present as a pollutant in non-ferrous metal smelters and the recycling of electronic waste. Volcanic activity, the gradual process of erosion and abrasion of rocks and soil, and forest fires are among the reasons for the increase in Cd concentrations in the living environment (atmosphere, soil, and water); even zinc, lead, and copper mines

contribute to the release of this metal into the atmosphere, resulting in the contamination of soil [106].

The absorption of Cd takes place mainly through the respiratory tract and to a smaller extent via the gastro-intestinal tract, while skin absorption is relatively rare. When cadmium enters the body, it is transported into the bloodstream via erythrocytes and albumin and is then accumulated in the kidneys [107], liver, and gut [108]. Cadmium excretion from the body is slow and occurs via the kidneys, urine, saliva, and milk during lactation. In humans, Cd exposure can result in a variety of adverse effects, such as renal and hepatic dysfunction, pulmonary edema, testicular damage, osteomalacia, and damage to the adrenals and hemopoietic system [109]. An association between Cd exposure markers (blood and urine) and coronary heart disease, stroke, peripheral artery disease, and atherogenic changes in lipid profile was also observed [110]. In addition to its cytotoxic effects that could lead to apoptotic or necrotic events, cadmium is a proven human carcinogen (group I of International Agency for Research on Cancer classification) [111]. Occupational or environmental cadmium exposure has been related to lung, breast, prostate, pancreas, urinary bladder, and nasopharynx cancers [112].

The generation of reactive oxygen species, accumulation of Cd^{2+}, upregulation of caspase-3, downregulation of bcl-2, and deficiency of p-53 lead to Cd-induced apoptosis. Recently, it has also been demonstrated that cadmium arsenite in yeast cells may interfere with the folding of nascent proteins, which reduces cellular viability and is probably responsible for various pathological conditions, such as neurodegenerative diseases and age-related disorders, and Alzheimer's and Parkinson's diseases [113]. Additionally, exposure to cadmium is recognized as one of the risk factors for osteoporosis, although critical exposure levels and the exact mechanisms are still unknown [114], and a relationship between prenatal Cd exposure and cognitive and kidneys development in fetuses has been demonstrated [115,116].

Cadmium may interfere with the activity of antioxidant enzymes, such as catalase, manganese superoxide dismutase, and copper-zinc superoxide dismutase. Metallothionein is a zinc-concentrating protein that can act as a free-radical scavenger. Cells containing

metallothioneins are resistant to cadmium toxicity, while cells that cannot synthesize metallothioneins are sensitive to its intoxication [117]. Metallothionein expression determines the choice between apoptosis and necrosis in Cd-induced toxicity [118]. The most severe form of Cd toxicity in humans is "itai-itai", a disease characterized by excruciating pain in the bone [119]. Other health implications of Cd in humans include kidney dysfunction, hepatic damage and hypertension. However, it has been suggested that overall nutritional status (rather than mere Cd content of food) is a more critical factor in determining Cd exposure. The WHO recommended safe limits of Cd in wastewater effluent are 0.003 mgL^{-1} [120].

2.1.2. Dyes

Dyes are used at the beginning of human civilization for different purposes. They offer fascinating colour to clothing and other stuff. In recent time, multi-coloured clothing leads to an increasing consumption of dyes that resulted in an augmented amount of polluted water discharged in industrial effluent. Dyes are the major source of color in textile effluents. In typical dyeing processes, 50-100% of the dye is fixed on the fiber, and the unfixed dyes are discharged in spent dye-baths or in the wastewater from subsequent textile-washing operations. Difficulties in the effluent treatment arise from the low level of aerobic biodegradation and/or adsorption of dyes onto adsorbents during treatment. Furthermore, discharged wastewater contains salts whose removal is unattainable by conventional treatment systems. Most of the dyes are toxic for aquatic biota and humans due to their suspected carcinogenic and mutagenic effects [121]. Therefore, it is recommended to remove it early as possible.

Dye wastewater treatment has always been a concerning environmental issue from the industrial effluent emission in this modern era. Most of the industrial effluents from manufacturing sectors like textiles, cosmetics, paper and printing, rubber, leather, pharmaceutical, food, and plastics consisted of a large number of toxic dyes that are harmful to the environment and aquatic life forms [122]. Other than the carcinogenic and mutagenic negative effects, the dyes have the propensity to sequester metal which could lead to the cause of micro toxicity towards the aquatic organisms [123]. Among different dyes, methylene blue

(MB) is a cationic dye, widely used for different dyeing processes for wood, cotton, silk, etc [124]. It is an aromatic heterocyclic compound also widely used in different applications such as, medicine, biological, and textile industries. Its chemical structure is given in Figure 2. The dye is commonly found in industrial wastewater, which causes devastating effects on the environment [125]. Therefore, the removal of this dye from wastewater is the most significant issue worldwide. Thus, to remove it adsorption is an available method which has superior to the others in terms of initial cost, simplicity of design, and ease of operation, without producing harmful substances for the removal of dyes and other pollutants [122].

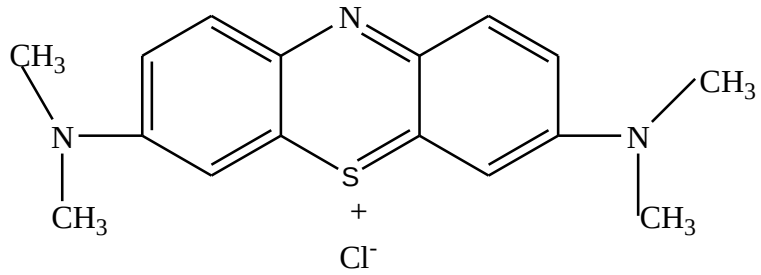

Figure 2. Chemical structure of MB.

2.2. Current Wastewater Treatment Technologies

Water is the most important molecule (compound) on earth for sustaining life all over the world. Due to different industrialization activities, untreated wastewater effluents with wide range of pollutants has been released into water bodies and severely affects the human health and aquatic animals. Therefore, several methods are used for the treatment of wastewater effluents, including chemical and physical methods. Thus, the treated wastewater by using these methods should be able to be discharged into the environment or to be used by industries without any negative consequences. The wastewater treatment technologies have strong future perspectives which create challenging condition in water treatment development. Therefore, wastewater treatment technologies are on high priority among other technologies.

Recently, several wastewater treatment technologies are available for decontamination of organic and inorganic pollutants from wastewater called physical, chemical and biological including chemical oxidation and reduction, membrane separation, liquid extraction, ion exchange, electrolytic treatment, electroprecipitation, coagulation, flotation, evaporation,

hydroxide and sulfide precipitation, crystallization, ultrafiltration, bio-degradation and electrodialysis [82, 126].

The comparison of these treatment technologies regarding the effectiveness and cost are reported by different research articles. Among these, adsorption gained popularity among environmentalists in recent years because; it produces high quality treated effluent with least operating cost. It is a well-known equilibrium separation process; it is effective, efficient, and economical method not only for the water treatment but also for analytical separation techniques both in small and large scale [127]. Different physicochemical wastewater treatment techniques with their advantages and disadvantages are presented in Table 1.

Table 1. The main merits and demerits of the different physico-chemical approaches for wastewater purification.

Treatment approaches	Merits	Demerits	References
Adsorption	Low-cost, easy working principle, high pollutant uptake capacities	Low selectivity, production of waste products	[82]
Electrolysis	Simple operation and management, stable effluent quality, impressed decolorization effect and less area-covering	The processing cost is high due to the high energy consumption	[128]
Membrane filtration	Simple process and convenient operation	The membrane module is expensive and prone to being polluted	[129]
Electrocoagulation	Economically reliabile	low efficiency, generates a large amount of chemical sludge and difficult to completely remove pollutants	[130]
Chemical precipitation	Simple method and high degree of selectivity - Precipitants are relatively inexpensive	Ineffective to treat water containing high concentration of heavy metals, requires large amount of precipitating agents, production of large quantity of toxic sludge, chemical stabilization and proper precipitant disposal are needed.	[131]
Ion exchange	Regeneration of materials and its selective property for metal ions	Expensive	[132]

2.2.1. Adsorption process modeling

The removal efficiency of adsorbent will be easily identified by using adsorption process modeling. It is applied to describe the experimental data by using adsorption isotherm and kinetic models [133]. The most commonly used isotherms for modeling adsorption processes in liquid phase are the Freundlich, Langmuir, Temkin and Dubinin-Radushkevich isotherm models [142]. These models help to find out a deviation between experimental data and isotherm models, describe surface processes of adsorbent, type of adsorbate monolayer or multilayer and capacity of adsorbent.

According to the Langmuir model, adsorption occurs uniformly on the active sites of the adsorbent. The Langmuir isotherm model is described by the following formula:

$$qe = \frac{Q_o Ce}{1 + bCe} \quad (1)$$

To derive the model parameters Q_o and b, Equation 1 can be linearized. The linear Langmuir isotherm allows the calculation of adsorption capacities and is equated by using Equation 2 [134].

$$\frac{Ce}{qe} = \frac{1}{bCo} + \frac{Ce}{Qo} \quad (2)$$

The essential characteristics of a Langmuir isotherm can be expressed in terms of a dimensionless constant separation factor or equilibrium parameter R_L, which is given by Equation 3 [135].

$$RL = \frac{1}{1 + bCe} \quad (3)$$

For all the above equation (1-3), C_o is the initial adsorbate concentration in solution (mg/L), C_e is the adsorbate residual concentration in solution, q_e is the equilibrium concentration in milligrams of adsorbate accumulated per gram of the adsorbent material, Q_o is the maximum uptake corresponding to the site saturation and b is the ratio of adsorption and desorption rates.

According to the Freundlich isotherm model, adsorption occurs on multi-component system. Its equation is an empirical expression that encompasses the heterogeneity of the surface and the exponential distribution of sites and their energies and improved to describe adsorption in

aqueous solutions. This model is commonly given by the non-linear equation presented in Equation 4:

$$q_e = K_f C_e^{\frac{1}{n}} \quad (4)$$

Where K_f is the adsorption or distribution coefficient and represents the quantity of adsorbate adsorbed onto adsorbent for unit equilibrium concentration and called a constant for the system related to the bonding energy. 1/n is an empirical constant describes the magnitude of the adsorption driving force onto the sorbent.

If its value gets closer to zero, then it becomes more heterogeneous. Batch experiments, using logarithmic equation of the data and the linearized form of the Freundlich equation to determine both K_f and n are given in Equation 5 [136].

$$\log qe = \log Kf + \frac{1}{n}\log Ce \quad (5)$$

Kinetics of adsorption gives information about the prediction of adsorption rates and modeling of the processes. Its parameters describe how fast the adsorbate adsorbed onto adsorbent surfaces. Successful application of the adsorption demands innovation of cheap, easily available and abundant adsorbents of known kinetic parameters and sorption characteristics. Till now, several kinetic models (pseudo first- and second-order equations and intra-particle diffusion) are used to interpret the time dependent experimental data and examine the controlling mechanism of adsorption process. The Pseudo-first order model is represented in Equation 6 [137].

$$\log(qe - qt) = \log Qe - \frac{K1t}{2.303} \quad (6)$$

The pseudo-second-order kinetic model equation is given in Equation 7 [138].

$$\frac{t}{qt} = \frac{1}{K_2 qe^2} + \frac{t}{qe} \quad (7)$$

The spontaneity of the adsorption processes is easily determined by obtaining information from thermodynamics concept. Therefore, one can understand the concept of Gibb's free energy change (ΔG) to determine a given process is whether spontaneous or non-spontaneous. If the value of ΔG is negative, then the reactions occur spontaneously at a given temperature

Thethermodynamic parameters such as change in standard free energy (ΔG), enthalpy (ΔH) and entropy (ΔS) can be calculated by using Equation 8, 9, and 10 [139].

$$\Delta G = -nRT \ln K_C \quad (8)$$

$$\ln K_C = -\Delta \frac{H^O}{RT} + \Delta \frac{S^O}{R} \quad (9)$$

$$\Delta G^o = \Delta H^o - T\Delta S^o \quad (10)$$

Where R (8.314 J/molK) is the gas constant, T (K) is the absolute temperature and K_c is the standard thermodynamic equilibrium constant defined by q_e/C_e. By plotting the graph of $\ln K_c$ versus T^{-1}, the value of ΔH^o and ΔS^o can be estimated from the slopes and intercept, respectively.

Regeneration of used adsorbents is a process of getting again the used adsorbents through desorption process. If adsorption is thought of as surface complexation reaction a high concentration of H^+ ions shifts the equilibrium so that less adsorbate (metal ions) is bound to the surface. In addition to this, the surface acid/base reaction is shifted more towards positively charged species, which hinders adsorption of cations such as metal ions. As a result, a pH decreases due to the use of HCl, shifts the adsorption equilibrium and can result in desorption of the adsorbate. If the adsorption capacity can be regained in this process, the adsorbent is regenerated. In many studies [26,42], hydrochloric acid (HCl) solution has been shown as suitable regenerant for CNMs adsorbents as well as composite materials. The adsorbate ions desorbability is given in Equation 11.

$$\%desorptionefficiency = \frac{desorbed}{adsorbed} * 100 \quad (11)$$

Where,

Desorbed: the concentration of the metal ions after the desorption process

Adsorbed: $(C_o - C_e)$ for each recovery process.

2.3. Basic Concepts and Theory of Adsorption

Adsorption is a surface phenomenon which occurs when a gas or liquid solute accumulates on the surface of a solid or a liquid (adsorbent), forming a molecular or atomic film (the adsorbate). It is not similar to absorption, in which a substance diffuses into a liquid or solid to form a solution and sorption encompasses the activities of both adsorption and absorption. Desorption is the reverse process of adsorption. Adsorption might be chemical or physical process, or combination of those, which occurs at the common boundary of two phases, such as liquid-solid, gas-solid, gas-liquid or liquid-liquid [140].

Moreover, based on surface interaction, adsorption is divided in to four types: ion exchange, physisorption, chemisorption, and specific adsorption [77]. Ion exchange adsorption involves an attachment of ionic species to the opposite charge at the surface of an adsorbent. Physisorption occurs when van der Waals forces are involved, this type of adsorption has the characteristics of low enthalpy (less than 80 kJ/mol), can be monolayer or multilayer adsorption, no dissociation of adsorbed species, and decreasing adsorption capacity with increasing temperature [77]. On the contrary, chemisorption involves chemical forces or bonding between adsorbent and adsorbate that resulting in a change in the chemical form of adsorbate. Due to its strong interaction, chemisorption has high enthalpy (80–800 kJ/mol), adsorption occurs at monolayer only, and involves dissociation of adsorbed species [77]. Specific adsorption is resulted from specific interaction between adsorbate molecules and adsorbent which do not result in chemical change of adsorbate. This type of adsorption has binding energy value in between those of physisorption and chemisorption [141].

Adsorption is an important technique for different industries including gas, petroleum, and water purification. Adsorption is also used for gas separations, such as N_2 from O_2, acetone and C_2H_2 from vent stream, and CO, CH_4, CO_2, N_2, Ar from hydrogen. In the liquid phase, adsorption is applied, for example, for organic and inorganic removal, and decolourization. Classically, the adsorption mechanisms can be divided into three steps (Figure.3): a) diffusion of adsorbate to adsorbent surface, b) migration into pores of adsorbent c) monolayer build-up of adsorbate on the adsorbent. Firstly, diffusion of adsorbate on the adsorbent surface occurs

by intermolecular forces between adsorbate and adsorbent. Secondly, migration of adsorbate into pores of adsorbent occurs. Lastly, when the adsorbate's particles are distributed on the surface and filled up the volume of pores, particles of adsorbate are building up the monolayer of reacted molecules, ions and atoms to the active sites of adsorbent [141].

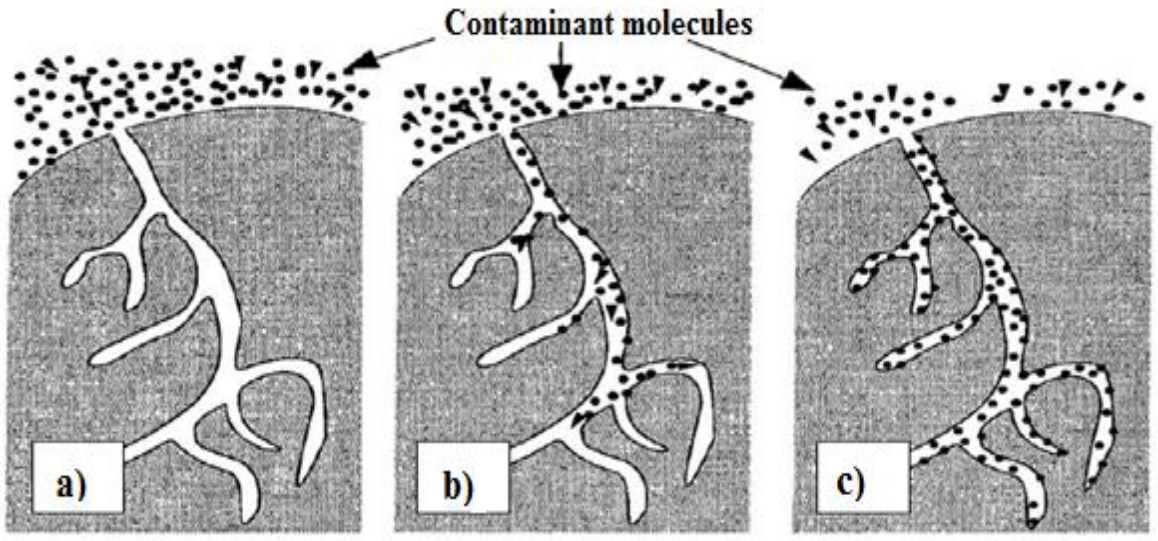

Figure 3. Three steps of adsorption mechanism: a) diffusion of adsorbate to adsorbent surface b) migration into pores of adsorbent c) monolayer build-up of adsorbate on adsorbent [142].

Adsorption is influenced by adsorbate-solvent properties, system properties, and adsorbent properties. For adsorbate-solvent properties, it can be shown in the form of solubility. If the adsorbate molecule has high solubility in water, then adsorption removal will decrease. System properties such as pH can give major influences on adsorption mechanism. In many published works [42,77], the authors always studied the effect of pH since in some pH the adsorbent can either be protonated or deprotonated. Adsorbent properties are usually referred to surface area and the distribution of area with respect to pore size as a primary determinant in adsorption capacity [143]. Adsorption occurs in three consecutives step as shown in Fig. 3: bulk diffusion, external diffusion, and intraparticle diffusion. Bulk diffusion is usually rapid due to the effect of mixing. External diffusion concerns about the diffusion of adsorbate molecule through a hydrodynamic boundary layer. Then adsorbate molecules diffuse to the active sites of adsorbent, where this step is called intraparticle diffusion. Usually, the rate limiting step lays on the second step where it controls the diffusion of solute through boundary layer to the external surface of adsorbent [143].

2.4. Lignocellulostic Biomasses

Biomass is commonly referred to various organisms that come from plants, animals, and microorganisms [144]. In other words, biomass may refer to all non-fossil organic matter that can participate in carbon cycling and regeneration. Lignocellulosic biomass (LCB) is estimated to be the most widely spread biopolymer on earth. Global annual production of this biopolymer is roughly calculated to be $1.3 * 10^{10}$ metric tons [145]. It encompasses agriculture wastes (palm residues, empty fruit bunch, straw, bagasse, corncob, Nile rose and stover), etc [146,147], forest wastes (branches, unwanted stems, withered leaves) [148].

Also, LCB refers to plant biomass that is composed of cellulose, hemicellulose, and lignin. It includes various natural organic matters which mostly refer to the plants or plant based materials, which is the largest amount of sustainable carbon material group and the most promising feedstock for the sustainable production of biochemical, bioethanol, biofuels and Nanocellulose [149]. Especially, LCB is a source of natural fiber which can substitute the petroleum-based polymers due to its outstanding environmentally friendly properties. Furthermore, the wastes from biomass such as agricultural wastes and forest residues have high potential for reuse as fuel, or feedstock for production of high value-added materials without the competition with human and animal food chains. In addition to this, it is the most promising adsorbent material for wastewater treatment. This is, due to the biodegradability, biocompatibility, non-toxicity, low cost, ease regeneration without production of pollution, high pollutant up take capacity and easy for several surface modifications [150]. Therefore, here we focus different locally available indigenous plants and wastes that are used as biomass, such as, *Erythrina Brucei, Millettia ferruginea and* wastes like *Eichhornia crassipes*, respectively. The details will be discussed as follows.

2.4.1. *Erythrina brucei*

Erythrina Brucei is a leguminous tree endemic to Ethiopia. It belongs to the family fabaceae with leaf symbiotic N-fixing characteristics. *Erythrina Brucei* is adapted to grow in areas with an altitude ranging from 1400–2600 m. It fixes atmospheric nitrogen through its leaves in

contrast to angiosperms of *Rubiaceae* and *Primulaceae*. It is a fast growing tree that reaches up to 3 m in height within 6 months of planting [151]. *Erythrina Brucei* has important agro-forestry attributes such as spreading leaves; source of large quantities of swiftly decomposable litters, vigorous re-growth, high coppicing ability as well as rapid recovery after a spell of prolonged drought. It is propagated both by seed and cuttings. The pruned branches and leaves are used by farmers as animal feed in times of animal feed shortage. In the Southern Nations Nationalities and Peoples and Oromia Regions in Ethiopia, *Erythrina Brucei* is grown abundantly as live fences, along farm boundary and inside farmlands in alleys as Agro-forestry tree [152]. Production of up to 50 kg of fodder biomass (Leave + twigs) per tree per year is potential of *Erythrina brucei*. Optimal doses of 10 tons of biomass per hectare of *Erythrina Brucei* can easily be obtained from only 200 trees [151]. The Organic carbon value determined by calcination method is fifty percent which was considered to be the total organic carbon value [152] and the cellulose content in *Erythrina brucei* wood was 50-55%. Therefore, this initiates to use this plant for cellulose preparation. The image of *Erythrinia Brucei* was presented in Figure 4.

Figure 4. The picture of *Erythrinia Brucei taken from* Bekoji on Novmeber, 2019.

2.4.2. *Millettia ferruginea*

Millettia ferruginea (Hoechst) Baker is a useful endemic tree species of Ethiopia with great potential for agroforestry. It is belonging to the family Fabaceae (Leguminosae) sub-family Papilionnodeae. This plant is known to have two subspecies, namely, ferruginae and darassana [153]. Subspecies ferruginae is known to occur at North Ethiopia within the range of 1,000 and 2,500 m above sea level, while subspecies darassana is located in the southern part of the country (particularly in Sidama) within the range of 1,600 and 2,500 m above sea level. The hybrid of the two subspecies believed to be found in the central and western part of Ethiopia. According to Andualem and Gessesse [153], *Millettia ferruginea* found in the following regions: subspecies ferruginea; Tigray, Gondar, Gojam, Shewa, Welega and Hararge. The subspecies darassana is commonly found in Welega, Shewa, Hararge, Bale, Ilubabor, Kefa and Sidama [154]. This species are found not only in the listed regions of Ethiopia, but also it is found in Gamo, Gofa, Gedeo, Konso, Shouthern Omo, etc. *Millettia ferruginea* contains high amount of organic matter and its wood also contains increased amount of cellulose in its composition. Therefore, *Millettia ferruginea* is a valuable lignocellulostic source for nanocellulose extraction for this study. The picture of *Millettia ferruginea* is presented in the Figure 5.

Figure 5. Picture of the plant Millettia Ferruginea taken from Hawassa on Novmeber, 2019.

2.4.3. *Eichhornia crassipes*

Eichhornia crassipes is a floating plant species that live in water. Rapid breeding led to water hyacinth plant has turned into a weed in some areas in Ethiopian waters such as in many lakes (Lake Tana, Abaya, etc. or other basins). *Eichhornia crassipes* is called the world's worst aquatic weed due to its ability to rapidly cover whole waterways. The growth of water hyacinth within 6 months reaches 125 tonnes wet weight in the area of 1 ha [155]. It forms dense, impenetrable mats over the water surface, and other specific impacts such as blocking irrigation channels and rivers, restricting livestock access to water, destroying natural wetlands, eliminating native aquatic plants, reducing infiltration of sunlight, changing the temperature, pH and oxygen levels of water, reducing gas exchange at the water surface, increasing water loss through transpiration (greater than evaporation from an open water body), altering the habitats of aquatic organisms, restricting recreational use of waterways, reducing aesthetic values of waterways, reducing water quality from decomposing plants, destroying fences, roads and other infrastructure when large floating rafts become mobile

during flood events, and destroying pastures and crops when large floating rafts settle over paddocks after flood events [156].

Eichhornia crassipes can grow easily in polluted wastewater and its pH tolerance is estimated at 5.0-7.5. Thus it is considered to be a potential green remediation method for the removal of pollutants presented in wastewater [157]. High cellulose content in *Eichhornia crassipes* has potential to be used as raw material for cellulose preparation, which has a higher economic value, because using this completely waste material for the remediation of wastewater.

For long time, nanocellulose have been extracted from different biomasses including woods, cultivated plants, agricultural wastes, industrial crops, and others [158]. Nevertheless, fewer studies have focused on aquatic weed water hyacinth. It is one of the fastest growing aquatic species commonly found in water basin, cannel, river, etc. Unfortunately, water hyacinth has rather caused the negative effects on environmental and ecological system since it is considered as an invasive aquatic species. Surprisingly, water hyacinth is composed of relatively high cellulose content, which is approximately 60% (wt/wt) in comparison with other cultivated plants such as bamboo; corncob, oil palm frond, sugarcane bagasse, and banana stem [159]. According to its all impressive feature, water hyacinth has been considered as a raw material for preparing nanocellulose. Until now, there are several studies focusing on the isolation of nanocellulose including nanocrystals and nanofibers from water hyacinth. For example, cellulose nanocrystals were successfully isolated from *Eichhornia crassipes* weed by acid hydrolysis and ultrasonication, respectively. It was found that the obtained nanocellulose exhibited a rod-like structure with 15.61 nm wide and 147.4 nm long [159]. Its picture is given in Figure 6.

Figure 6. The picture of Eichhornia crassipes taken from Lake of Abaya on Novmeber, 2019.

2.4.4. Bio-based adsorbents in wastewater treatment

The substances that act as adsorbents can be from organic, mineral, or biological origins: activated carbons, natural zeolites, alumina, and silica beads. They can also be low-cost adsorbents, i.e. the industrial by-products, agricultural wastes, biomass and polymeric materials such as organic polymeric resins, and macro-porous hyper crosslinked polymers [160]. Most of conventional adsorbents, such as, activated carbon, zeolites, kaolin, and can be energy intensive, expensive, and emit greenhouse gases. From these bio-based adsorbents called low-cost adsorbents and materials derived from different biological and natural sources like agricultural by-products, plants, animals, algae etc. Bio based adsorbents are prepared from the lignocellulosic biomasses through different chemical, biological and mechanical techniques. Due to its abundant availability and broad range of applicability, lignocellulosic materials have attracted the attention of various researchers to utilize it for environmental application. Or, the use of bio-based adsorbents like cellulose, chitin, chitosan, gelatine, alginate and starch for the removal of contaminants from water has the advantages of biocompatibility and non-toxicity over the non-biological adsorbent counterparts. One of the

promising applications of lignocellulosic material is as the adsorbent for wastewater treatment. Among these lignocellulosic materials, cellulose has better advantages of relatively large abundance in nature, non-toxicity, renewable characteristics and possession of hydroxyl functional groups which are used in several modification processes [161,162].

This natural polymer has been investigated as bio-sorbent in its natural or chemically modified form. In natural form, it exists in agricultural wastes and plants such as banana peel saw dust, corncob, bagasse and different soft and hard woods [163]. Modified cellulose can be divided into two groups, which are direct modification and monomer grafting. The main routes of direct cellulose modification in the preparation of adsorbent materials are esterification, etherification, halogenation, oxidation, alkaline treatment, and silynation [164]. Monomer grafting or graft copolymerization is a process where side chain grafts are covalently attached to the main chain of a polymer backbone to form a branched copolymer. Well known techniques that commonly used in graft copolymerization are photografting, high energy radiation grafting, and chemical initiation grafting [165-177].

The uses of sustainable bio-based adsorbent materials, such as cellulose-based materials reduced our dependence on activated carbons and also reduce the carbon foot print as several cellulose-based adsorbents have demonstrated excellent adsorption capacity. Nowadays, researches focus on these low cost and environmentally friendly bio-based adsorbents for the removal of pollutants from wastewater. It is also a useful tool for protecting the environment because bio-based adsorbents are abundant, biodegradable, non-toxic, and renewable with a capacity to associate with a variety of molecules via physical and chemical interactions [178].

2.4.4.1. Cellulose

The word “cellulose” originates from a French word called “cellule”, meaning a living cell and glucose. This was discovered by a French chemist called Anselme Payen in 1838 [179]. Cellulose is the most abundant polymer in the world [180], found in wood, hemp, cotton, cereal straws and other plant-based materials [181,182]. It is estimated that about 10^{10}–10^{12} tons of cellulose are produced annually [183] and about 6×10^{9} of the produce is processed

by various industries such as textile, paper, etc. [184]. Similarly, Payen found the chemical formula of cellulose to be $C_6H_{10}O_5$ through elemental analysis and it is one of the most widespread biopolymer found globally, existing in a variety of living species such as plants, animals, bacteria and some amoebas. It is a linear polysaccharide with long chains that consists of β -D-glucopyranose units joined by β-1.4 glycosidic linkages [185]. Its' natural fibers mainly consist of cellulose, lignin, and hemicellulose.

Being a carbohydrate polymer the molecular structure of cellulose possesses a large number of hydroxyl groups (three per anhydroglucose unit), which forms vast intra- and intermolecular hydrogen bonds. In one repeating unit of cellulose molecule, there are methylol (1) and hydroxyl (2) groups as functional groups. Due to the absence of side chains or branching, cellulose chains can exist in an ordered structure. Therefore, cellulose is a semi-crystalline polymer, and it contains both crystalline and amorphous phases. Although it is a linear polymer and contains two types of hydroxyl groups, primary hydroxyl in the methylol group ($-CH_2OH$) at C-6 and secondary hydroxyl groups (-OH) at C-3 and C-4, both of which are hydrophilic, it does not dissolve in water and in common solvents due to strong hydrogen bonds between the cellulose chains. As a result, the hydrogen bonds between the cellulose chains and van der Waals forces between the glucose units lead to the formation of crystalline regions in cellulose [164].

Cellulose can be derived from a variety of sources, such as woods, plants, microbes, and different agricultural wastes. These include seed fiber (cotton), wood fibers (hardwoods and softwoods), bast fibers (flax, hemp, jute, ramie), grasses (bagasse, bamboo), algae (*Valonicaventricosa*), and bacteria (*Acetobacterxylinum*). In addition to cellulose, these materials also contain hemicelluloses, and a comparably small amount of lignin. Wood and cotton are the raw materials for the commercial production of cellulose. Cellulose in its natural state serves as a structural material within the complex architecture of plant cell walls with variation in its content. In wood, it constitutes about 40–50%; in leaf fibers, it constitutes about 55–73%, in bast fibers: flax, it constitutes about 70–75%, in hemp, it constitutes about 75–80%, in jute, it constitutes about 60–65%, in ramie, it constitutes about 70–75%, in kenaf, it constitutes about 47–57%, in baggase, it constitutes about 33–45%, in barley, it constitutes

about 48%, in oat, it constitutes about 44–53%, in rice, it constitutes about 43–49%, in rye, it constitutes about 50–54%, and in wheat, it constitutes about 49–54%. Cotton seed hairs, the purest source, contain 90–99% cellulose [164].

Understanding the chemistry, cellulose is very important in the wastewater treatment. In 1838 Payen coined the name cellulose, which means the sugar (the "ose") from cells. However, cellulose chemistry did not arise until established the basic chemical formula of cellulose [184]. In 1926, the macromolecular nature of cellulose was finally recognized and accepted. Following those studies reported that cellulose was a linear homopolymer of anhydro–D-glucose units linked together by β-1-4 linkage, as shown in Figure 7. Each glucose unit is oriented 180 degree to its neighbours [184].

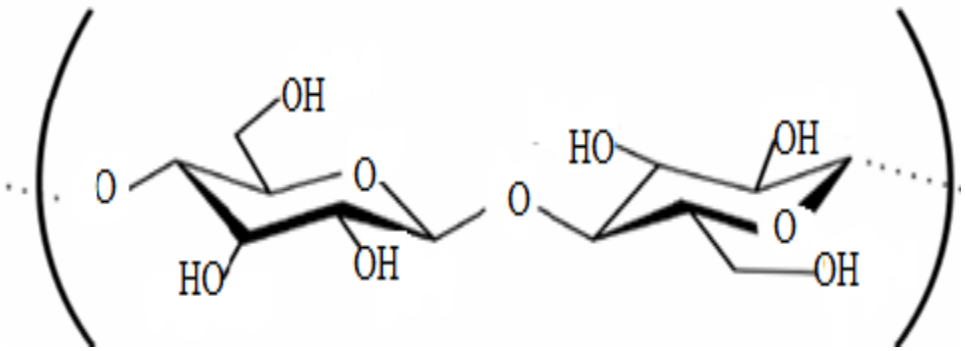

Figure 7. Structure of cellulose which shown the anhydro–D-glucose units linked together by β-1,4-linkag.

Furthermore, the monomer of cellobiose, named anhydroglucose unit, consists of three hydroxyl groups which form strong hydrogen bond with the adjacent glucose unit in the same chain and with the different chains, called as intramolecular and intermolecular hydrogen bonding networks, respectively (Figure 8). These hydrogen bonding networks are strong and tightly packed in the crystalline parts of cellulose fibrils which lead to the tough, strength, fibrous, insoluble in water, and high resistant to most organic solvents in plant cell wall [150].

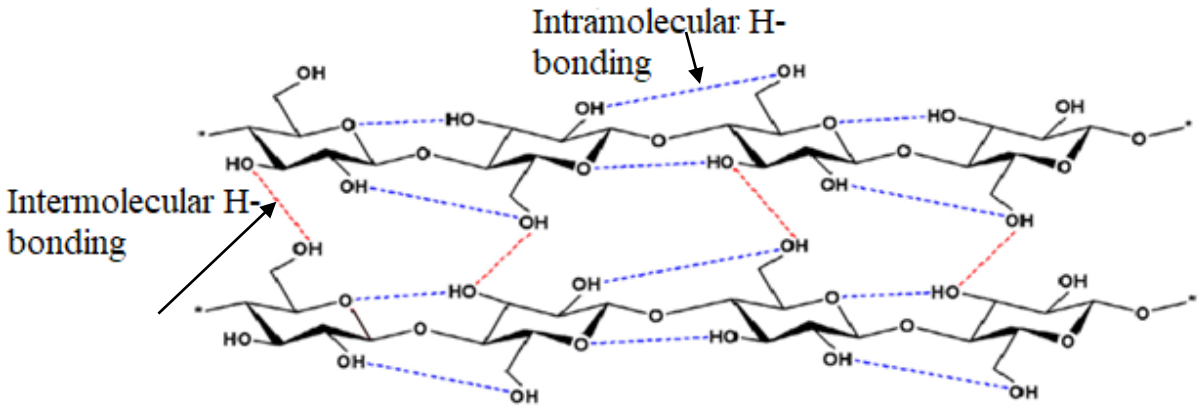

Figure 8. Intramolecular and intermolecular hydrogen bonding networks in cellulose structure.

2.4.4.2. Nanocellulose

Nanocellulose (NC) has been considered a most abundant and inexpensive biopolymer with a wide variety of applications in different areas. NC has acquired an extra reputation relative to conventional cellulose fibers due to their huge surface area, high aspect ratio and high Young's modulus of 145 GPa resulting from high crystallinity [186]. Furthermore, being as natural materials, nanocelluloses are biodegradable, biocompatible and renewable. The lateral size of cellulose molecule chains is about 0.3 nm, and these chains form bundles of elongated fibrils still with nano-scale diameters [187].

Cellulose particles with at least one dimension in nanoscale (1–100 nm) are referred to as NC. Depending on the production conditions, which influence the dimensions, composition and properties, NC can be divided into two main categories: (i) cellulose nanocrystals (CNC) or cellulose whiskers and (ii) cellulose nanofibrils (CNF), also known as nanofibrillated cellulose (NFC) [178]. Besides, Bacterial cellulose (BC) and electrospun cellulose nanofibers (ECNF) are also considered as NC. However, CNC and CNF are much more common, since they are produced by disintegration of cellulose fibers into nanoscale particles (top-down process), whereas BC and ECNF are generated by a buildup of nanofibers (bottom–up process) from low molecular weight sugars by bacteria or from dissolved cellulose using electrospinning, respectively [178].

CNFs in the form of nanocellulose can be extracted from the lignocellulosic bio-resources by using appropriate chemical, mechanical, enzymatic or combination of more than one method. It has been attracted considerable research attention in recent years due to its many exceptional properties and potential for the diverse applications [179]. Nano-biomaterials derived from abundant and renewable natural resources could have the potential to replace synthetic nanomaterials [180]. They have many interesting features such as nano dimension (higher surface area to volume ratio), nontoxicity, biodegradability, biocompatibility etc. These interesting properties could find applications in the biomedical field, reinforcement in polymer matrix in order to fabricate nanocomposite, energy, and environment. Also they have fundamental properties including morphology, crystallinity; dimension and surface chemistry vary highly depending on the raw material source and extraction process. These key properties are of crucial for the end use of isolated nanocellulose [179].

Owing to the hierarchical structure of cellulose molecules in the lignocellulosic biomass, nanocellulose can be extracted by using appropriate extraction methods [181]. Various types of plant biomasses can be used to extract nanosized cellulose, and the yield of nanocellulose could depend on the source of lignocellulosic biomass, when same method of extraction would be employed [89]. The development of nanotechnology research encourages scientists to develop nanomaterials from renewable bio-resources which have significantly lowered environmental impact for water treatment. Therefore, nanocellulose extracted from various lignocellulosic biomasses is paramount important for removing pollutants from water.

2.5. Nanocellulose Preparation Techniques and Applications

Recently, the innovation and development of more sustainable products and more efficient processes results in a large improvement in the quality of life. In order to meet this growing trend, there is a need to exploit resources that are renewable and sustainable. Thus, cellulose is by far the most abundant biopolymer on earth, and is being produced at a rate of 1.5×10^{12} tons per year. In its native form, such as cotton or wood, it can be used to clothe and shelter us, and through additional chemical and mechanical treatments, pulp fibers are extracted to

make paper. Additionally, these pulp fibers can undergo further mechanical and chemical treatments to yield a more useful class of materials, called nanocellulose.

Nanocelluloses are accounted for various types of cellulosic nanomaterials with at least one of its dimensions is less than or equal to 100 nm by the definition of nanomaterials. Typical examples of nanocelluloses are CNFs, CNCs and BNCs [182,183]. Nanocellulose can be extracted from various lingocellulosic plant resources by using mechanical, chemical or enzymatic methods. LCB is complex biomaterial which consists of cellulose, hemicellulose, and lignin. Cellulose in the LCB can be disintegrated to nano dimension materials by using appropriate methods.

Extraction of NC from the cellulosic biomass includes two major steps viz. pretreatment and removal of amorphous phase by appropriate methods [184]. Prior to the mechanical, chemical or enzymatic treatment, pretreatments such as alkali treatment and bleaching are required. The prime objective of pretreatment is to remove certain amount of lignin, hemicellulose, wax and oils which cover on the external surface of the fibre cell wall. Alkali treatment depolymerizes the native cellulose structure, defibrillates the external cellulose microfibrils and exposes short length crystallites. Further, bleaching treatment is required in order to remove the cementing material completely from the fiber [77].

2.5.1. Chemical Method

Acid hydrolysis is a common method to extract nanocelluose from the lignocellulosic biomass [185]. After the hemicellulose removal and prior to the acid hydrolysis treatment, the lignocellulosic biomass can be treated with chemicals such as dimethyl sulfoxide to swell the matrix of biomass so that acid could diffuse into the domain structure of lignocellulosic biomass easily and disintegrate the nanowhisker. In an acid treatment method, yield of NC depends on the content of lignocellulosic biomass and the reaction conditions such as acid concentration, time and temperature. Optimization of experimental parameters is required to obtain maximum yield and to preserve the NC morphology [186].

Yield as well as nano dimension of NC decreases with the increase of acid treatment time of cellulosic biomass. Preparation of NC from the lignocellulosic biomass by using catalysts could be a green approach. Ionic liquid based catalyst has several advantages viz. wide range of electrochemical stability, good electrical conductivity, high ionic mobility and selective dissolution properties to many organic and inorganic substances as well as excellent chemical and thermal stabilities [157].

Cellulose based nanomaterials produced by chemical method are applied in water treatment technology because of their high specific surface area, high specific strength, hydrophilicity, biodegradability and surface functionalization capabilities. Also it is applied in biomedical application including antimicrobial application, tissue engineering, drug delivery and others.

2.5.2. Mechanical Method

NC can be obtained by disintegrating cellulose from the lignocellulosic biomass by mechanical means [187]. Cherian et al. reported acid coupled steam treatment method for the preparation of nanocellulose from pineapple leaf fiber [186]. The surface morphology of biomass changes with the removal of primary components. Pretreatment of biomass at high temperature steam explosion with alkali hydrolyzes hemicellulose and depolymerizes the lignin. Further, lignin is rapidly oxidized by chlorine and accelerates the degradation of lignin. Formation of various groups such as hydroxyl, carbonyl and carboxylic groups facilitates the lignin solubilization in the alkaline medium. Acid coupled steam treatment helps to disintegrate fibrils to form the NC. Hettrich et al. reported a combined chemical and mechanical method for the preparation of NC by using various cellulosic bioresources such as bleached pulp, cotton linters and microcrystalline cellulose [185].

Prior to the mechanical treatment, pretreatments such as grinding, acid hydrolysis, decrystallization and derivatization are used for the preparation of nanocellulosic materials. The extracted NC has spherical shape with diameter of less than 200 nm [188]. NC can be derived from the lingocellulosic biomass by high pressure homogenization. The biomass could be suspended by high speed stirring coupled with ultrasonication treatment prior to the

high pressure homogenization [189]. Ionic liquid can be used to treat the lignocellulosic biomass prior to the mechanical treatment. The ionic liquid permeates through the microstructure of cellulose and subsequently, attacks the hydrogen bonds between cellulose molecules. During high pressure homogenization, inter and intra molecular bonds are further destroyed, hence, nanocellulose is disintegrating from the biomass. The extracted NC has a width of 10–20 nm [190].

2.6. Modification of Nanocellulose (NC)

An important aim of chemical functionalization is the introduction of stable negative or positive electrostatic charges on the surface of cellulose [191]. This is done to obtain better colloidal dispersion and to tune the surface characteristics of cellulose to improve its compatibility, especially when used in combination with non-polar or hydrophobic matrices in nano-composites. Due to the abundance of –OH groups on the surface of cellulose, different chemical modifications have been carried out including treatment with base solutions (NaOH, $Ca(OH)_2$, $Na_2(CO_3)$, with mineral and organic acid solutions (HCl, HNO_3, $H_2(SO_4)$, citric acid, etc.), with organic compounds (EDTA, formaldehyde, CH_3OH), and with H_2O_2. Pristine cellulose has a low heavy metal adsorption capacity as well as variable physical stability.

However, a chemical modification of cellulose can be executed to achieve adequate structural durability and an efficient adsorption capacity for heavy metal ions and other water pollutants. The properties of cellulose, such as its hydrophilic or hydrophobic character, elasticity, water sorbency, adsorptive or ion exchange capability, resistance to microbiological attack and thermal resistance, are usually modified by chemical treatments. The β-D glucopyranose on the cellulose chain contains one primary hydroxyl group and two secondary hydroxyl groups. Functional groups may be attached to these hydroxyl groups through a variety of reactions. The main routes of direct cellulose modification in the preparation of adsorbent materials are esterification, etherification, halogenations, oxidation and alkali treatment [39].

2.6.1. Esterification

The esterification of free –OH groups of the cellulose with one or more acids, whereby cellulose reacts as a trivalent polymeric alcohol is a process in which the derivatives of cellulose (Cellulose esters) can be produced. Cellulose esters are commonly derived from natural cellulose by reacting with organic acids, anhydrides, or acid chlorides. Table 2 presents the esterification methods of cellulose leading to adsorbent materials for water treatment.

Table 2 Cellulose modification using esterification methods and associated adsorption capacities

Adsorbent	Modifying chemicals (Chelating group)	Maximum adsorption (mg/g)	Reference
Cellulose	Succinic anhydride a)(Carboxyl) b)(Carboxylate	Cu(II) 30.4 Cd(II) 86 Pb(II)205.9	[190]
Cellulose	Succinic anhydride +Triethylenetetr amine (Carboxyl, Amine)	Cr(VI) 43.1	[191]
Cellulose	Triethylenetetramine (Amine)	Cu(II) 56.8 and 69.4 Cd(II) 68.0 and 87.0 Pb(II) 147.1 and 192.3	[192]
Cellulose	Maleic anhydride (Carboxyl)	Methyl violet dye 106.4 (Unfunctionalized 43.7)	[193]
Pineapple peel fibers	Succinic anhydride (Carboxyl)	Cu(II) 27.7 Cd(II) 34.2 Pb(II) 70.3	[194]
Bagasse fibers	Succinic anhydride (Carboxyl)	Cu(II) 95.3 Ni(II) 105.7 Cr(II) 130.0 Fe(II) 346.0	[195]
Cotton cellulose	Sulfuric acid	Au(III) 6.	[196]
Jute fiber	Maleic acid modified cellulose	Pb(II) 115	[197]
Cellulose (junpier)	Sulfuric acid(Carboxyl)	Cd(II) 16.6	[198]

Table 2. indicates the treatments of cellulose with cyclic anhydrides, such as succinic anhydride, are widely studied methods to add carboxyl groups to the surface of cellulose [195]. EDTA dianhydride, citric acid anhydride and maleic anhydride were also used for esterification. The reaction of succinic anhydride on cellulose is presented in Figure 9. The mercerization of cellulose before a succinylation reaction is commonly used due to the fact that the mercerization of cellulose increases the separation of polysaccharide chains and reduces the packing efficiency, thereby facilitating the penetration of succinic anhydride. It was observed that the modified mercerized cellulose showed a higher adsorption capacity for Cu (II), Cd(II) and Pb(II) ions than modified non-mercerized cellulose. Modified mercerized cellulose in relation to modified non-mercerized cellulose presented an increase in the mass gain and concentration of carboxylic functions of 68.9% and 2.8 mmol/g, respectively, and an increase in the adsorption capacity for Cu(II) (30.4 mg/g), Cd(II) (86 mg/g) and Pb(II) (205.9 mg/g); it demonstrated that metal ion adsorption efficiency was proportional to the number of carboxylic acids introduced. Chemically modified cellulose (CMC) and sugarcane bagasse (CMSB) were also prepared from mercerized cellulose and twice-mercerized sugarcane bagasse using ethylenediaminetetraaceticdianhydride (EDTAD) as the modifying agent [191].

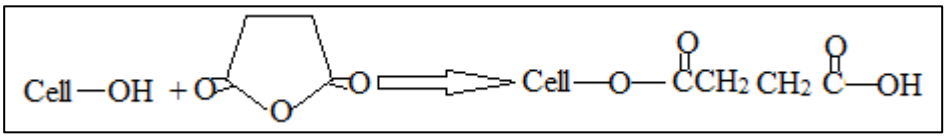

Figure 9. Modification reactions between cellulose nanomaterial and succinic anhydride.

Further processing after esterification would give better properties for binding metals from water solutions. The esterified cellulose is commonly treated with a saturated sodium bicarbonate solution because carboxylate functions have better chelating capacities than the carboxylic group. The other pre-tretatment method was reacting carboxylic groups with triethylenetetramine to introduce amine functionality to carboxylated material [191].

The new cellulose-based ion exchanger polysaccharide was prepared by adding cellulose directly to molten succinic anhydride in a quasi-solvent-free procedure [195]. This biopolymer/anhydride ion exchange was able to exchange cations from an aqueous solution

through a batch wise methodology to obtain 144.9 mg/g and 144.4 mg/g adsorption capacities for Co(II) and Ni(II) cations, respectively.

The sawdusts of oak and black locust hardwood were found to possess good adsorption capacities for heavy metal ions. The leaching of coloured organic matter during the adsorption could be prevented by the following adsorbent pre-treatments: with formaldehyde in acidic medium, with sodium hydroxide solution after formaldehyde treatment, or with sodium hydroxide only. With this respect the adsorption of Zn(II) and Cu(II) was studied. The studies indicated that the leaching of coloured matter from modified hardwood sawdust was less than that from unmodified hardwood sawdust, namely between 70 and 94%, depending on the wood species and the method of modification. At the same time, the adsorption capacities of modified adsorbents were higher than those of unmodified adsorbents when sodium hydroxide was applied for modification. When formaldehyde was applied, the adsorption capacities of adsorbents remained unchanged.

Only the application of sodium hydroxide was recommended for modification of hardwood sawdust. The adsorbent for the removal of Pb(II) and Hg(II) was prepared through two common reactions, which included the esterification of starch with excess maleic anhydride in the presence of pyridine, and the cross-linking reaction of the obtained macromonomer with acrylic acid by using potassium persulphate as the initiator [199]. It was found that the adsorption capacities of the adsorbent for lead and mercury ions were 123.2 and 131.2 mgg^{-1}, respectively.

Meanwhile, most acids used for the treatment of cellulosic plant wastes, such as sulfuric acid, hydrochloric acid and nitric acid, have been in a dilute form. When rice husk is treated with hydrochloric acid, adsorption sites on the surface of the rice husk are protonated, leaving the heavy metal ions in the aqueous phase rather than being adsorbed on the adsorbent surface. The adsorption study of copper was carried out by modifying rice husks using various kinds of carboxylic acids (citric acid, salicylic acid, tartaric acid, oxalic acid, mandelic acid, malic and nitrilotriacetic acid) and it was reported that the highest adsorption capacity was achieved

by citric acid modified rice husk [200] and also the highest adsorption capacity (115 mgg^{-1}) of Pb was reported by maleic acid modified cellulose [197].

It was reported that when corncobs were treated with sulfuric acid while heating at 150 °C, the functional groups present in the adsorbent were mainly oxygen-containing groups such as –OH and –COO. The maximum adsorption capacity for copper was 31.5 mg/g. Adsorption was more favoured at a higher pH value (4.5) due to the low competing effect of protons for the adsorption sites. The effect of interfering ions, such as Zn(II), Pb(II) and Ca(II), was also studied. It was noticed that copper removal efficiency was reduced by 53%, 27% and 19% in the presence of Pb(II), Ca(II) and Zn(II), respectively. A regeneration study indicated that sulfuric-acid-treated corncobs could be regenerated by acidified hydrogen peroxide solution and as much as 90% of the copper was recovered.

HCl, HNO_3, NaOH, tartaric, citric and oxalic acids were used to modify agave bagasse and the obtained materials were tested for the removal of Cd(II), Pb(II) and Zn(II) ions from water [200]. Raw bagasse had an adsorption capacity of approximately 8.0, 14.0 and 36.0 mg/g for zinc, cadmium and lead, respectively and this was improved by 27–62% upon modification with HNO_3 and NaOH. Treatments with citric, oxalic and tartaric acid did not have any significant effect on the adsorption capacities. Raw agave bagasse had appreciable adsorption capacity for metal cations and it could be partly regenerated (45%), since the biosorption mechanism involved ion exchange and complexation.

Cellulose sulfates are the most frequently investigated of all other inorganic cellulose esters. Sulfonated juniper was found to have at least twice the sorption capacity for cadmium removal from water compared to that of untreated juniper [196]. Cotton cellulose was chemically modified with concentrated sulfuric acid to prepare a novel kind of adsorption gel for gold [197]. The maximum adsorption capacity for Au(III) was evaluated as 6.21 mmol/g.

2.6.2. Oxidation

Chemical modification of cellulose using oxidation method was given in Table 3. Therefore, we can say cellulose derivatives can also be prepared by oxidation and the subsequent functionalization of the oxidized cellulose. The behavior of the ion exchange of carboxylate groups in the 2,2,6,6-tetramethylpiperidine-1-oxy radical (TEMPO)-oxidized fibrous cellulose prepared from cotton linters was compared with that of fibrous carboxymethyl cellulose (F-CMC) with almost the same carboxylate content as that of the TEMPO-oxidized cellulose. The native cellulose was treated by catalytic oxidation with 2,2,6,6-tetramethylpiperidine-1-oxy radical (TEMPO)/NaBr/NaClO under aqueous conditions. The adsorption selectivity of metal ions on the TEMPO-oxidized cellulose was also studied using aqueous solutions containing multiple metal salts and the following selectivity order was obtained:

Pb(II)>La(III)>Al(III)>Cu(II)>Ba(II)>Ni(II)>Co(II)>Cd(II),>Sr(II),>Mn(II)>Ca(II)>Mg(II).

Dialdehyde cellulose was prepared by the periodate oxidation of cellulose. This dialdehyde cellulose was further oxidized using mildly acidified sodium chlorite. The adsorption capabilities for Ni(II) and Cu(II) were 184.0 mg/g and 236.0 mg/g, respectively. Cellulose-hydroxamic acid derivatives were synthesized from dialdehyde cellulose obtained by the previous periodate oxidation method and their heavy metal adsorption capacities were investigated. These materials were capable of adsorbing 246 mg/g of Cu(II) from an aqueous solution [201]. Oxidized cellulose was effectively used in the form of filter sheets to remove some metal ions from water and from aqueous solutions. Furthermore, oxycellulose was applied in an ion exchange column and in a batch process [202].

Table 3. Cellulose modification using oxidation methods and associated adsorption capacities.

Adsorbent	Modifying chemicals (Chelating group)	Maximum adsorption (mg/g)	Reference
Cellulose powder	Sodium metaperiodate (Carboxyl)	Ni(II) 184.0 Cu(II) 236.0	[203]
Cellulose powder	Sodium metaperiodate Hydroxamic acid (Amino)	Cu(II) 246	[204]
Softwood pulp	Nitrogen tetroxide	Cd(II)30.9 Ni(II) 9.6 Zn(II) 16.9	[202]

2.6.3. Alkaline treatment

Alkaline treatment induces changes on the wood's surface by increasing its surface area, average pore volume, and pore diameter. Sodium hydroxide is a good reagent for saponification or the conversion of an ester group to carboxylate and alcohol. A detailed analysis on the ideal concentration of NaOH for modifying juniper fiber for the adsorption of cadmium ions was carried out by Min et al. [205]. Based on the FTIR analysis, it was found that as the concentration of NaOH increased (from 0 to 1.0 M), the amount of carboxylates also increased. After a base treatment, the maximum adsorption capacity of cadmium increased by approximately three times (from 9.2 to 29.5 mgg^{-1}) compared to untreated juniper fiber despite a decrease in specific surface area for the treated adsorbent.

Two kinds of sawdust, poplar and fire wood, were treated with NaOH (fiber-swelling agent) and Na_2CO_3 solutions, and the adsorption capacities were compared with the untreated sawdusts. For unmodified sawdust, both types of woods showed higher uptakes of Cu(II) ions than Zn(II) ions, and adsorption followed the Langmuir isotherm model. Equivalent amounts of adsorption capacities were recorded by both types of sawdust for Zn(II) and Cu(II) ions,

although these two adsorbents have different anatomical structures and chemical compositions. After treating with NaOH, a marked increase in adsorption capacity was observed for both heavy metal ions, and especially for Zn(II) ions. The increase was 2.5-fold for Cu(II) and 15-fold for Zn(II).

A comparative study on the adsorption efficiency of untreated and NaOH-treated sawdust of cedrus deodar wood was conducted by [205]. Cadmium removal was more favored by NaOH-treated sawdust as the value of adsorption capacity was four times greater than that of untreated sawdust.

2.7. Different Characterization Techniques

Characterization studies are very important to know the significant properties of adsorbent materials. They can also be used to correlate structure with properties. There is a number of characterization techniques used to characterize the adsorbent materials. They include Fourier transform infrared spectroscopy (FTIR), X-ray diffraction (XRD), scanning electron microscopy (SEM), thermogravimetric with differential analysis (TGA-DTA), and energy dispersive x-ray (EDX) techniques.

2.7.1. Fourier transform infrared spectroscopy (FTIR)

Infrared spectroscopy is a very useful technique for characterization of materials, not providing only information about the composition and the structure of molecules, but also morphological information. The advantages of infrared spectroscopy include wide applicability, non-destructiveness, measurement under ambient atmosphere and the capability of providing detailed structural information. Besides these intrinsic advantages (of the known as dispersive infrared spectroscopy), the more recent infrared spectroscopy by Fourier transform (FTIR) has additional merits such as: higher sensitivity, higher precision (improved frequency resolution and reproducibility), quickness of measurement and extensive data processing capability (as FTIR is a computer based technique, it allows storage of spectra and facilities for processing spectra).

FTIR has always been a powerful tool for the identification of organic materials. It is a qualitative verification of functional groups and structural behaviors of materials. Also it is a technique based on the measurement of the absorption of electromagnetic radiation with wavelengths within the mid-infrared region (4000–400 cm^{-1}). If a molecule absorbs IR radiation, the dipole moment is somehow modified and the molecule becomes IR active. A recorded spectrum gives the position of bands related to the strength and nature of bonds, and specific functional groups, providing thus information concerning molecular structures and interactions. Generally, in FTIR spectroscopy, a sample is irradiated with infrared light. The device measures the amount of absorbed, transmitted, and/or reflected light after the light has interacted with the sample and reports the absorbance as a function of wavenumber. The resulting plot provides information on molecular vibrations, which can be used to identify the chemical and physical properties of functional groups within the sample. Basically, FTIR instruments collect interferograms using an interferometer and then perform a Fourier transform of the latter to yield the IR spectrum that can be analyzed. Here, FTIR spectrometers collect all wavelengths simultaneously, which is a major advantage of the technique along with high spectral resolution and high signal to noise ratio [206]. Also, FTIR stands as a key technique to establish the presence of specific groups and bonds on the surface of the nanomaterials and is therefore commonly used to validate the effectiveness of the adsorption mechanisms on chemical reactions targeting onto a specific functionality of the materials.

For a molecule to present FTIR absorption bands it is required that it has a permanent dipole moment. When a molecule with at least one permanent dipole vibrates, and can interact with the oscillating electric field of incident infrared radiation. In order for this normal mode of vibration of the molecule to be infrared active, that is, to give rise to an observable infrared band, there must be a change in the dipole moment of the molecule during the course of the vibration. Thus, if the vibrational frequency of the molecule, as determined by the force constant and reduced mass, equals the frequency of the electromagnetic radiation, then adsorption can take place. As the frequency of the electric field of the infrared radiation approaches the frequency of the oscillating bond dipole and the two oscillate at the same

frequency and phase, the chemical bond can absorb the infrared photon and increase its vibrational quantum number by +1, or what is the same, increase its vibrational state to a higher level.

The larger the strength of the bond the higher the frequency of the fundamental vibration observed. In the same way, the higher the masses of the atoms attached to the bond the lower the wavenumber of the fundamental vibration. The infrared spectrum can be divided into two regions, one called the functional group region and the other called the fingerprint region. The functional group region is generally considered to range from 4000 to 1500 cm^{-1} and all frequencies below 1500 cm^{-1} are considered characteristic of the fingerprint region. The fingerprint region involves molecular vibrations, usually bending motions, which are characteristic of the entire molecule or large fragments of the molecule. Thus these are used for identification. The functional group region tends to include motions, generally stretching vibrations, which are more localized and characteristic of the typical functional groups, found in organic molecules. Basically, an IR spectrometer is composed by the source, the monochromator and the detector. Between the source and the detector there must be some kind of device to analyze the radiation so that intensity can be evaluated for each wavelength resolution element.

2.7.2. X-ray diffraction (XRD)

One of the phenomena of interaction of X-rays with crystalline matter is its diffraction, produced by the reticular planes that form the atoms of the crystal [207,208]. Relevance X-ray diffractometric analysis can in principle is applied to all cellulosic materials, including CNMs. However, the significance of this approach is to use XRD analysis as a means not only to obtain a measure of crystallinity, which is a bulk property as determined by XRD, but also to systematically examine the factors influencing the transition and distribution of highly-ordered to least-ordered regions. The method, approach and analysis described in here are applicable to CNMs. X-ray diffraction (XRD) is one of the most extensively used techniques for the characterization of adsorbent materials. Typically; XRD provides information regarding the crystalline structure, nature of the phase, lattice parameters and crystallite size.

The latter parameter is estimated by using the Scherrer equation using the broadening of the most intense peak of an XRD measurement for a specific sample. An advantage of the XRD techniques, commonly performed in samples of powder form, usually after drying their corresponding colloidal solutions, is that it results in statistically representative, volume-averaged values.

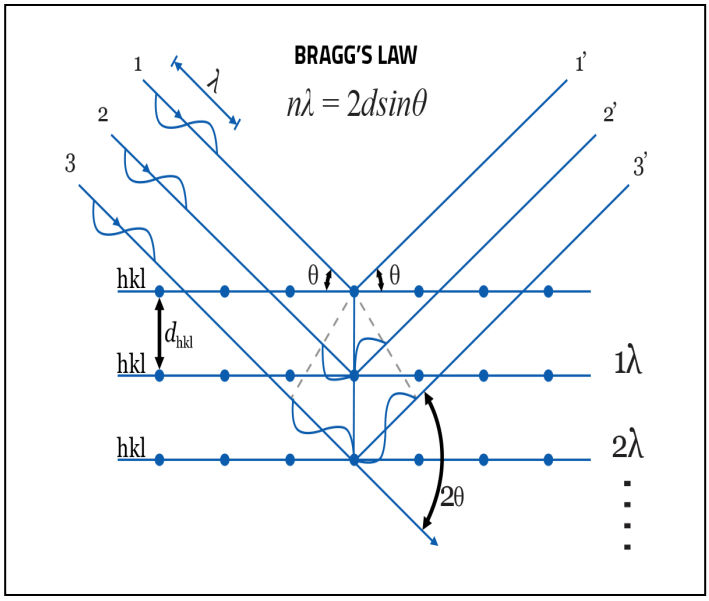

Figure 10. Principles of Bragg's law.

A crystal diffracts an X-ray beam passing through it to produce beams at specific angles depending on the X-ray wavelength, the crystal orientation and the structure of the crystal. In the macroscopic version of X-ray diffraction, a certain wavelength of radiation will constructively interfere when partially reflected between surfaces (i.e., the atomic planes) that produce a path difference equal to an integral number of wavelengths. This condition is described by the Bragg's law in Equation 12:

$$n\lambda = 2dsin\theta \quad \text{.....(12)}$$

Where

λ = wavelength of the X-rays (1.5418 Å for Cu Kα),

n = reflection order,

d = inter-planar distance

θ =angle of incidence of the X-ray beam on the lattice plane.

Figure 10 presents the principles and parameter relations of Bragg's law. This relation demonstrates that interference effects are observable only when radiation interacts with physical dimensions that are approximately the same size as the wavelength of the radiation. So, through X-ray spectra one can identify and analyse any crystalline matter. The degree of crystallinity or order will provide the quality of the obtained result. In order to do this, a diffractometer is needed. Basically, an X-ray diffractometer consists in an Xray generator, a goniometer and sample holder and an X-ray detector, such as photographic film or a movable proportional counter. The most usually employed instrument to generate X-rays is X-ray tubes, which generate X-rays by bombarding a metal target with high energy (10-100 keV) electrons that knock out core electrons. Thus, an electron in an outer shell fills the hole in the inner shell and emits an X-ray photon. The common target used is Cu, which have strong K X-ray emissions at 1.5418Å. Apart from the main line, other accompanying lines appear which have to be eliminated in order to facilitate the interpretation of the spectra.

2.7.3. Scanning electron microscope (SEM)

Scanning electron microscope (SEM) is an important electron microscopy technique that is capable of achieving a detailed visual image of a particle with high-quality and spatial resolution. It is also a powerful characterization technique for surface analysis and morphology of the materials. SEM is a multipurpose state-of-the-art instrument which is largely employed to observe the surface phenomena of the materials. The working principle of SEM is given as the sample is exposed in SEM to the high-energy electron beam and gives information about topography, morphology, composition, chemistry, orientation of grains, crystallographic information, etc. of a material, and therefore SEM is a useful tool to be used for the characterization of materials. Morphology indicates the shape and size, while topography indicates the surface features of an object or "how it looks", its texture, smoothness or roughness.

The main working principle of an SEM is as follows and presented in Figure 11. The electron gun emits a beam of electrons by applying a voltage to a thermionic tungsten filament. Then these electrons are attracted by the anode and accelerated vertically through the column of the

SEM. On its way, the beam passes through different magnetic lenses before reaching the sample surface. The objective lens focuses the beam on the sample surface. The sample is scanned with the help of scan coils. Specialized detectors collect and amplify the signals to produce an image of the surface.

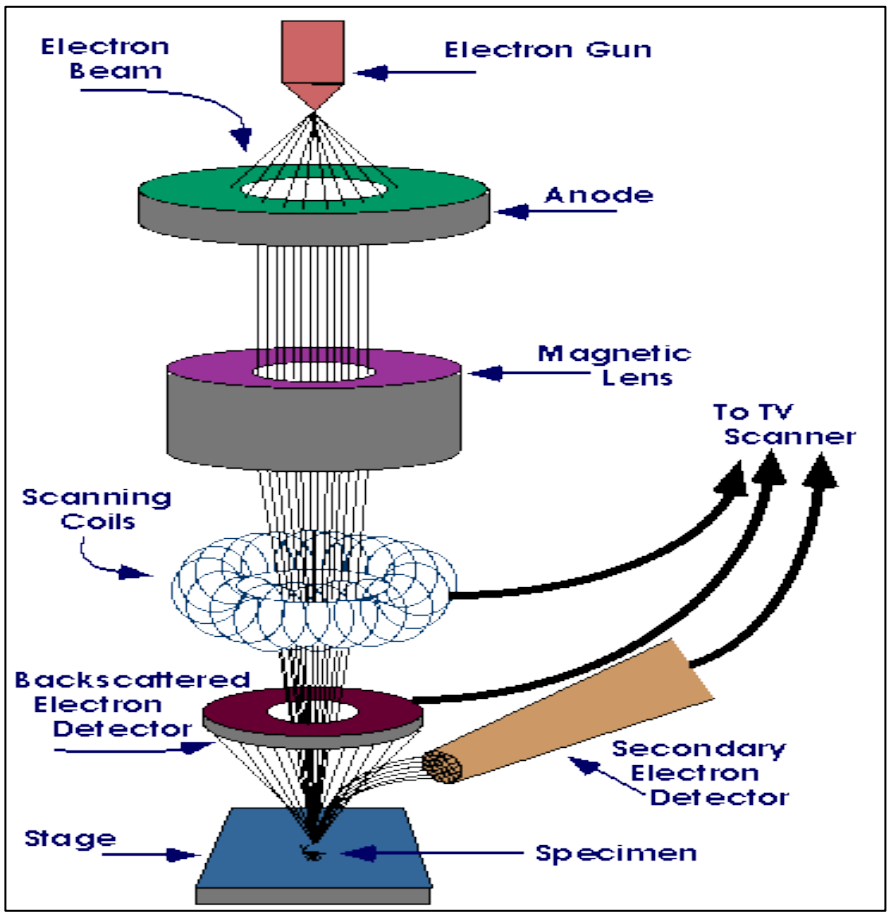

Figure 11. Schematic of scanning electron microscope.

2.7.4. Thermogravimetric (TG) analysis with differential thermal (DT) analysis

Thermogravimetry deals with the branch of thermal analysis which investigates the change in weight for a substance as a function of time or temperature. The weight change profile is recorded when the sample is subjected to heating or cooling environment in a controlled manner. The main principle of thermogravimetry analysis (TGA) includes mass change for a sample can be studied under programmed condition. Therefore, TGA is mainly used for understanding certain thermal events such as absorption, adsorption, desorption, vaporization,

sublimation, decomposition, oxidation and reduction. In addition to this, TGA can be utilized for evaluation of volatile or gaseous products lost during such chemical reactions for samples such as nanomaterials, polymers, polymer nanocomposites, fibers, paints, coatings and films. Along with the prediction of thermal stability for samples, it is also possible to study the kinetics of chemical reactions under various conditions using TGA.

Differential Thermal Analysis (DTA) is a technique in which the difference in temperature between the sample and a reference material is monitored against time or temperature while the temperature of the sample, in a specified atmosphere, is programmed. DTA works by placing the sample and the reference symmetrically in the furnace. The furnace is controlled under a temperature program and the temperature of the sample and the reference are changed. During this process, a differential thermocouple is set up to detect the temperature difference between the sample and the reference. Also, the sample temperature is detected from the thermocouple on the sample side. Therefore, in this study the thermal stability and the carbon nature of pristine and chemically modified CNMs were determined by using thermogravimetric analysis with differential thermal analysis (TGA-DTA)

2.7.5. Energy Dispersive X-Ray (EDX) Analysis

Generally elemental analysis (EA) techniques are often the fastest and most inexpensive methods to determine the purity of samples. These methods of chemical analysis are particularly useful in cellulosic materials because they can provide validation and quantification of chemical modification, can help identify sulfur and other elements in a sample, can provide verification of acid hydrolysis of cellulose-containing compounds, and can assist in determining impurities in materials containing cellulosic materials.

Among EA techniques EDX is an analytical technique where a high-energy beam of charged particles or an X-ray is used to characterize a sample. Atoms within the sample contain ground-state electrons in discrete energy levels bound to the nucleus which, when excited by an outside source, can be ejected from their shells creating an electron hole. An electron from an outer shell can then fill this hole, releasing an X-ray with energy equal to the energy

difference between the outer-shell and inner-shell [209]. The number and energy of these X-rays are measured by an energy-dispersive spectrometer and are used to characterize the sample. EDX is a particularly useful EA technique for the characterization of cellulosic materials because it is often attached to SEM devices. Because of this, one can easily obtain the chemical composition of surfaces that are visually identified on the SEM.

In summary, this section briefly reviwed the past studies which is related to the present study. Hence, points such as the sources of water pollution, current wastewater treatment thechniqes, basic concepts and theories of adsorption, lignocellulosic biomass, bio-based adsorbents in wastewater treatment, cellulose nanomaterials preparation methods, modification of cellulose nanomaterials, and different characterization techniques of cellulose nanomaterials were briefly discussed. In that, the major research gaps based on pollutants removal technologies, adsorbent materials, adsorbent preparation methods, and the surface chemical modification methods were reviewed. Also, it reviews how the current research fills the stated research gap on cations removal by using different techniques and materials. Furtheremore, this section reviewed suitable methods which have been used to prepare cellulose-based adsorbents and their chemical modification method which is prefer to remove cations from wastewater effluents. Since, this study was focused on the use of cellulose, cellulose nanomaterials, and its modified forms, for the effective removal of Cr(VI), Cd(II), Pb(II), and MB dye cations from wastewater effluents. Therefore, the present research fills the research gap of cost, energy, materials recyclability, environmental friendly, and removal efficiency.

3. MATERIALS AND METHODS

3.1. Materials and Instruments

The following materials and instruments were used in order to perform the study. Materials such as, different size beakers, measuring cylinders, micropipette, volumetric flasks, burettes, funnels, test tubes, thermometer, stopwatch, mortar and pestle, 2 mm sieve, oven, electronic mill, plastic bags, stirrer, Erlenmeyer flask (different sizes), refrigerator, filter papers № 42, homogenizer, and shaker.

Instruments such as, digital analytical balance (Explorer, Ohaus, Model E11140, Switzerland), Atomic Absorption Spectrophotometer (AAS, Shimadzu, USA), X-ray diffraction (XRD) (XRD-7000 X-Ray diffractometer, Shimadzu Co., Japan), Fourier transforms infrared spectroscopy (FTIR) (Perkin Elmer65, PerkinElmer, Inc., Waltham, USA), scanning electron microscopy (SEM) (JCM-6000plus, JEOL/EO, USA), thermogravimetric analysis with differential gravimetric analyses (TGA-DTA, Shimadzu TGA-DTA -60H, Japan), a potentiometric digital pH meter (Hanna instruments, model MP 220, UK), Conductivity meter (model 4310), UV-VIS spectrophotometer (SM-spectrophotometer UV-VIS 1600, MaaLab Scientific Equipment Pvt. Ltd., India), digital Sonicator, (Branson digital Sonicator, S-450D, South Korea), and a water deionizer (Elgalan Instrument Purified-Water, Cartridge type C114, B114 deionizer, UK) were used throughout the study.

3.2. Chemicals and Reagents

All the chemicals and reagents used throughout the experiments were analytical grade. These includes toluene (99%), (Loba Chemie Pvt. Ltd, India), ethanol (97%), (Tradewell International Pvt. Ltd, India), sodium hydroxide, (99%), (Shraddha Associates GUJ, Pvt. Ltd., India), conc. hydrochloric acid (35%), (Loba Chemie Pvt. Ltd., India), conc. sulfuric acid (69%), (Loba Chemie Pvt. Ltd., India), conc. nitric acid (69%), (Loba Chemie Pvt.Ltd., India), sodium chlorite (80%), (Shanghai ZZ New Material Tech. Co., Ltd., China),

Methylene Blue trihydrate, $C_{16}H_{18}ClN_3S{\cdot}3H_2O$ (80%), (Sigma-Aldrich, India), sodium bicarbonate, 99%, (Shraddha Associates GUJ Pvt. Ltd., India), $Pb(NO_3)_2$ (99%), (BDH chemicals Ltd, England), $Cd_2(NO_3)$ (99%), (SDFCL, India), and $K_2Cr_2O_7$ (99%), (SDFCL, India).

3.3. Methods

3.3. 1. Collection of plant samples

Before collecting the plant samples it is suggested to use sample collection protocols of EPA, USA, such as, identifying suitable collecting equipment, data recording equipment and storing equipment [210]. Then, sample collection was performed following sample collection protocols of EPA, USA, [210]. Accordingly, the stem of *Erythrina brucei* plant sample was collected from purposly selected location of Bekoji Twon, Arsi zone**,** Oromia Region. Bekoji in afan Oromiffa: Boqqojji is a town in Oromia reginonal state, Ethiopia. It has latitude and longitude of 7°35′N 39°10′E with an elevation of 2810 m. It was located about 226 Km in the south waste of Addis Ababa. The stem of *Millettia ferruginea* plant sample was collected from Hawasa Town, Sidama and Southern Regional state. Hawassa is a city in southern Ethiopia; Located in the Sidama Region and the Southern Nations, Nationalities, and Peoples Region (SNNPR) about 273 Km south of Addis Ababa. It has latitude and longitude of 7°3′N 38°28′E with an elevation of 1708 m. Also, *Eichhornia crassipes* sample was collected from Arba Minch, (Ganta Garo), Gamo, Zone, Ethiopia. Arba Minch (Ganta Garo) is a city in southern Ethiopia; Located in the Gamo Zone of the Southern Nations, Nationalities, and Peoples Region about 500 kilometers south of Addis Ababa. It has latitude and longitude of 6°2′N 37°33′E with an elevation of 1285 m. All these samples were collected as per the EPA sample collection protocol [210]. Next to this, the collected plant materials were identified in the National Herbarium of Ethiopia in AAU; and samples were transported to Adama Science and Technology University, Department of Chemistry Research Laboratory. The dried stem of plant material was cut into small pieces and finally grinded into course powder using a grinder. Finally, it was sieved through 30–80 mesh size sieves and stored at room temperature in a plastic bag.

3.3. 2. Collection of wastewater (WW) samples

Wastewater samples were collected from near industrial outfalls of tannery and textile industries from city Zone of Modjo, Oromia Regional State, Ethiopia, and Hawassa, SNNPR and Sidama regional State, Hawassa, Ethiopia, respectively, in a sterilized bottles in dry seasons (January, 2020). Here, the sampling strategy follows the representativeness of the WW effluents enough to analyze the corresponding pollutant sources. The collected WW samples were transported to Arba Minch University, Department of Chemistry research laboratory for analysis and treatment. During sampling, preservation of samples is essential for controlling biological action, hydrolysis of chemical compounds and complexes, and reduction of volatility of constituents. Therefore, the WW sampling was performed by using the EPA, South Australia, WW sampling protocol standards [211].

3.3.3. Physico-chemical analysis of WW

The purpose of industrial WW analysis was to decide upon what physical, or chemical treatment should be given to make them suitable. Thus, the analysis of quality of WW is the prime consideration to assess its effect on the entire ecosystem. Firstly, the collected samples were filtered through filter paper (Whatman No 42, Diameter 125 mm) to remove large materials of the effluents. The filtrate was used to analyze the pH and conductivity in the field. The pH of the WW sample was measured by a potentiometric digital pH meter. Firstly, the instrument was calibrated with two standard buffer solutions of pH 4.0 and pH 9.0. The electrode was dipped into the solution whirled and paused up to one minute for stable reading. The reading performed after the indicated value remains fixed for about a minute. For electrical conductivity (EC) measurement a standard of a 0.1 N KCl solution was used to calibrate the cell. The cell was washed carefully with distilled water and wisely wipe with tissue paper. The cell was a dipped into the sample solution, twirled and paused up to one minute for steady reading. The reading was taken after the reading stayed fixed for about a minute. After this, the samples were transported to Arba Minch University, Department of Chemistry research laboratory for other parameter analysis and treatment. WW samples were

stored at 4 °C, while all physicochemical properties of WW samples were immediately processed or stabilized via freezing, according to established protocols [212].

In the laboratory, the previously filtrated and (pH and EC) measured sample was used to analyze the rest physicochemical parameters. The concentrations of Cl^- ions was determined using Mohr method, because it is a simple and inexpensive classical titration method, based on the reaction between chloride ions and standardized $AgNO_3$ solution, in presence of K_2CrO_4 as indicator. Both the total content of nitrogen (TN) was determined using persulphate digestion method [212]. The concentration (mgL^{-1}) of Mg (II) and Ca(II) ions in real WW was determined using flame photometry. The concentration (mgL^{-1}) of Cu(II), Cd(II), Cr(VI), and Pb(II) was determined using AAS.

3.3.4. Stock solutions of heavy metals and cationic dyes

The stock solutions of Pb(II), Cr(VI), Cu(II), and Cd(II), ions were prepared by dissolving $Pb(NO_3)_2$, $K_2Cr_2O_7$, $CuSO_4.5H_2O$, and $Cd_2(NO_3)$, respectively in 1000 mL volumetric flasks. The standard series of solutions for calibration curves of each metal ion was performed from the stock solution by dilution methods. Next to this, the WW sample was spiked with a suitable amount of $Pb(NO_3)_2$, $K_2Cr_2O_7$, $CuSO_4.5H_2O$ and $Cd_2(NO_3)$ standard solutions and reserved for the successive batch adsorption experiments.

For Methylene Blue (MB) dye stock solution preparation, the required amount of $C_{16}H_{18}ClN_3S{\cdot}3H_2O$ was dissolved in distilled water to prepare a solution of 1000 mgL^{-1}. Desired concentrations were then prepared from the stock solution. UV-Vis spectrometer was used to determine the dye concentrations of MB dye. The calibration curve was determined using the maximum absorbance at λ_{max} of 664 nm in the MB concentrations ranged from 10 - 40 mgL^{-1}. Here, the batch adsorption experiments were performed within 48 hours after immediate sampling.

3.3.5. Preparation of cellulose nanomaterials (CNMs)

3.3.4.1. Preparation of CNMs from the stems of *Erythrina brucei, Millettia ferruginea,* and Eichhornia crassipes

The collected plant and weed samples were washed with distilled water repeatedly until free of any dust particles; and then dried with air at room temperature. The dried samples were grinded into coarse particle using grinder. Then, the coarse particles were ready for cellulose extraction. Cellulose extractions was performed by mixing 10 g of coarse particles of each plant and weed samples and conjugated solvents of a 125 mL toluene and 75 mL ethanol in ratio for 48 hours at 50 ℃ in water bath. The extracted mixtures was washed with boiled water; filtrated and dried in oven at 50 ℃ for 10 hours. Then the obtained dried fibers were cut into short fibers. These short fibers were treated with 100 mL of 2.5 M NaOH solution at 50 ℃ for 3 hours to remove the lignin and hemicelluloses present in LCB. Afterwards, this mixture was washed well with deionized water repeatedly until it became neutral.

Thereafter, the neutral mixture was centrifuged, filtered and dried in an oven at 50 ℃ for 10 hours. Then the dried mixture was grinded into a pulp form and bleached with a ratio of 100 mL of sodium chlorite ($NaClO_2$) to 25 mL of glacial acetic acid (CH_3COOH) at 60 ◦C for 4 hours under mechanical stirring. This procedure was repeated with half of the initial amount of bleaching agent. In this second bleaching procedure, the insoluble micro crystallites remained after-bleaching treatment-stage, was washed in order to remove phenols and lignin. Then, this mixture was centrifuged, filtered and form cellulose suspension. After this, the cellulose suspension was hydrolyzed by 100 mL of 6 M H_2SO_4 for 2 hours to break up the cell wall and to separate the fibrils present for the production of cellulose nanomaterials (CNMs) suspension through sonication for 2 hours. Then the prepared CNMs suspension was centrifuged at 1600 rpm to separate the CNM from non-cellulose constituents and homogenized in homogenizer at 12,000 rpm for 2.5 h. Then washed, filtered and dried in oven at 50 ℃ for 10 hours. Finally, the prepared CNM was kept in suitable place for characterization purpose. This procedure was adapted from Abraham et al, [213] with

different parameter modification and the procedure was used throughout the experiments. The flow chart representation for the preparation of CNM is given in Figure 12.

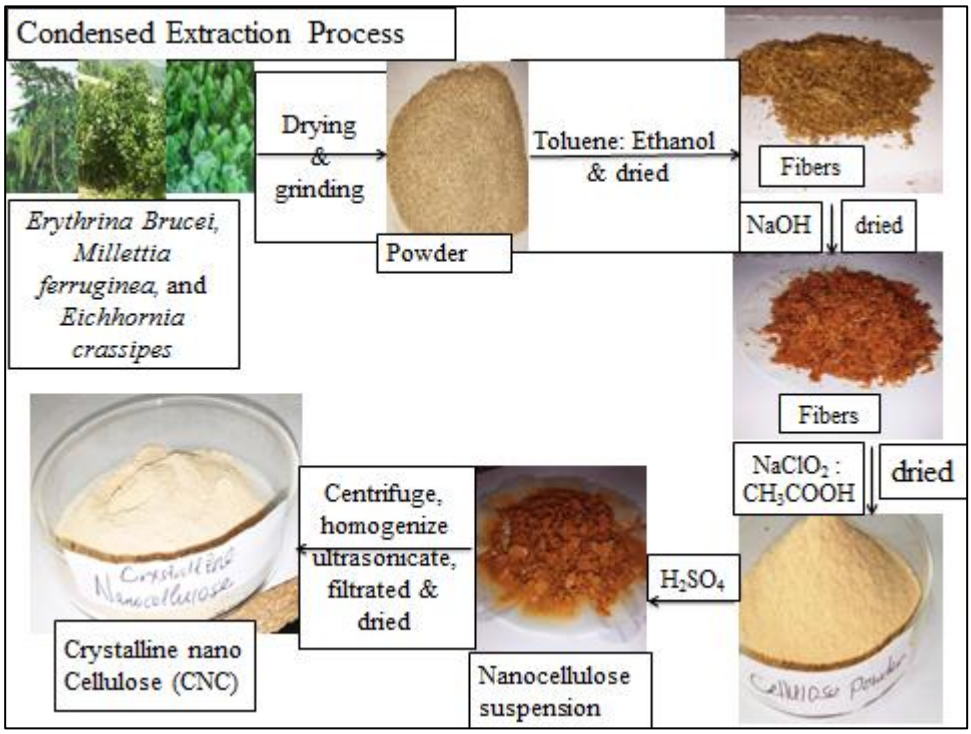

Figure 12. Flow chart representation for cellulose nanomaterials preparation from the stem of *Erythrina Brucei, Millettia ferruginea,* and *Eichhornia crassipes.*

3.3.5. Preparation of chemically modified CNMs:

3.3.5.1. Preparation of sodium periodate modified CNMs

The vicinal hydroxyl groups at carbon atoms number 2 and 3 in an anhydroglucose unit of cellulose was oxidized to two aldehyde groups through simultaneously breaking the carbon–carbon bond between the carbon atoms number 2 and 3 by using sodium periodate reagent (Figure 13). Therefore, sodium periodate is considered as specific oxidant for cellulose based materials. Thus, 0.2 gmL^{-1} of $NaIO_4$ was dissolved in approximately 2 wt% of CNM suspension in 250 mL flask. The light-induced decomposition of periodate was prevented by cautiously covering the flask with aluminum foil and agitated at 50 °C in the dark for 4 hours [41]. By the addition of 1 g ethylene glycol the excess oxidizing agents were consumed, and after 28 min the reaction was completed.

This procedure produces dialdehyde cellulose nanomaterial (DACNM) through centrifugation at 1600 rpm for 40 min and purified by successive water addition and centrifugation. This was sonicated for 30 min using a 24 kHz Sonicator. DACNM was separated by centrifugation at 1600 rpm at 20 °C and filtrated using filter paper no 42. Finally, it was dried in dark place in order to prevent any light induced photo decomposition. Then, it was stored under safe place for characterization purpose. The modification mechanism is given in Figure 13.

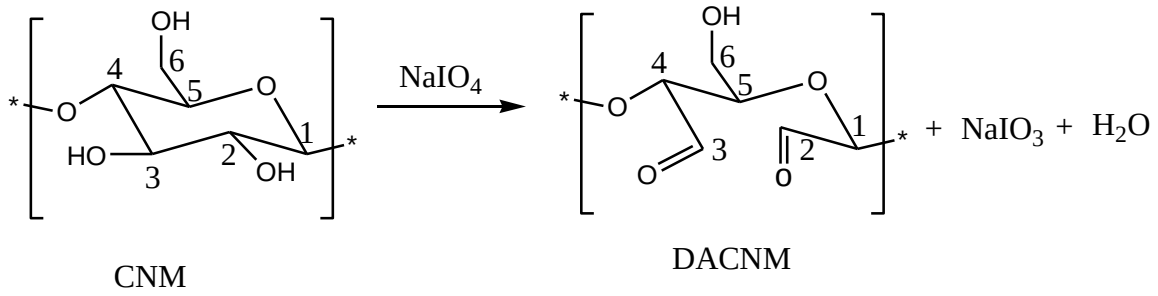

CNM DACNM

Figure 13. Sodium periodate oxidation of cellulose nanomaterial (CNM).

3.3.5.2. Preparation of succinic and maleic anhydride modified CNMs

A definite amount (30 g) of the early prepared CNM was treated with 0.20 L of NaOH solution (20 wt.%) at room temperature at least for 16 hours through magnetic stirring. The alkali-cellulose formed was separated from the solution using centrifuge and washed with distilled water down to neutral pH, filtered and dried. Then 20 g of the separated cellulose was reacted with 32 g of succinic anhydride for 24 hours. This CNM suspension was centrifugated and filtered, washed in sequence with dimethylformamide (DMF), ethanol 95%, distilled water, HNO_3 (0.01 $molL^{-1}$) and finally with acetone. In order to get carboxylate functional group for a better chelating function than the carboxylic group, succinylated celluloses were treated with a saturated sodium bicarbonate solution for 30 min under constant stirring and afterwards filtered, finally washed with distilled water and then acetone and dried in oven to yield S-CNM. This procedure was taken from study reported by Hokkanen et al., [189] on removal of heavy metals using succinic anhydride modified CNM with a slight modification.

About 10 g of CNM and 5 g of maleic anhydride were dissolved in 50 mL glacial acetic acid followed by 10 mL of ceric ammonium nitrate initiator (0.5 g of CAN in 10 mL of 1N nitric acid) was added to initiate the polymerization process in the above mixture. This mixture was then stirred well at 70 ℃ for 45 min and then poured into 200 mL of 10% NaOH solution to precipitate the graft copolymer. After this process is over the precipitated graft copolymer was filtered, washed and dried for 2 hours to form maleic anhydride cellulose material (MA-CNM). Afterwards the prepared S-CNM and MA-CNM adsorbents were ready for characterization and placed safe and clean place. The functionalization chemical reaction of succinic anhydride and maleic anhydride was represented in Figure 9 & 14, respectively.

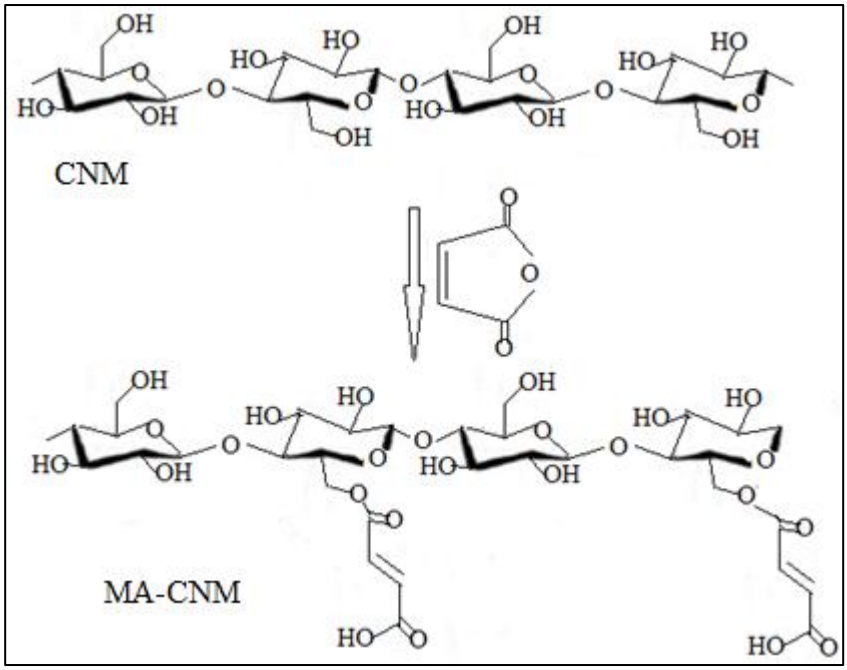

Figure 14. Functionalization reactions between CNM and maleic anhydride.

3.4. Characterization

3.4.1. Fourier transform infrared spectroscopy (FTIR)

In this study FTIR with 50 mg of KBr pelleting method was used to determine the functional groups of the synthesized pristine and chemically modified cellulose nanomaterials (CNMs). For this procedure, CNMs sample and KBr powder was careful dryied in order to minimize

the water content. Then, 5 g of the CNMs sample was taken and mixed with 50 g of KBr to form the pellets. The FTIR spectrum of CNMs was recorded at the wavenumber range of 4000 to 400 cm^{-1}.

3.4.2. X-ray diffraction (XRD)

Generally, XRD provides information regarding the crystalline structure, nature of the phase, lattice parameters and crystalline grain size. Specifically, in this study the crystallite size of the pristine and chemically modified CNMs adsorbents were characterized by using x-ray diffraction XRD with a Cu-Kα radiation (λ=0.154 nm) at 40 kV and 30 mA under a 2θ diffraction angle from 10° to 80° at a scan rate of 3°/min.

3.4.3. Scanning electron microscope (SEM)

Scanning electron microscope (SEM) is an important electron microscopy technique that is capable of achieving a detailed visual image of a particle with high-quality and spatial resolution. The working principle of SEM is given as the sample is exposed in SEM to the high-energy electron beam and gives information about topography, morphology, and composition. Thus, in this study the surface morphology of the pristine and chemically modified CNMs were examined using scanning electron microscope (SEM) with a beam of electrons in the range between 100-30,000 electron volts.

3.4.4. Thermogravimetric (TG) analysis with differential thermal (DT) analysis

Generally, thermogravimetric analysis with differential thermal analysis (TGA-DTA) deals with the branch of thermal analysis which determines the stability and carbon nature of adsorbent materials. Specifically, in this study thermogravimetric analysis with differential thermal analysis (TGA-DTA) with purge gas flow rate of 50 $mLmin^{-1}$, sample weight of 8.223 mg, and DTG-60H detector was used to determine the thermal stability and the carbon nature of the as-prepared pristine and chemically modified CNMs adsorbents.

3.4.5. Energy Dispersive X-Ray (EDX) Analysis

EDX is an analytical technique where a high-energy beam of charged particles or an X-ray is used to characterize a sample. Atoms within the sample contain ground-state electrons in discrete energy levels bound to the nucleus which, when excited by an outside source, can be ejected from their shells creating an electron hole. EDX is a particularly useful elemental analysis technique for the characterization of CNMs because it is often attached to SEM devices. Because of this, one can easily obtain the chemical composition of surfaces that are visually identified on the SEM.

3.5. Adsorption studies

All the adsorption studies were performed in Erlenmeyer flasks of 250 mL having suitable amount of adsorbent to adsorbate solutions. In the case of Cr(VI) ions adsorption, the adsorption process was performed mixing 0.3 g of CNM and S-CNM adsorbents and 2 mgL^{-1} of Cr(VI) ions solution together. Similarly, in the case of Cd(II) ions adsorption, the adsorption process was performed mixing 0.5 g of CNM and MA-CNM adsorbents and 20 mgL^{-1} of Cd(II) ions solution together. Pb(II) ions and cationic MB dye adsorption process also done by mixing 1 g of CNM and DACNM adsorbents and 30 mgL^{-1} of Pb(II) ions and cationic MB dye solution together. The pH of Cr(VI), Cd(II), Pb(II) ions, and cationic MB dye solution was adjusted using 0.1M HCl and 0.1 M NaOH solutions by using pH meter. Equilibration for all adsorption experiments were maintained after continuously shaking the mixture on the rotary shaker.

The absorbance measurement of each metal ions solution was done by atomic absorption spectrophotometer and cationic MB dye solutions was done by UV-visible spectrophotometer at a λ_{max} of 664 nm. All sample solutions containing more Cr(VI), Cd(II), Pb(II) ions, and cationic MB dye than the highest concentration that could be detected by the AAS and UV-Vis instruments were diluted and the dilution factor for each case was first corrected when calculating the results. These experiments were done by determining different parameters that were influencing the metal ions and cationic MB dye ions adsorbents adsorption capability

such as, solution pH, adsorbent dose, contact time, agitation speed and initial metal ions concentration for metal ions removal and initial MB dye solutions for MB dye removal.

The influence of each parameter on the pollutant uptake capability was carried out by keeping the rest parameters at optimum values. That is, solution pH ranged from 2-9, adsorbent dose ranged from 0.02-2.5 g, contact time ranged from 30-180 min, agitation speed ranged from 100-350 rpm and initial adsorbate concentration ranged from 0.5-4.5 mgL^{-1} for Cr(VI) ions. Also, the initial concentration of Cd(II) ions were ranged from 5 to 40 mgL^{-1}, adsorbent dose ranged from 0.04 to 1.5 g, contact time ranged from 30 to 150 min., solution pH ranged from 2 to 12. Similarly, the initial concentration of Pb(II) ions were ranged from 5 to 50 mgL^{-1}, adsorbent dose ranged from 0.01 to 2.5 g, contact time ranged from 30 to 180 min., solution pH ranged from 1 to 9 for Pb(II) ions. For the MB dye adsorption purposes, each parameter such as, pH, contact time and initial MB dye concentration was determined by keeping other parameters at optimum value. That is contact times ranged from 10 to 90 min., MB initial concentration ranged from 10 to 40 mgL^{-1}, adsorbent dose ranged from 0.4 to 2 g, and solution pH ranged from 3 to 10 by making other parameters at fixed manner. For all this experiments, the influence of temperature on adsorption efficiency was carried out by varying the temperature from 25 to 45 ℃ by keeping the remaining parameters constant. All adsorption processes was performed by covering each flask with aluminum foil in order to prevent the solution from any side reactions and after the reaction completion; it was carefully filtered with filtrate paper No 42.

3.5.1. Adsorption isotherms

Adsorption isotherms are mathematical models that describe the distribution of the adsorbate species among the liquid and solid phases based on a set of assumptions that are related to the heterogeneity or homogeneity of the solid surface, the type of coverage, and the possibility of interaction between the adsorbate species. The relation ship between adsorbates equilibrium concentration and equilibrium adsorption capacity of the adsorbent was determined by performing adsorption isotherm experiments. In order to construct adsorption isotherms for the adsorbents, experiments were carried out by varying the initial Cr(VI) ion concentration

from 0.5-4.5 mgL^{-1} and the (CNM & S-CNM) dose of 0.3 g for Cr(VI) adsorption. For Cd(II) ion adsorption, experiments were carried out by varying the initial Cd(II) ion concentration from 5 to 40 mgL^{-1} and the (CNM & MA-CNM) dose of 0.5 g. Similarly, for Pb(II) ion adsorption, experiments were carried out by varying the initial Pb(II) ion concentration from 5 to 50 mgL^{-1} and the (CNM & DACNM) dose of 1 g. Finally, for cationic MB dye adsorption experiments were carried out by varying the initial cationic MB dye concentration from 5 to 40 mgL^{-1} and the DACNM dose of 1 g. For each adsorbates adsorption the following optimum parameters were kept constant during the study: pH 5 in the case of Cr(VI), pH 8 in the case of Cd(II) and cationic MB, and pH 6 in the case of Pb(II); contact time 90 min. in the case of Cr(VI), 120 min. in the case of Cd(II) and Pb(II), 60 min. in the case of cationic MB dye. Then, the quantity of Cr(VI), Cd(II), Pb(II), ions, and cationic MB dye adsorption by using both adsorbents were carried out using Equation 13 and 14.

$$q_e = \frac{C_i adsorbate - C_e adsorbate}{S} \qquad (13)$$

$$q_t = \frac{C_i adsorbate - C_t adsorbate}{S} \qquad (14)$$

Where q_e and q_t are represents the equilibrium adsorbates concentration in mgg^{-1}. C_i and C_e are represents the initial and equilibrium concentration in mgL^{-1} of the pollutant ions in the WW sample, respectively, and C_t is the concentration in mgL^{-1} of pollutant ions in wastewater samples at a specified time. S represents the slurry dosage defined as the ratio between the mass of pristine and chemically modified CNMs adsorbents (g) to the initial volume of WW sample (L). Initial and equilibrium concentration were used to determine the percent pollutant ions removal and represented in Equation 15.

$$\%\ Removal = \frac{C_i adsorbate - C_e adsorbate}{C_i adsorbate}\ x\ 100\%\ [214] \qquad (15)$$

The adsorption isotherms including Langmuir and Freundlich were investigated and the appropriate model was selected. The correlation coefficient (R^2) was used to estimate the fitting of models between the experimental data.

3.5.1.1. Point of zero charge (PZC)

The point of zero charge experiments for each adsorbate adsorption processes were performed by using salt addition methods. Experiments were carried out taking the required amount of solutions with an initial pH ranging from 2.0 to 9.0. Then, 0.20 g of each adsorbent was added to 40.0 mL of 0.1 M $NaNO_3$ in 50 mL beaker. The pH was adjusted using 0.1 M NaOH and 0.1 M HCl. The suspensions were shaken for 120 min. in water bath at a shaking speed of 250 rpm to reach equilibrium. After this, the resulting pH was measured and the initial pH (pH_o) vs. the difference between the initial and final pH values (pH) was plotted. The PZC was taken as the point where pH = 0 and calculated using Equation 16:

$$\Delta pH = pH_1 - pH_2 \quad (16)$$

Where pH_1 is the pH value before the experiment and pH_2 is the pH value after the experiment. In the plot of ΔpH vs pH, the intersection points at which ΔpH = 0 specifies PZC.

3.5.2. The thermodynamic of adsorption

The thermodynamic study of the adsorption process was studied by investigating the basic thermodynamic parameters such as a change in Gibbs free energy (ΔG), change in enthalpy (ΔH), and change in entropy (ΔS) values [215-217]. Therefore, in order to determine the spontaneity and fevarability of the adsorption processes, all predetermined and optimized values of parameters (solution pH, sorbent dosage, contact time, agitation speed, and Pb(II), Cr(VI), Cd(II) ions, and cationic MB dye initial concentration) was used and the temperatures were varied from 20-45℃.

3.5.3. Kinetics of adsorption

The rate of Pb(II) ions, Cr(VI) ions, Cd(II) ions and MB dye adsorption mechanisms was conducted by using the contact time ranged from 30 to 180 min by putting all parameters such as, solution pH, sorbent dose, agitation speed and adsorbate initial concentration at optimum value.

3.6. Desorption studies

The release of adsorbates from the surface of adsorbents is termed as desorption. Desorption is an essential factor considered during determination of methods dependent on the principle of adsorption. Desorption activity is explained by the ratio between solid and liquid (S/L ratio) where the solid phase is the adsorbent on which adsorbates are adsorbed and the liquid phase is the desorbing eluent. Desorption helps in understanding the reusability of the biosorbents without any loss of effectiveness of the biosorbent. Also, desorption reduces the cost of the biosorption process due to the re-use of the sorbents. Different desorbents like acids, alkalis and alcohols are applied in removing the sorbates from the biosorbents [26].

In this study, 10 mL of 0.1 M HCl was used to desorb Cr(VI), Cd(II), and Pb(II) ions and cationic dye from S-CNM, MA-CNM, and DACNM adsorbents, respectively. This procedure was made by mixing the suitable amount of previously used adsorbents for adsorbates removal purpose with 10 mL of 0.1 M HCl through vigoursly shaking the mixture. In the case of Cr(VI) ions desorption, 0.3 g of S-CNM sorbent used before for adsorption of Cr(VI) ions from WW was mixed to a flask containing 10 mL of 0.1M HCl solution for 20 min. and then sonicated for 4 min. Next to this, the S-CNM sorbent was separated from the solution using centrifugation. The separated S-CNM sorbent was then washed with deionized water for four times, dried and ready for reuse as adsorbent. In the case of Cd(II) ions desorption, 0.5 g of MA-CNM adsorbent previously used for removing purpose was mixed with 10 mL of 0.1 M HCl solution and added to a 100 mL flask. Then, this mixture was sonicated and centrifuged to separate the adsorbent from the mixture. The separated MA-CNM sorbent was then washed with deionized water four times, filtered, and dried. In the case of Pb(II) ions desorption, 1 g of DACNM adsorbent previously used for removing purpose was mixed with 10 mL of 0.1 M HCl solution and added to a 100 mL flask. Then this mixture was stirred in an orbital shaker for 25 min. Thereafter, the DACNM sorbent was separated from the solution using centrifugation. In case of cationic MB dye desorption, 1 g DACNM adsorbent dosage was added into the saturated mixture and the mixture was shaken carefuly. Then, 10 mL of 0.1 M

HCl solution was added into the mixture and shaken by an orbital shaker for 60 min. After this, DACNM adsorbent was separated from the mixture and washed with deionized water.

3.7. Regeneration Test

Reuse of spent adsorbent materials after regeneration is an important requirement in industrial application for efluent treatment in order to reduce cost of operation by increasing amount of times an adsorbent can be used while recovering the adsorbate ions from the liquid [26]. Due to this reason, the chemical modified adsorbents, such as, S-CNM, MA-CNM, and DACNM from both adsorbents were selected for regeneration study. This is due to the higher, Cr(VI), Cd(II), Pb(II), and cationic MB dye uptake abilities, respectively. The previously regenerated adsorbents in desorption study was reused as adsorbents for the removal of adsorbates from wastewater until significant efficiecy loss is observed.

4. RESULTS AND DISCUSSION

4.1. Characterization

Different characterization techniques, such as, TGA-DTA, FTIR, XRD, SEM and EDX were performed to determine thermal stability, functional groups, crystallinity, surface morphology and elemental analysis, respectively, of both pristine and chemically modified CNMs adsorbents prepared from the *Erythrina Brucei* (EB) and *Millettia ferruginea* (MF) plants and *Eichhornia crassipes* (EC) weed samples. Specifically, the identification of functional groups of raw cellulose, CNM and chemically modified CNMs sorbents were carried out by the help of FT-IR spectroscopy technique. Figure 15a shows the FTIR spectra of raw cellulose prepared from *Erythrina Brucei* (EB), CNM, and DACNM adsorbents. Results show that samples indicate almost similar spectra presenting no changes in their chemical composition during the pretreatment processes for raw cellulose and CNM adsorbents, but a significant structural change observed on the DACNM. That means all samples have shown similar vibration spectra, namely at 3385, 2925, 1741, 1458, and 1058 cm^{-1} except DACNM adsorbent. The broad peaks at 3385 were related to the stretching vibrations of the O-H groups of cellulose [245]. The peak at 2925 cm^{-1} was attributed to the C–H stretching. The peaks detected at 1458 cm^{-1} are correlated to the C-C stretching and/or CH_2 symmetric bending in aromatic groups of cellulose I [218]. The peak at 1058 cm^{-1} was attributed to the stretching vibration of C–O–C pyranose ring (anti-symmetric in phase ring) stretching vibration [219].

Compared with the FTIR spectra of pristine CNMs, additional peaks observed in oxidized cellulose nanomaterial (DACNM) at 1730 cm^{-1}, referring to the stretching vibration of carbonyl group (C=O) for aldehyde due to the formation of aldehyde cellulose nanomaterial (DACNM) [220]. This result suggests sodium periodate efficaciously oxidizes the adjacent hydroxyl groups of cellulose at locations of carbon number 2 and 3 into aldehyde groups. This reaction occurs by concurrently breaking the corresponding carbon-carbon bond of the glucopyranose ring and produce DACNM.

In the same fashion, the FTIR spectra of raw cellulose prepared from *Millettia ferruginea* (MF), CNM and S-CNM adsorbents are presented in Figure 15(b). It has been reported that raw cellulose and CNM adsorbents shown the characteristic absorption peaks at 3372, 2931, 2850, 1741, 1637 and 1062 cm^{-1}. The broadened band at 3372 cm^{-1} is associated to the stretching vibration of hydroxyl groups and the band at 2931 cm^{-1} associated to the C–H stretching vibration. The peak at 1637 cm^{-1} relates to the bending vibration of the absorbed water [221]. The peak at 1062 cm^{-1} was attributed to the O–H bending vibration [222]. Compared to the raw cellulose and CNM adsorbents, the esterified cellulose nanomaterial (S-CNM) shows the additional peak at 1731 cm^{-1} which corresponds to the asymmetric and symmetric stretching of ester C=O functional groups in the spectrum of S-CNM [189]. Also the peak at 2850 cm^{-1} was attributed to the stretching vibration of carboxylic acid (-COOH) functional groups. The presence of this additional peak confirms the formation of esterification reaction between CNM and succinic anhydride. In addition to this, appearance of the peak at 1369 cm^{-1} related to the asymmetric and symmetric stretching vibrations of the ionic carboxylic groups. This indicates the formation of carboxylic groups on the surface of S-CNM [189]. Furthermore, the peak at 674 cm^{-1} related to ß-glycosidic links between the glucose units of cellulose. The presence of this band in the S-CNM adsorbents spectra is attention-grabbing, since it is suggestive that cellulosic material may have not been lost during the esterification [189].

Finally, the spectra of raw cellulose prepared from *Eichhornia crassipes*, CNM and MA-CNM sorbents prepared with the help of sulfuric acid hydrolysis obtained from the FTIR spectroscopy is shown in Figure 15c. The result shows that raw cellulose prepared from *Eichhornia crassipes*, CNM and MA-CNM displayes the representative broad band around 3355 cm^{-1} which corresponds to O-H free stretching vibration of the CH_2-OH structure on cellulose I and OH groups which resemble to intra and intermolecular hydrogen bonds existing in cellulose I and water absorbed [221]. The spectra located at 2925 cm^{-1} are as a result of C-H stretching vibration in cellulose I and the spectra found in zone four at 1735 cm^{-1} are recognized to the carbonyl functional groups of cellulose I in maleic anhydride cellulose nanomaterial (MA-CNM). The peaks detected at 1458 cm^{-1} are correlated to the C-C stretching and/or CH_2 symmetric bending in aromatic groups of cellulose I. The peak

located at 1058 cm^{-1} is connected to C-O-C stretching of cellulose I [219]. Compared with the spectra of raw cellulose prepared from *Eichhornia crassipes* and CNM adsorbents, the appearance of new strong band at 1593 cm^{-1} corresponding to the presence of C=C stretching of maleic anhydride molecule in MA-CNM confirmed the insertion of ester groups on the surface of CNC sorbent [193]. Furthermore, the spectra at 1265–1325 cm^{-1} are indications for the presence of C-O-C groups on the adsorbent. These tells maleic anhydride efficaciously oxidizes the adjacent hydroxyl groups of cellulose at locations of carbon number 2 and 3 into aldehyde groups, concurrently breaking the corresponding carbon-carbon bond of the glucopyranose ring in order to obtain maleic anhydride cellulose nanomaterial (MACNM).

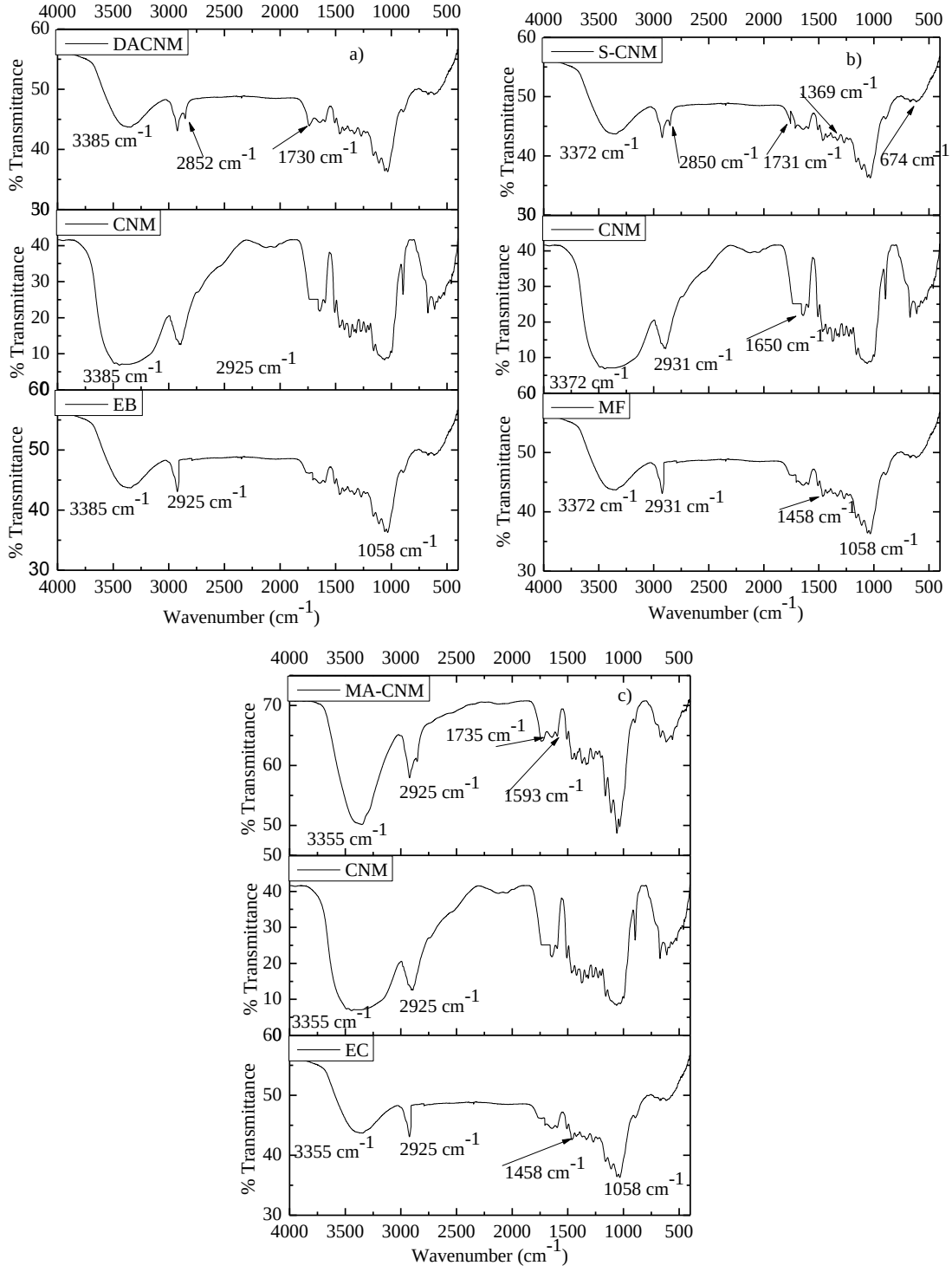

Figure 15. FT-IR Spectra of EB, CNM, & DACNM (a), MF, CNM, & S-CNM (b), and EC, CNM, & MA-CNM (c), respectively. Where EB, MF, & EC are raw cellulose prepared from *Erythrina Brucei*, *Millettia ferruginea* & *Eichhornia crassipes*, respectively.

The X-ray diffraction (XRD) pattern of (EB, CNM, and DACNM), (MF, CNM, and S-CNM), and (EC, CNM, and MA-CNM) as well as the cellulose I standard crystal from JCPDS No. 00-050-22411 for comparison purpose are depicted by Figure 16(a-c). The pattern evidently presented the amorphous and semi-crystalline nature because the adsorbent materials were prepared from polymeric materials. From the spectra, the main peaks observed at 15.35° and 22.48° have shown the representative cellulose-I structure and the crystals displayed the characteristic designation of (110) and (200) planes, respectively, for EB, CNM, and DACNM adsorbents (Figure 16a). This is because, these peaks are located in a similar position as the peaks of cellulose I standard crystal, 15.9° (110) and 22.6° (220). Furthermore, from these spectra, the average crystallite particle size was calculated using Debye Scherrer formula (Equation 17). The calculated value of the average crystallite sizes for raw cellulose prepared from EB, CNM, and DACNM adsorbents were found to be 2.69, 2.70, and 2.28 nm, respectively.

$$D_s = \frac{0.9\lambda}{\beta \cos\theta} \text{ [223]} \qquad (17)$$

Where, D_s is mean crystallite size (nm), λ wavelength of the incident radiation (λ = 0.15405 nm), β pure diffraction broadening (radians) and θ the Bragg angle (degrees, half-scattering angle). Usually β is taken as the full width at half maximum of the major diffraction band (FWHM).

In addition to this, the representative peaks at 16.16° and 22.24° for the oxidized nanocellulose (DACNM) was revealed a reduced degree of crystallinity than the EB and CNM adsorbents (Figure 15a). This is owing to the non-compact region of the crystalline part was oxidized progressively by the reaction of $NaIO_4$ chemicals with cellulose nanomaterial suspension [224]. Generally, from the spectra it can be seen that similar spectra observed for EB, CNM, and DACNM adsorbents at 2θ = 15.35°, 22.27°, and 34.41° which are represented to (110), (220), and (004) crystallographic planes of cellulose I, respectively [50]. This interpretation arises by observing the detected peaks that are located in similar position as the peaks of cellulose I standard crystal of 15.9° (110), 22.6° (200), and 34.6° (004) from JCPDS No. 00-050-22411.

Similarly, Figure 16b represents the X-ray diffraction (XRD) pattern of raw cellulose prepared from MF, CNMs, and S-CNM and the cellulose I standard crystal from JCPDS No. 00-050-22411 for comparison purpose. Results show that the peaks at 15.09^{o}, 22.50^{o}, and 34.50^{o} are the representative cellulose-I structure and the crystals displayed the characteristic designation of (110), (200), and (004) planes, respectively [40] as these peaks are located in a similar position as the peaks of cellulose I standard crystal, 15. 9^{o} (110) and 22.6^{o} (220), and 34.6^{o} (004) from JCPDS No. 00-050-22411. The crystallite size was calculated for adsorbents and the values were 2.73, 2.75, and 2.30 nm for raw cellulose prepared from MF, CNM, and S-CNM adsorbents, respectively. This result agrees with research reported by Andreas, et al. [225] on correlating cellulose nanocrystal particle size and surface area. The peaks generally, exhibited that a semi-crystalline with an amorphous widened hamp and crystalline bands. This is due to the fact that the sorbent materials were prepared from polymeric source materials, which clearly shows semi-crystalline nature. The crystallinity appears in the peaks probable due to the use of a chemical method (acid hydrolysis), which ultimately resulted in a loss of amorphous structure of the cellulose chain [226]. In comparison, the representative diffraction peaks found at 15.09° and 22.4° for the esterifiied cellulose nanomaterials (S-CNM) that exhibited a decreased degree of crystallinity than the raw CNM. This is because of the non-compact region of the crystalline parts that were transformed progressively with the addition of succinic anhydride into CNM suspension during the esterification process to form a carboxylate group (COO^{-}) on the surfaces of CNM.

Furthermore, Figure 16c represents the XRD pattern of raw cellulose prepared from EC, CNMs, and MA-CNM and the cellulose I standard crystal from JCPDS No. 00-050-22411 for comparison purposes. The crystallographic planes of cellulose I structure were certainly fixed to the peaks attributed at 2θ = 15.87°, 22.50° and 34.82° are (110), (220) and (004), respectively [222]. This is because these peaks are located in a similar peak position as the peaks of cellulose I standard crystal, 15.9° (110), 22.6^{o} (220), and 34.6^{o} (004) from JCPDS No. 00-050-22411. From the XRD patterns, the raw cellulose and CNM adsorbents have the same peaks to that of the esterified (MA-CNM) except the increased degree of crystallinity for the raw cellulose and CNM adsorbents. The average crystallite particle sizes of raw cellulose, CNM, and MA-CNM adsorbents were calculated by using Equation 17 and their

values are 2.83, 2.71, and 2.25 nm, respectively. Even though, the increased degree of crystallinity possessed by the raw cellulose and CNM adsorbents, all adsorbents undoubtedly displayed the semi-crystalline nature because *Eichhornia crassipes* material is polymeric material. The diffractogram of raw cellulose, CNM, and MA-CNM adsorbents have an obvious sharp band focused at 22.50° which is attributed to the semi-crystalline structure of the cellulose-based adsorbents. The functionalized nanocellulose exhibited the reduced percent of crystallinity and broad peak than the raw cellulose and CNM adsorbents because of the oxidation of the crystalline region by the addition of maleic anhydride into the raw nanocellulose suspension [193].

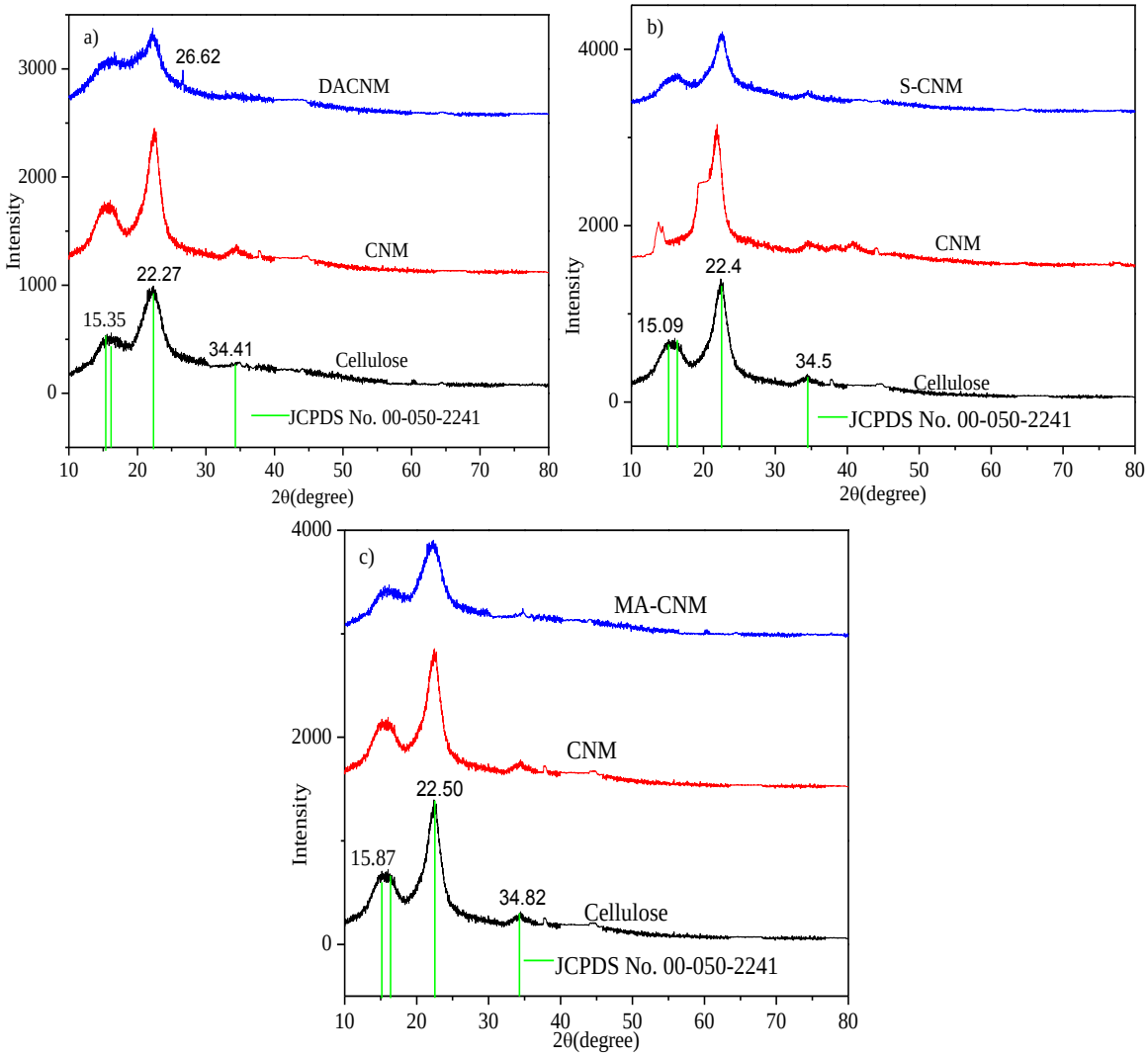

Figure 16. XRD Spectra of EB, CNM, & DACNM (a), MF, CNM, & S-CNM (b), and EC, CNM, & MA-CNM (c), respectively.

SEM characterization was carried out to give information about the surface morphology and microstructure of prestine CNM and chemically modified CNM adsorbents prepared from lignocellulosic biomass. Figure 17 shows the SEM image of cellulose prepared from (EB, CNM, & DACNM), (MF, CNM, & S-CNM), and (EC, CNM, & MA-CNM) adsorbents, respectively. From the SEM images it is possible to predict that the shape of the adsorbents as plate like for EB, plate like with elongated morphology and fibrous for CNM, and plate like and rod like structures with less distinct morphology for DACNM. Also, the shape of MF was flake like and a rod, the shape of CNM was flake like, and the shape of S-CNM was not clearly showed. Similarly, the shape of EC was flake like, the shape of CNM was flake like with associated rod like structure, and the shape of MA-CNM was fibrous structure. Furthermore, from these pridictions the chemically modified CNM adsorbents have shown probabllity to agglomerate in comparison with the pristine CNM adsorbent after drying. Addition of reagents such as, $NaIO_4$, succinic anhydride and maleic anhydride to CNM suspension during the oxidation process initially degrades the amorphous regions of modified CNM and the progressive oxidation reaction takes place into crystalline regions. Finally, aldehyde and carboxyl groups gained from the oxidation reaction were added to the hydroxyl groups to yield dialdehyde cellulose and carboxyl functional group containing CNMs [227]. These variations in biochemical arrangements also caused the variations in surfaces of the modified CNM [228,229].

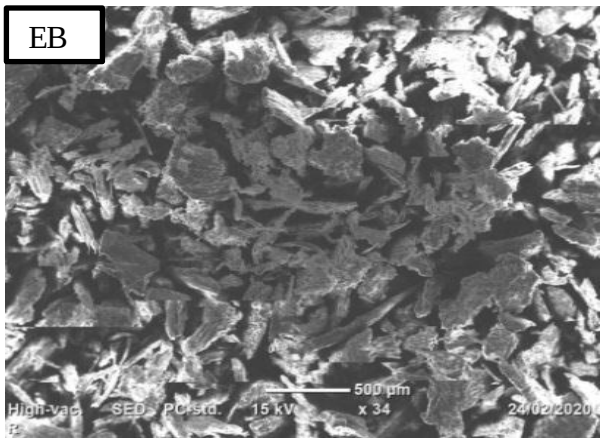
EB
500 µm
High-vac. SED PC-std. 15 kV x 34 24/02/2020

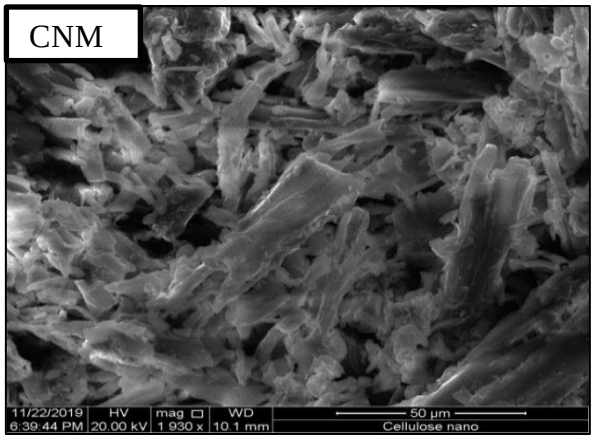
CNM
11/22/2019 6:39:44 PM
HV 20.00 kV
mag 1 930 x
WD 10.1 mm
50 µm
Cellulose nano

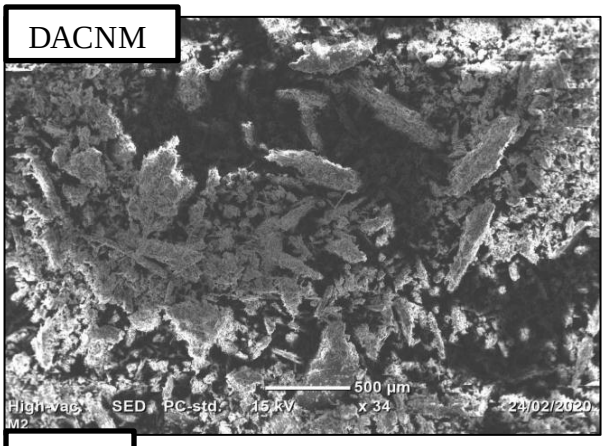
DACNM
500 µm
High-vac. SED PC-std. 15 kV x 34 24/02/2020

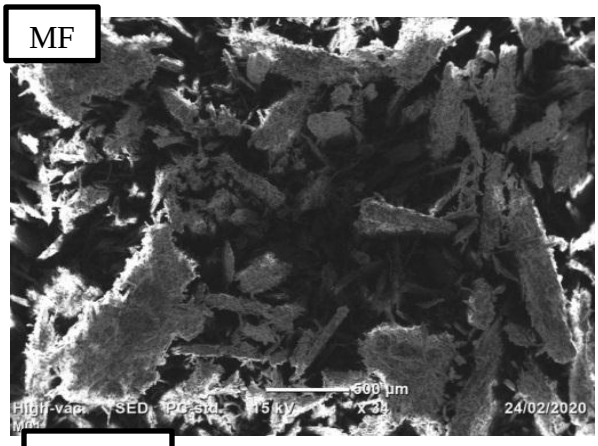
MF
500 µm
High-vac. SED PC-std. 15 kV x 34 24/02/2020

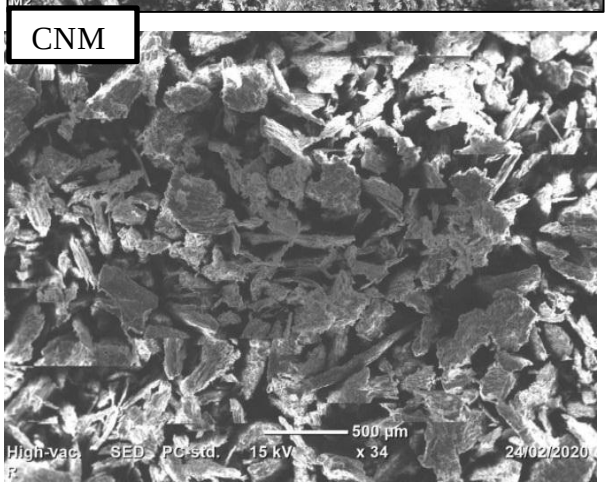
CNM
500 µm
High-vac. SED PC-std. 15 kV x 34 24/02/2020

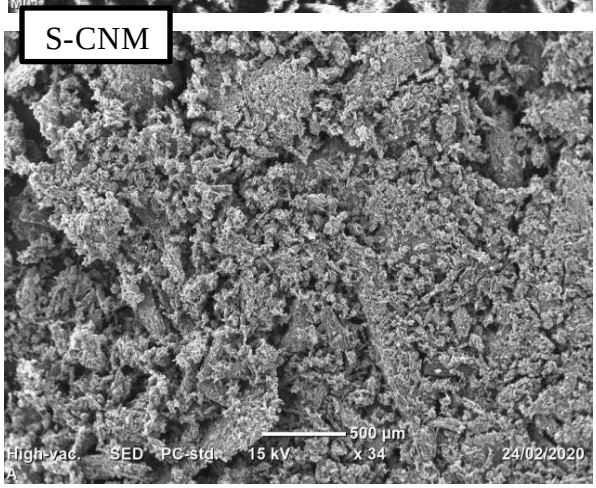
S-CNM
500 µm
High-vac. SED PC-std. 15 kV x 34 24/02/2020

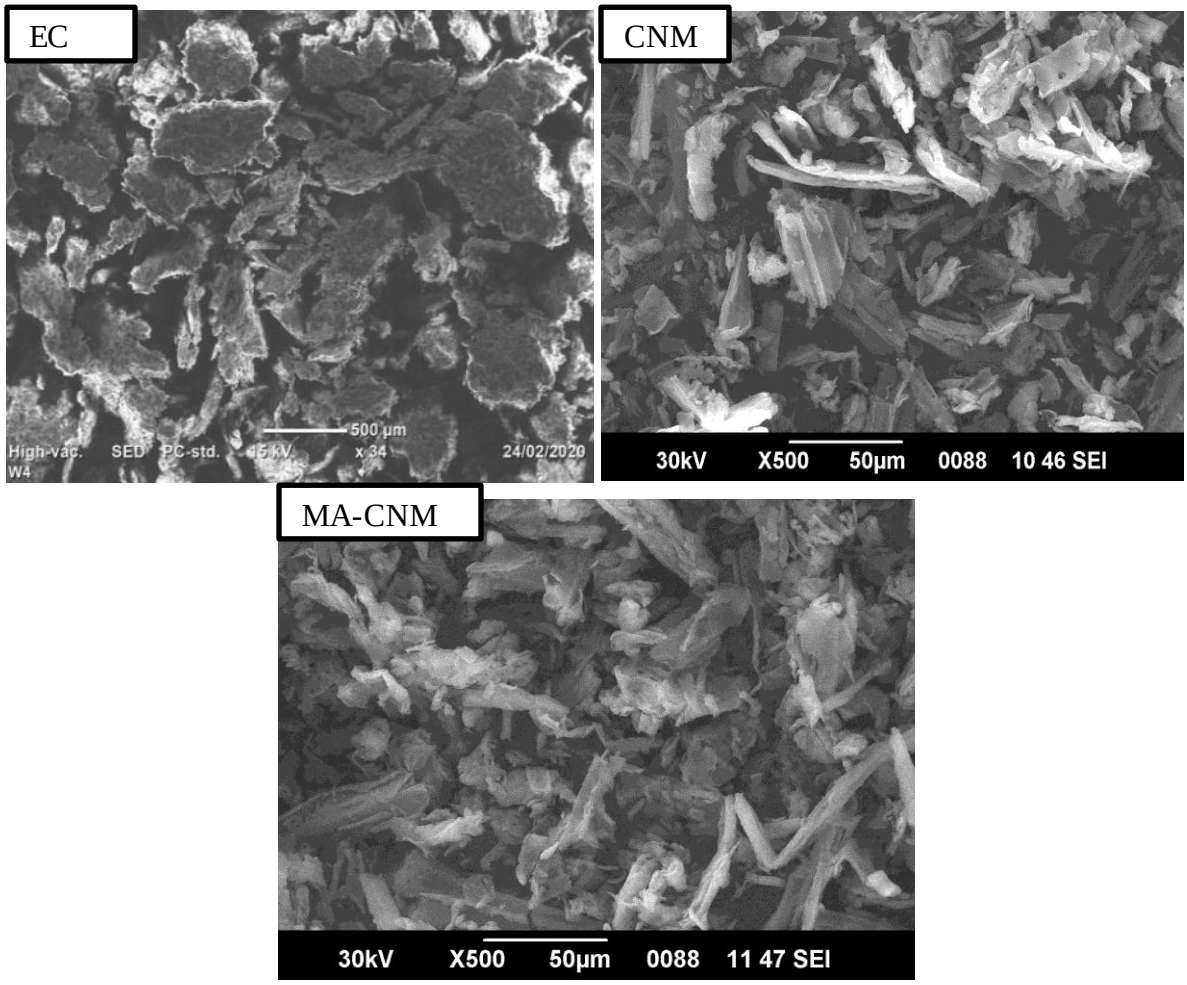

Figure 17. SEM images of cellulose prepared from (EB, CNM, & DACNM), (MF, CNM, & S-CNM), and (EC, CNM, & MA-CNM) adsorbents, respectively.

The elemental analyses of the pristine and chemically modified adsorbents were done by using EDX analysis. The EDX spectrum shown in Figure 18(a & b) exhibited the peaks for carbon, oxygen, chlorine and sulfur corresponding to their atomic weights, respectively. The pristine CNM adsorbent was observed to contain the elements such as carbon, oxygen, chlorine, sufur, silcon and phosphorous with their respective composition: carbon 52.68%, oxygen 44.65%, chlorine 2.16%, sulfur 0.21%, silicon 0.18% and phosphorus 0.12%. The chemically modified adsorbent contain relatively increased oxygen wt% than carbon as shown in Figure 18(a & b). This variation is due to the functionalization of cellulose suspension with oxygen bearing reagents.

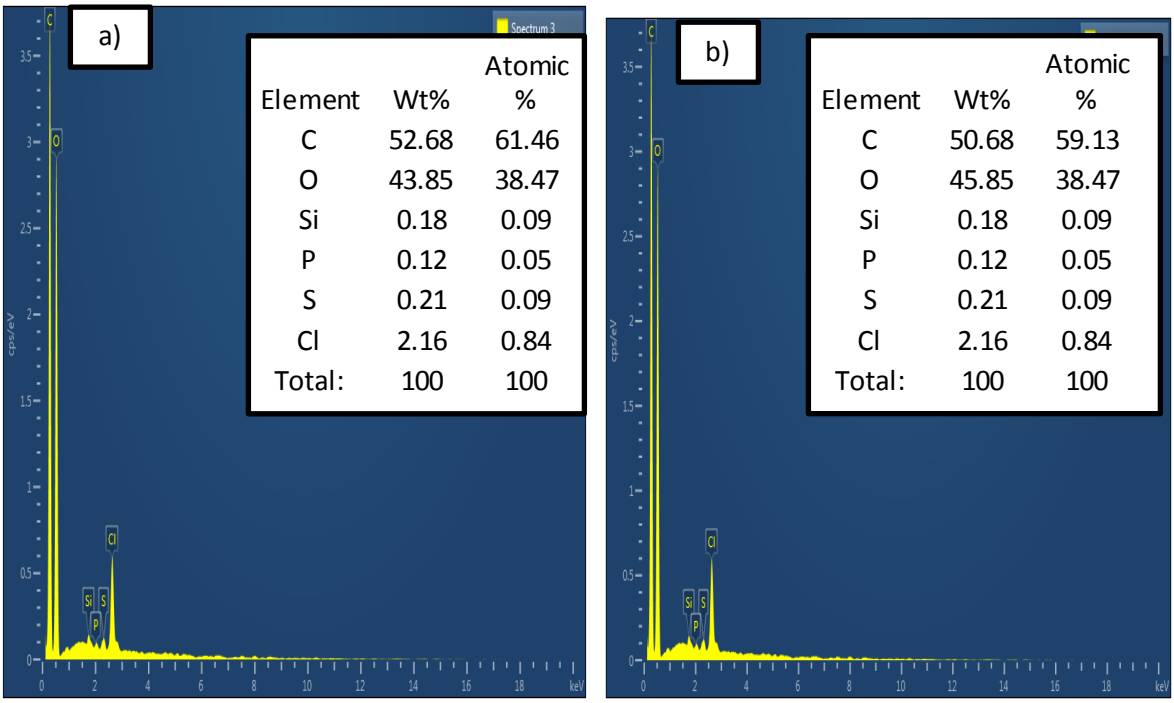

Figure 18. EDX analysis of pristine CNM (a) and chemically modified (C-CNM) (b), respectively.

The thermogravimetric analyses with derivative thermal analysis (TGA-DTA) behaviors of the adsorbents were presented in Figure 19 (a&b), respectively. Analyses of samples revealed that the TGA curves illustrated three phases of decompositions and indicated in Figure 19a. Initially 10% of mass loss in the temperature range 40–83.03 °C was attributed to the vaporization of absorbed water and decomposition of cellulose nanomaterials. In the second phase, almost 48.853% of mass loss was observed in the temperature range 252.25–385.309 °C attributed to the scission of cellulose structure and chain thereby release of CO, CO_2 and carbonaceous residues were formed [230]. The third phase which occurred after 500 °C, demonstrated a very slow mass loss of about 14.097%, was revealed the decomposition of residual substances due to the oxidation of char. While the DTA curves in Figure 19b determined the thermal decomposition peaks of the maximum weight loss as 411.22 °C and 397.17 °C for CNM and C-CNM, respectively. In addition to this, the initiating temperature of degradation for C-CNM was slightly lower than that of CNM, which is may be expected as the periodate oxidation disrupts the ordered bonding of the highly crystalline CNM [231]. In general, a slight shift of C-CNM curves for both TGA and DTA was possibly attributed due to

the addition of carbonyl, carboxyl, and ester bearing modifiers on the backbone of CNM adsorbent. This increases the hydrophilicity of C-CNM and induces a lower thermal decomposition temperature for C-CNM adsorbent [47].

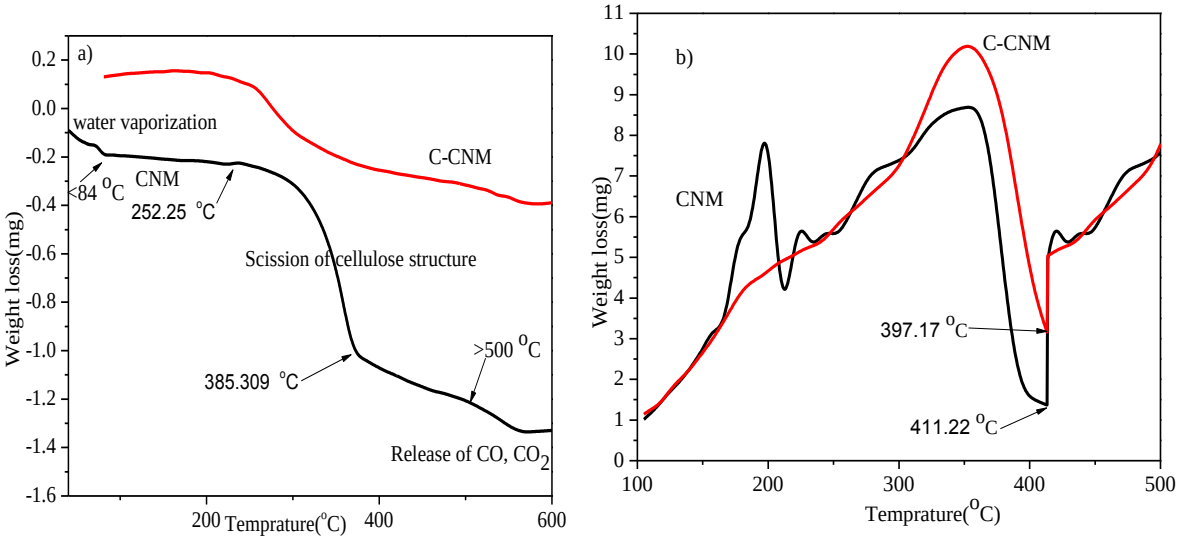

Figure 19(a&b). TGA and DTA analysis of pristine CNM and chemically modified CNM adsorbents, respectively.

4.2. Physicochemical Properties of the WW

Table 4 displays the values for the physicochemical analysis of the tannery wastewater (WW) samples. The analysis was carried out in triplicate and reported as the average amount of each parameter. From the pH values the finding suggests that the WW sample taken from the run of Modjo River was nearly acidic. The findings have showed that there are certain amounts of ions present in the wastewater and negatively affect the %R of Cr^{6+}, Cd^{2+}, Pb^{2+} ions from WW. In addition, it is believed that the presence of ammonia nitrogen element exhibit complexation affinity for all the studied metals under the conditions that reduce the %R of Cr^{6+}, Cd^{2+}, Pb^{2+} ions from WW at high ammonium ion concentration. Thus, physicochemical analysis of WW sample before adsorption helps to understand whether the presence of matrix components affects the %R of Cr^{6+}, Cd^{2+}, Pb^{2+} from real WW samples or not. From the whole results, it is possible to concluded that the presence of competing ions in the real WW was negatively affected the %R of Cr^{6+}, Cd^{2+}, Pb^{2+} from real WW samples. This is because

most of the calculated mean values for each parameter were greater than the standard provisional limit values provided by WHO [120].

Table 4. Physico-chemical properties of the WW collected from the run of Modjo River (for tannery waste water).

Parameter	**Lowest value**	**Maximum value**	**Average**	**WHO Limit [96,97,120]**
pH	4.8 ± 0.03	6.0 ± 0.03	5.3 ± 0.03	6–9.0
EC(µS cm^{-1})	250± 0.5	270± 0.5	260± 0.5	0.288
NH_4^+(mgL^{-1})	3.5 ± 0.04	5.9 ± 0.04	9.4 ± 0.04	<2
Cu^{2+} (mgL^{-1})	0.26 ± 0.03	0.54 ± 0.03	0.40 ± 0.03	2
Cl^- (mgL^{-1})	36.9 ± 0.02	45.5 ± 0.02	42.3 ± 0.02	<350

4.3. Adsorption of Heavy Metal Ions

An optimum parameter is essentially required to maximize the interactions between heavy metal ions and adsorption sites of the adsorbents in the solution [39]. In the case of Pb(II) adsorption, for an optimum CNM and DACNM adsorbents dose evaluation 0.01 to 2.5 g of CNM and DACNM adsorbents were added to 100.0 mL of wastewater spiked with 30.0 mgL^{-1} Pb(II) solution through shaking. Also, for an optimum contact time evaluation 1 g of CNM and DACNM adsorbents were added to 100.0 mL of wastewater spiked with 30.0 mgL^{-1} Pb(II) solution through shaking by orbital shaker for contact time of 30 to 180 min. Similarly, 1 g of CNM and DACNM adsorbents were added to 100.0 mL of wastewater spiked with 30.0 mgL^{-1} Pb(II) solution through shaking by orbital shaker for solution pH of 1 to 9.

In the case of Cd(II) adsorption, for an optimum CNM and MA-CNM adsorbents dose evaluation 0.04 to 1.5 g of CNM and MA-CNM adsorbents were added to 100.0 mL of wastewater spiked with 20.0 mgL^{-1} Cd(II) solution through shaking by orbital shaker. Also, for an optimum contact time evaluation 0.5 g of CNM and MA-CNM adsorbents were added to 100.0 mL of wastewater spiked with 20.0 mgL^{-1} Cd(II) solution through shaking by orbital

shaker for contact time of 30 to 180 min. Similarly, 0.5 g of CNM and MA-CNM adsorbents were added to 100.0 mL of wastewater spiked with 20.0 mgL^{-1} Cd(II) solution through shaking by orbital shaker for solution pH of 2 to 12 for solution pH optimization.

In the case of Cr(VI) adsorption, for an optimum CNM and S-CNM adsorbents dose evaluation 0.02 to 2.5 g of CNM and S-CNM adsorbents were added to 100.0 mL of wastewater spiked with 2.0 mgL^{-1} Cr(VI) solution through shaking by orbital shaker. Also, for an optimum contact time evaluation 0.3 g of CNM and S-CNM adsorbents were added to 100.0 mL of wastewater spiked with 20.0 mgL^{-1} Cr(VI) solution through shaking by orbital shaker for contact time of 30 to 180 min. Similarly, 0.3 g of CNM and S-CNM adsorbents were added to 100.0 mL of wastewater spiked with 2.0 mgL^{-1} Cr(VI) solution through shaking by orbital shaker for solution pH of 2 to 9 for solution pH optimization.

4.3.1. Effect of contact times

The effects of contact time on the adsorption of Cr(VI), Cd(II) and Pb(II) ions from wastewater was conducted by varying the contact times ranged from 30-180 min at optimized agitation speed of 300 rpm, adsorbent dose of 0.3 g, temperature (T) of 25 °C, and concentrations (C_i) of Cr(VI) ions of 2 mg L^{-1} for Cr(VI) adsorption. Similarly, at optimum adsorbent dose of 0.5 g, temperature (T) of 25 °C, agitation speed of 250 rpm, and initial concentration (C_i) of 20 mg L^{-1} for Cd(II) adsorption. Also, at optimum adsorbent dose of 1 g, temperature (T) of 25 °C, agitation speed of 250 rpm, and initial concentration (C_i) of 30 mg L^{-1} was used for Pb(II) adsorption (as shown in Figure 20(a & b). For all studied metals the adsorption pattern showed fast adsorption kinetics up to an optimum time followed by slow sorption kinetics. This fast kinetics observed due to the presence of greater number of hydroxyl groups on the surface of CNMs adsorbents and after the optimum time the slow process is because of saturation of available active sites on CNMs adsorbents with heavy metal ions after the optimum time [232]. Specifically, in the case of Cr(VI) ions removal, the increasing trends were observed by increasing the contact time from 30 to 90 min for both CNM and S-CNM adsorbents because of the presence of active sites available in this short period of time [232]. The higher % removal (%R) of Cr(VI) ions (64.25 and 90.9%) was

detected at the optimum time of 90 min for CNM and S-CNM adsorbents, respectively. After this, the removal processes reaches at equilibrium and proceed with a constant amount. Furthermore, the greater Cr(VI) ions uptake capabilities were detected for S-CNM adsorbent than CNM due to the presence of numerous active sites which easily bind the Cr(VI) ions onto the surfaces possessing a large number of reactive carboxyl groups resulted from succinic anhydride modified reaction. This result agrees with previous researches reported by Hu *et al.* [194] on the removal of Cu(II), Cd(II), Pb(II) from aqueous solutions using pineapple peel fibers modified with succinic anhydride adsorbent.

The results shown that the Cd(II) ions removal capacity increases by increasing the contact time from 30 to 120 min for both CNM and MA-CNM sorbents because of the excess active sites are available on the surfaces of CNM and MA-CNM sorbents and remains unchanged after this optimum time [233]. This was because with increased contact time the ratio of surface active sites to the total metal ions in the solution was low and hence all active sites had metal ions in solution and had occupied [234]. The maximum %R of Cd(II) ions of 67.80 and 88.84% was observed at the optimum time of 120 min for CNM and MA-CNM adsorbents, respectively. Next to this optimum contact time, the Cd(II) ions removal processes remains unchanged. In comparisons of MA-CNM sorbent with CNM, the maximum Cd(II) ions uptake capabilities were observed for MA-CNM sorbent than CNM because of the increased number of active sites resulted from esterification reaction of maleic anhydride. This result was in agreement with researches reported by Madivoli et al. [234] on adsorption of heavy metals using modified nanocellulose.

The %R of Pb(II) ions for CNM and DACNM adsorbents were raised with rising the time up to 120 min, due to the presence of high active sites on the surfaces of the adsorbent [59]. The maximum %R of Pb(II) ions was observed to be 72.55% and 96.8% for CNM and DACNM adsorbents respectively. After this, the %R processes become at equilibrium and proceed with a fixed manner. The maximum adsorption capacity was detected for DACNM adsorbent than CNM adsorbent mainly due to the presence of oxygen bearing aldehyde carbonyl groups and carboxylate groups.

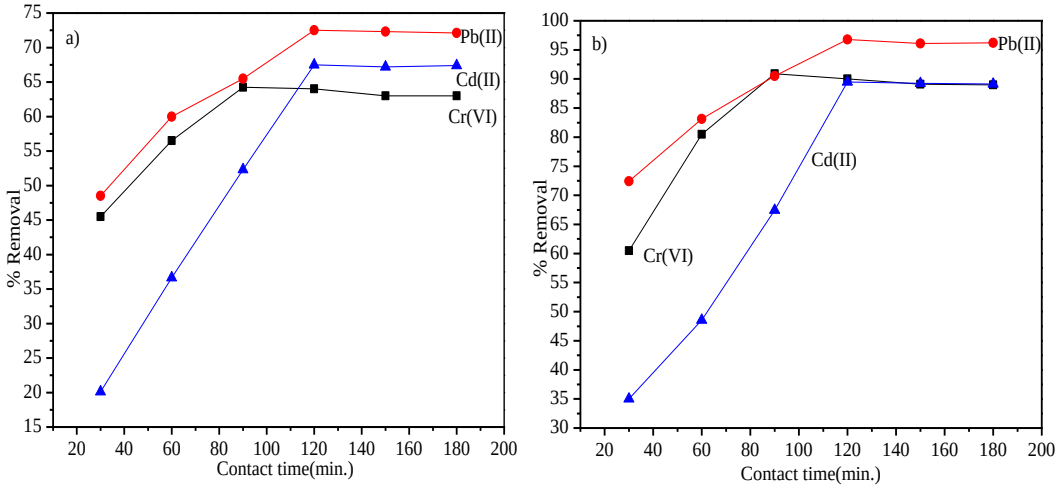

Figure 20. The effect of contact times on the removal of Cr(VI), Cd(II) and Pb(II) ions by CNM (a) and S-CNM, MA-CNM and DACNM (b) respectively, at optimum pH of (5, 8, & 6), dose of (0.3, 0.5, & 1 g), room temperature, C_i of (2, 20, & 30 mgL^{-1}), and agitation speed of (300, 250, & 250 rpm).

4.3.2. Effect of initial concentration

The effect of Cr(VI), Cd(II) and Pb(II) ions initial concentration on the %R of Cr(VI), Cd(II) and Pb(II) ions from wastewater are presented in Figure 21(a&b) by pristine and chemically modified CNMs. In all cases, initially the %R of Cr(VI), Cd(II) and Pb(II) ions were increased upto the optimum initial concentration values and beyond this value it becames fixed. This observation was may be the greater number of heavy metal ions in solution than the number of the active sites in the surface of adsorbents [235]. Specifically, in the case of Cr(VI) ions removal, the removal processes proceed quickly and reaches the optimum value of 2 mgL^{-1}. The observed sharp increase in removal processes at low initial concentration was because of the presence of large unoccupied sites on the CNM and S-CNM adsorbents resulted from greater number of hydroxyl functional groups on the surface of the adsorbents. At this initial optimum initial concentration value, both adsorbents clearly displayed higher Cr(VI) ions adsorption capability. In addition to this, the higher adsorption capability of S-CNM adsorbent is obviously perceived compared to CNM adsorption capability. This is due to the presence of carbonyl, carboxyl, and ester functional groups in addition to the hydroxyl

functional groups on the surface of S-CNM adsorbent resulted from the grafting of succinic anhydride on the surface of CNMs [235].

In similar fashion, the Cd(II) ions removal process increases upto the optimum value of 20 mg/L. Initially, the ratio of surface active sites to the total metal ions in the solution was high and hence all Cd(II) ions are attracted to the surfaces of CNM and MA-CNM adsorbents [193]. At the optimum initial Cd(II) ions concentration of 20 mgL^{-1}, both adsorbents clearly displayed higher %R of 64.91 and 88.44 of Cd (II) ions from wastewater on to CNM and MA-CNM adsorbents, respectively. Compared to pristine CNM adsorbent, MA-CNM adsorbent has the higher removal capability of Cd(II) ions due to the presence of carbonyl, carboxyl, and ester functional groups in addition to the hydroxyl functional groups on the surface of MA-CNM adsorbent resulted from the grafting of maleic anhydride on the surface of CNMs [236]. Beyond the optimum value, the percentage of adsorption is almost constant indicating the greater number of Cd(II) ions in solution than the number of active sites on the adsorbent surfaces.

Furthermore, results from the Pb(II) ions adsorption process revealed that the uptake process was very fast initially. This fast removal processes, at low initial concentration of Pb(II) was due to the presence of large vacant surface area of the CNM and DACNM sorbents. At increased C_i, the removal ability gradually increases and move toward the optimum value at C_i of 30 mgL^{-1}. At this point, both adsorbents evidently displayed maximum Pb(II) ions uptake ability. In comparision, the DACNM adsorbent indicated the %R of Pb(II) ions than pristine CNM adsorbent. This is due to the presence of carbonyl functional groups in addition to the hydroxyl functional groups on the surface of DACNM adsorbent resulted from the grafting of $NaIO_4$ on the surface of CNMs. Supporting this result, Chen et al. [237] reported on the removal of As(III) by nanostructured dialdehyde cellulose−cysteine microscale and nanoscale fibers.

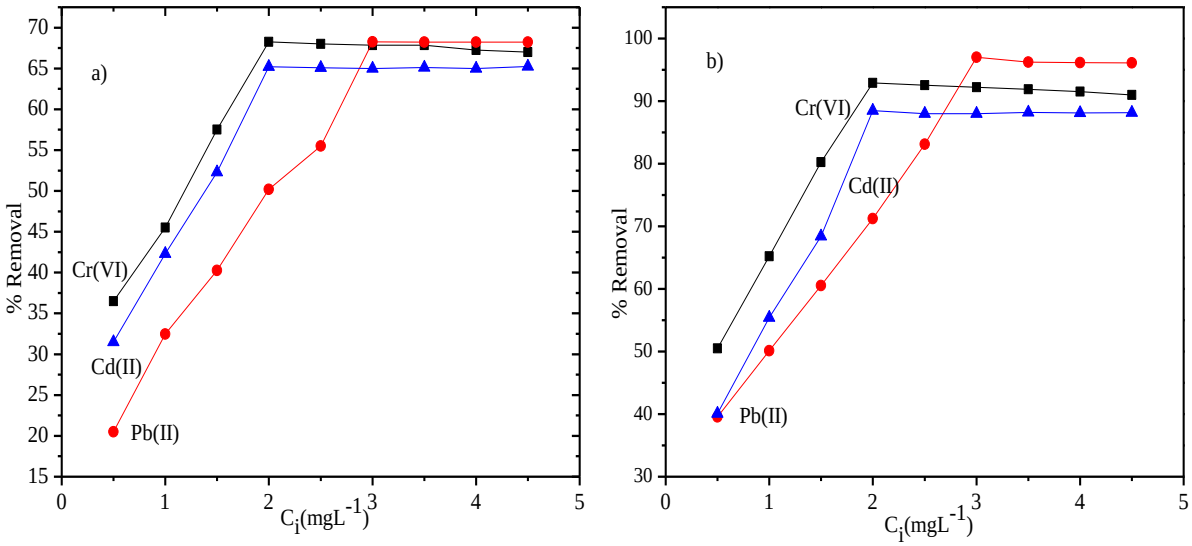

Figure 21. The effect of Ci on the removal of Cr(VI), Cd(II) and Pb(II) ions by CNM (a) and S-CNM, MA-CNM and DACNM (b) respectively, at optimum pH of (5, 8, & 6), dose of (0.3, 0.5, & 1 g), room temperature, contact time of (90,120,&120 min.), and agitation speed of (300, 250, & 250 rpm).

4.3.3. Effect of adsorbent dose

Figure 22 (a,b&c) indicates the consequences of pristine and chemically modified CNMs dosage on the (%R) of Cr(VI), Cd(II) and Pb(II) ions from the WW. Findings indicated that 61.3 and 90.25% of Cr(VI) ions can be eradicated from wastewater by using both CNM and S-CNM adsorbents represents with optimum adsorbent dosage of 0.3 g at 25 °C. The higher %R (90.25%) of Cr(VI) ions was observed by using S-CNM adsorbent than CNM because of the presence of extra ester and carboxyl groups to the surface of CNM. These extra functional groups resulted from the addition of succinic anhydride to CNM provide fresh and active sites for the functionalized adsorbent. The resulted fresh and active sites lead to the increased adsorption of Cr(VI) ions from WW. On the whole, it can be summarized that for both adsorbents, the % R of Cr(VI) ions was increased by increasing the adsorbents dosage up to the optimum values and then remains constant for the increment of dosage beyond the optimum value (0.3 g). This is anticipated because of the fact that, beyond this optimum adsorbents dose, the number of of ions bonded to the adsorbents and the nuber of mobile ions

in the wastewater becomes constant even with extra addition of the adsorbents dose [238,239].

Results exhibited that the increased trends of Pb(II) ions removal for both CNM and DACNM sorbents at the starting point. This trend is in agreement with research works reported by Alipour et al. [240] for Pb(II) ions removal using thiourea- functionalized magnetic ZnO/nanocellulose composite. Also the results indicated that, 97.8% of Pb(II) ions can be removed from wastewater by DACNM sorbent with optimum sorbent dosage of 1 g at 25 °C. Whereas, 72.5% of Pb(II) ions can be removed from wastewater by using CNM adsorbents with optimum sorbent dosage of 1 g at 25 °C. The increased %R of Pb(II) ions by DACNM sorbent was due to the presence of aldehyde carbonyl functional groups in addition to the hydroxyl functional groups on the surface of DACNM adsorbent resulted from the grafting of $NaIO_4$ on the surface of CNMs [237].

On the whole, it can be summarized that for both adsorbents the %R of Pb(II) ions increased by increasing the adsorbents dosage to optimum values and after that value the removal ability decreases. This is anticipated because of the fact that at increased concentrations of sorbents, maximum availability of replaceable surfaces for the ions. However, at further increased concentrations there is no further increase in adsorption owing to the quantity of ions bonded to the adsorbent and the quantity of mobile ions in the wastewater becomes fixed even with extra addition of the adsorbents dose [241].

Findings for Cd(II) ions removal indicated that the adsorption efficiency was increased with increase in CNM and MA-CNM adsorbents dose. This publicized that the uptake sites becomes unsaturated during the adsorption reaction, whereas the number of active surface areas available for adsorption site increased by increasing the CNM and MA-CNM adsorbents dose. The maximum %R of 70.3% and 90.4% was observed at optimum CNM and MA-CNM adsorbents dose of 0.5 g and optimum temperature of 20 °C, respectively. After this dose, the removal processes become unchanged due to the particle aggregation, which would lead to a decrease in total surface area of the adsorbent [242]. The higher %R (90.4%) of Cd(II) ions observed by using functionalized adsorbent was due to the insertion of ester and carboxyl

groups onto the surfaces of CNM lead to fresh and active sites for the Cd(II) ions uptake relative to non-functionalized adsorbent material.

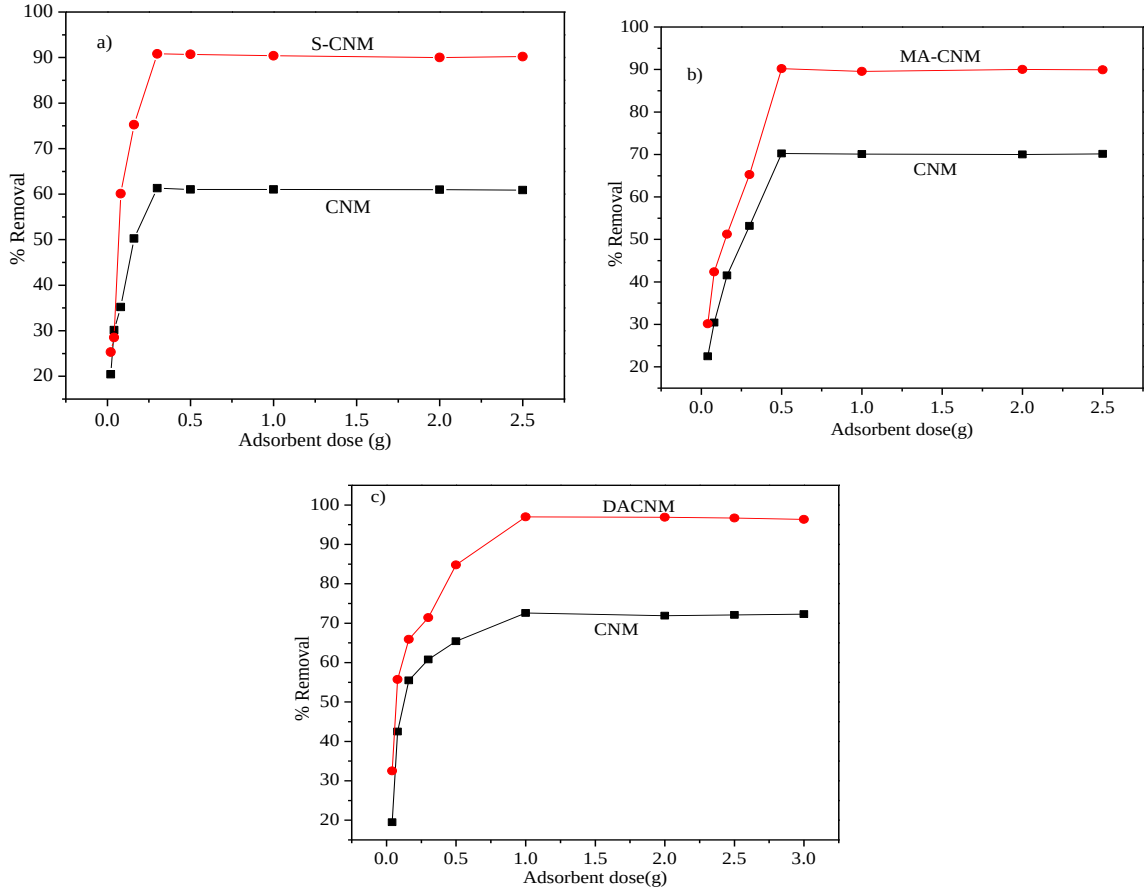

Figure 22. The effect of adsorbent dose on Cr(VI), Cd(II) and Pb(II) ions by CNM (a) and S-CNM, MA-CNM and DACNM (b) respectively, at optimum pH of (5, 8, & 6), room temperature, C_i of (2, 20, & 30 mgL^{-1}), contact time of (90,120,&120 min.), and agitation speed of (300, 250, & 250 rpm).

The temperature effects on the %R of Cr(VI), Cd(II) and Pb(II) ions from wastewater by using pristine and modified CNM sorbents is represented (Figure 23(a & b)). Findings indicated that the rise in temperature from 25 to 45 ℃ decreases the %R of Cr(VI) ions from WW. Both CNM and S-CNM sorbents exhibited that the maximum %R (61.3% and 90.3%) of Cr(VI) ions at optimum dosage (0.3 g) and optimum temperature of 25 ℃. This is due to at increased temperature; the slow rate of the chemisorption processes prevents the Cr(VI) ions to reach fresh active sites on the adsorbent surface for increased %R of Cr(VI) ions from wastewater [243]. Furthermore, the greater percentage of Cr(VI) ions remediation of 90.3%

was observed by using S-CNM sorbents than CNM sorbents. This is due to the increased specific surface area obtained due to the esterification of CNM with succinic anhydride in S-CNM adsorbents [190].

Similarly, increasing the temperature from 25 to 45 ℃ decreases in the %R of Pb(II) ions from wastewater by using both adsorbents. Both CNM and DACNM adsorbents shown the maximum %R (72.5% and 97.8%), respectively, of Pb(II) ions at optimum dosage of 1 g and optimum temperature of 25 ℃. This observation is in line with the reported narration that, at increased thermal behavior, the slow rate of the chemisorption processes prevents the metal ions to reach innovative active sites on the surfaces of the adsorbents [239]. Furthermore, the much higher percentage of Pb(II) ions removal of 97.8% was observed by using DACNM adsorbent than CNM adsorbent. This is due to CNMs adsorbent having the increased specific surface area and active sites was prepared resulted from the oxidation of CNM with addition of $NaIO_4$ [244].

Also, intensifying the temperature from 25 to 45 ℃ decreases the %R of Cd(II) ions from wastewater. Both CNM and MA-CNM sorbents showed that the maximum %R (70.3% and 90.4%) of Cd(II) ions at optimum temperature of 25 ℃. This shows the adsorption processes was dominated by physisorption rather than chemisorption [240]. Likewise, the greater percentage of Cd(II) ions removal of 92.5% was observed by using MA-CNM sorbents than CNM sorbents. This is due to MA-CNMs adsorbent contains hydroxyl, aldehyde carbonyl, and ester functional groups resulted from the esterification reaction [193].

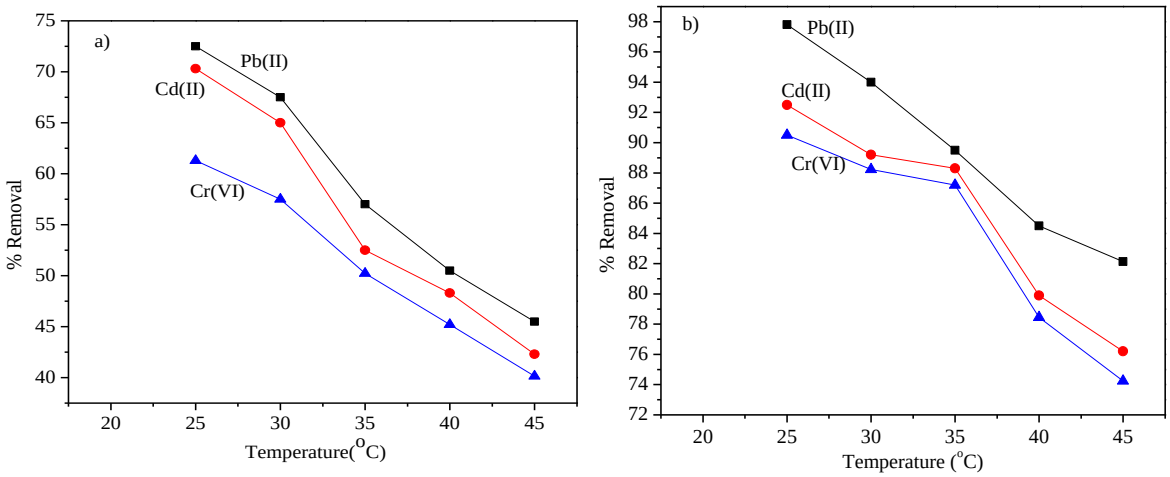

Figure 23. The effect of temperatures on Cr(VI), Cd(II) and Pb(II) ions by CNM (a) and S-CNM, MA-CNM and DACNM (b) respectively, at optimum pH of (5, 8, & 6), dose of (0.3, 0.5, & 1 g), room temperature, C_i of (2, 20, & 30 mgL^{-1}), contact time of (90,120,&120 min.), and agitation speed of (300, 250, & 250 rpm).

4.3.4. Effect of solution pH

The solution pH circumstance in which the surface charge density equals to zero is termed as the pH point of zero charge (pHPZC). Figure 24(a&b) indicated the pHPZC of the material and its value at pH =5.0. From the plot it is possible to deduce that, the adsorbent surface is positively charged at pH < 5.0 and becomes negatively charged at pH > 5.0. For pH < 5.0 uptake process is delayed by repulsive electrostatic force of attractions between the Cr(VI), Cd(II) and Pb(II) ions and positively charged functional groups of the CNM and ,S-CNM, MA-CNM and DACNM adsorbents, respectively [77]. Cr(VI) is toxic to living things, highly mobile in water bodies and found in the three forms CrO_4^{2-}, $HCrO_4^-$ and $Cr_2O_7^{2-}$ according to their respective pH values. Here, Cr(VI) ions adsorption on CNM and S-CNM adsorbents was effective at pH values ranged from 2-5.

Figure 24(c & d) represented the effect of solution pH on the %R of Cr(VI), Cd(II) and Pb(II) ions from the WW using both pristine CNM and chemically modified CNM adsorbents. Both CNM and chemically modified CNM adsorbents indicate increasing remediation abilities in the solution pH ranged from 2–5 and the maximum %R of Cr(VI) ions using both CNM and

S-CNM adsorbent was 60.25 and 90.24%, respectively. These are because of the consequences of cations (H^+) and anions (OH^-) on the binding of Cr(VI) ions to the surface of CNM and S-CNM adsorbents active sites. At high pH values, the interaction of Cr(VI) ions with adsorbents is decreased owing to the electrostatic repulsion between Cr(VI) ions and the negatively charged adsorbents.

In reverse, as the low pH, Cr(VI) ions adsorption to the CNM and S-CNM sorbents surfaces increases towards the optimum pH value of 5. Following this, for the pH of the solution medium less than 5, the levels of H^+ in WW enhances and the increased %R of Cr(VI) ions occurred. This results a greater number of Cr(VI) ions adsorption to the CNM and S-CNM sorbents surfaces and provides increased %R of Cr(VI) ions. Supporting this result Liu et al., [245] reported the maximum percent removal of Cr(VI) ions at nearly similar pH values of this study. In addition to this, results indicated that the higher %R of Cr(VI) ions were observed by S-CNM adsorbents than CNM sorbent systems at pH value of 5 (Figure 24 (a)). The differences in the reported %R for the Cr(VI) ions were related to the occurrence of functionalized groups in the structure of S-CNM adsorbents with different affinity to each metal than CNM sorbent [189]. Also, at alkaline medium, the Cr(VI) ions precipitates as $Cr(OH)_6$ and the adsorption rates gradually decreases [245].

In the case of Cd(II) ions removal, both CNM and MA-CNM adsorbents have shown the increasing removal abilities in the solution pH ranged from 2–8 and with the maximum %R for both CNM and MA-CNM adsorbent of 70.3 and 89.9%, respectively. At low pH values, the interaction of Cd(II) ions with sorbents is decreased owing to the competition of H^+ ions [244]. In reverse, as the WW pH raises starting from 2 (i.e. less H^+ ions), Cd(II) ions attachment to the CNM and MA-CNM adsorbents surfaces raises leading to high %R towards the optimum pH value of 8. Furthermore, when the pH is greater than the optimum value (i.e pH= 8), the removal efficiency becomes decreased due to the levels of OH^- in WW enhances. This decreased situation was observed because of the formation of insoluble hydroxyl complexes. Also, decreased removal efficiency is because of higher alkaline pH value, the Cd(II) ions precipitates as $Cd(OH)_2$. In addition to this, results specified that the higher %R of Cd(II) ions were observed by MA-CNM adsorbents than CNM adsorbents at pH value of 8.

The differences in the reported %R for the Cd (II) ions were related to the occurrence of additional functional groups in the structure of MA-CNM adsorbents with different affinity to Cd(II) ions than CNM adsorbent [190].

For Pb(II) ions removal, CNM and DACNM adsorbents show high removal capabilities in the solution ranged from 5–9 pH. These are because of the reaction of hydroxyl ions (OH^-) with the Pb(II) ions on the surface of CNM and DACNM adsorbents. At low pH values, the interaction of Pb(II) ions with sorbents is decreased because of the interference of H^+ ions and other matrix to the surfaces of CNM and DACNM. In other words, as the WW pH increases (i.e. less H^+ ions), the adsorption of Pb(II) ions to the CNM and DACNM adsorbents provides an increased %R at the optimum pH value of 6. Conversely, if the pH is greater than the optimum value 6, then the level of OH^- ions in the WW increases. This phenomena provides to the exchange of a few Pb(II) ions on the surfaces of CNM and DACNM adsorbents and gradually decreases the %R of Pb(II) ions.

Accordingly, the optimum pH for Pb(II) ions removal by CNM and DACNM adsorbents was found to be 6. In line with this study, Olivera et al., [168] reported the maximum adsorption capability (256 mgL^{-1}) of Pb(II) at pH value of 6. Also supporting this view we made similar report of our previous study [246]. Again, these results were in agreement with the study conducted by Qinghua Xu et al., [247] on the adsorption of Pb(II) from aqueous solutions using black wattle tannin-immobilized nanocellulose that showed increment with increasing the pH of solution form 2–6 and the highest adsorption capacity was observed at pH 6. At alkaline pH value, anions obtained from (HO^-) come to be more dominant and the force of attraction for Pb was raised. Yeol et al., [248] showed that the increased % R of Pb(II) ions in the pH ranges from 2 to 7 using thiol-functionalized cellulose nanofiber membranes. It was reported that for pH >7 the Pb(II) ions precipitate as $Pb(OH)_2$ [248]. Generally, results indicated that the higher %R of Pb(II) ions were observed by DACNM adsorbents than CNM sorbent at pH value of 6. This difference was due to the increased active sites in the surface of DACNM adsorbent than CNM adsorbent.

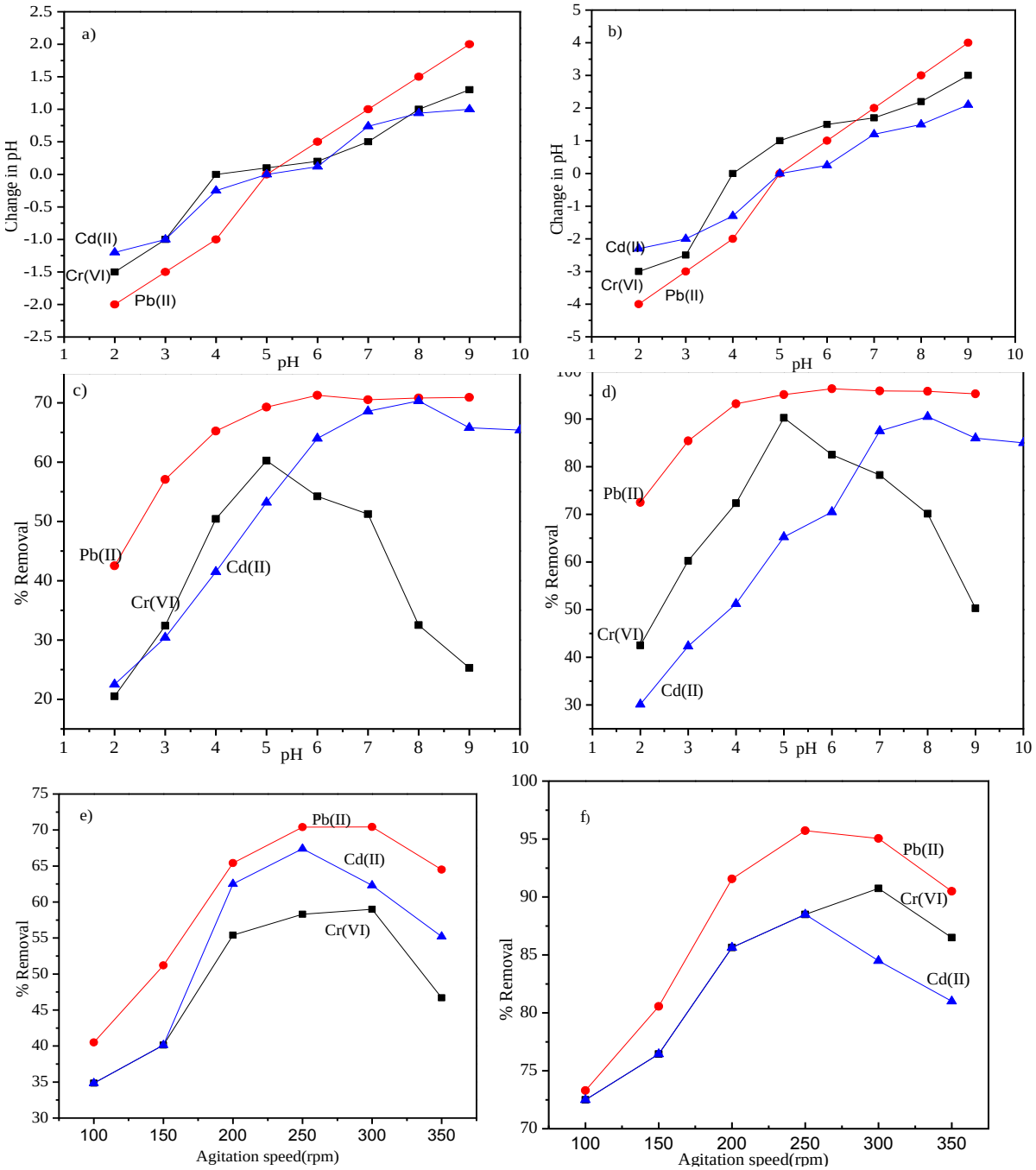

Figure 24. The effect of PZC, pH and agitation speed for the adsorption of Cr(VI), Cd(II) and Pb(II) ions by CNM (a,c,&e) and S-CNM, MA-CNM and DACNM (b,d,&f), respectively, at optimum dose of (0.3, 0.5, & 1 g), room temperature, C_i of (2, 20, & 30 mgL^{-1}), and contact time of (90, 120, & 120 min.).

4.3.5. Effect of agitation speed

The effect of agitation speed on the adsorption of Cr(VI) ions from WW is given in Figure 24(e & f). The findings exhibited that the increased %R of Cr(VI) ions was observed by increasing the agitation speed. This was resulted because of the presence of active smaller size adsorbent particles and more energetic sites on the adsorbing surface of the sorbents [249]. Therefore, the adsorption capability of Cr(VI) ions was increased from 34.85 to 59% by CNM adsorbent and 72.5 to 90.74% by S-CNM adsorbent with increasing the agitation speed from 100 to 300 rpm. The higher %R of Cr(VI) ions by both adsorbents were observed at the optimum agitation speed of 300 rpm. This result arises from the concept that, the interaction between CNMs and Cr(VI) ions is more effective at this moderate agitation speed. This was in agreement with a research reported by Mahmood et al. [250] on adsorption of heavy metals by using nanosorbents. Beyond this optimum agitation speed, it decreases, may be, because of the low mass transfer of Cr(VI) ions to the internal surface of CNMs adsorbent particle and also vigorous shaking makes the desorption of the already adsorbed Cr(VI) ions from the adsorbent. When compared to the pristine CNM Cr(VI) ions removal capability with the S-CNM capability, the functionalized (S-CNM) indicated the higher Cr(VI) ions capability due to the reaction of CNMs with succinic anhydride.

Results showed that, at the starting point, the agitation speed was slow, but, as the agitation speed increases subsequently, a rapid increase in the %R capability of Cd(II) ions observed. This is because of the presence of fresh and smaller sized sorbent particles and more number of active sites existing on the binding surface of the sorbent [249]. Thus, the removal capability of Cd(II) ions was increased from 72.2 to 88.55% as the agitation speed was raised from 100 to 250 rpm, on the surface of MA-CNM adsorbent. In the same way, the Cd(II) ions removal capability of the CNM sorbent was raised from 34.65 to 67.17% as the agitation speed increases from 100 to 250 rpm. After this optimum value of 250 rpm, the %R was decreased.

In addition to this, beyond this value it decreases, may be, because of the low mass transfer of Cd(II) ions to the internal surface of CNMs adsorbent particle and also vigorous shaking

makes the desorption of the already adsorbed Cd(II) ions from the adsorbent [249]. When the Cd(II) ions removal capability of the pristine CNM was compared with that of the functionalized cellulose nanomaterial (MA-CNM) removal capability, the higher removal capability was observed by MA-CNM due to the presence of more accessible surfaces resulted from the addition of maleic anhydride into the CNM. For both sorbents the maximum Cd(II) ions removal capability was obtained at the optimum agitation speed of 250 rpm. This result was in agreement with the study reported by Mahmood et al. [250]. Generally, an increase in the speed of agitation resulted in higher pollutant uptake capabilities and the agitation helps in overcoming the resistance of external mass transfer.

4.3.6. The chemistry of wastewater on the Cr (VI), Cd(II) and Pb(II) ions remediation

The %R of the Cr(VI), Cd(II) and Pb(II) ions from both synthetic and real wastewater is represented in Figure 25(a, b & c), respectively. Their values are represented in Table 5. From the findings, it was seen that the removal processes was negatively affected by the presence of cations and anions in real wastewater. The decreased %R of Cr(VI), Cd(II) and Pb(II) ions from the real wastewater than the synthetic solution might be the competition of cations and anions for the active sites of adsorbents in the real wastewater [251]. These are because of the presence of competing ions in the real WW decreases the interaction of active surfaces on S-CNM adsorbent and Cr(VI), Cd(II) and Pb(II) ions and results a decreased %R of Cr(VI), Cd(II) and Pb(II) ions [251]. The presence of these competing substances in the wastewater sample was measured and given in Table 4. The values of %R of Cr(VI), Cd(II) and Pb(II) ions are (99.7 & 90.25), (99.8 & 90.14), (99.99 & 96.5) for the synthetic solution and real wastewater, respectively and presented in Table 5.

Table 5. Comparison of %R analysis for Cr(VI), Cd(II), and Pb(II) removal from synthetic solution and real wastewater sample by S-CNM, MA-CNM, and DACNM, respectively.

	Percent Removal (%) of Heavy Metals		
Water samples	Cr(VI)	Cd(II)	Pb(II)
Synthetic solution	99.7	99.8	99.99
Real wastewater	90.25	90.14	96.2

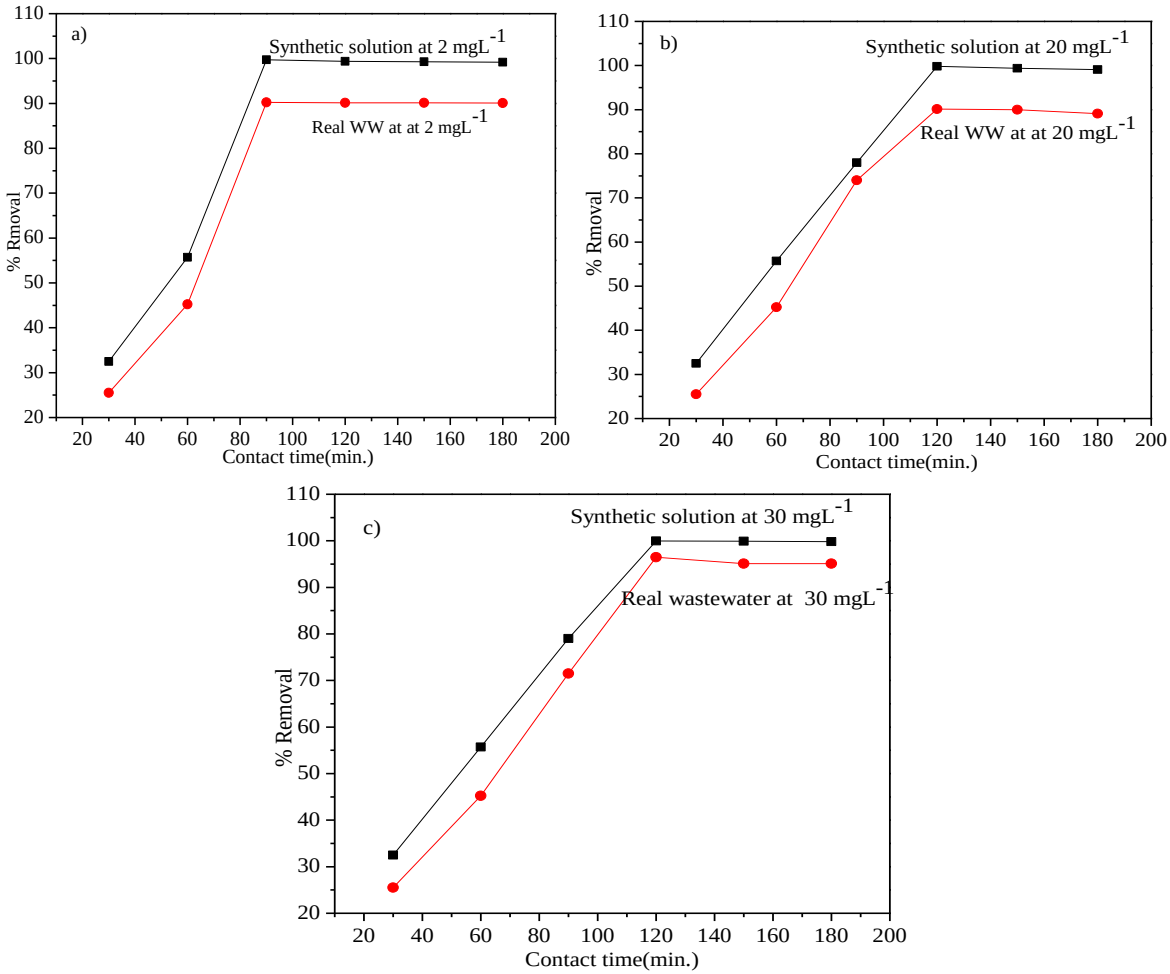

Figure 25. The effects of wastewater chemistry (both synthetic and real wastewater) on the percent removal of Cr(VI) ions (a), Cd(II) ions (b), and Pb(II) ions (c) at optimum pH of (5, 8, & 6), room temperature, C_i of (2, 20, & 30 mgL^{-1}), dose of (0.3, 0.5, & 1 g), and agitation speed of (300, 250, & 250 rpm), by using S-CNM, MA-CNM, DACNM, respectively.

4.3.7. Adsorption isotherms

Langmuir and Freundlich isotherm models for the adsorption of Cr(VI), Cd(II), and Pb(II) ions adsorption used and given in Appendix Figure 1(a,c,&f) & (b, d,&f), respectively. Clearly, Langmuir and Freundlich isotherm models describe the distribution of the Cr(VI), Cd(II), and Pb(II) ions among the liquid and solid states according to expectations related to the heterogeneity or homogeneity of the adsorbents surface, the category of coverages, and the prospect of contact between the Cr(VI), Cd(II), and Pb(II) ions. That is, Langmuir isotherms refer to the adsorption mechanism with monolayer, and recognize the distribution of Cr(VI), Cd(II), and Pb(II) ions between solid and liquid stages that is on the surface of the (CNM & S-CNM), (CNM & MA-CNM), and (CNM & DACNM) adsorbents, respectively. Its linear form of equation is represented in Equation 2. The linear form of Freundlich isotherm model is given in Equation 5 and indicates an exponential decay in the active sites density versus the heat of adsorption. Regarding this issue, Freundlich isotherms can be implemented as indicator of the heterogeneity of the adsorbent surfaces. In addition to this, a dimensionless equilibrium parameter (R_L) value for all level is calculated by using Equation 3 and it confirms the feasibility of Cr(VI), Cd(II), and Pb(II) adsorption on (CNM & S-CNM), (CNM & MA-CNM), and (CNM & DACNM) adsorbents, respectively. The findings from R^2 value showed that the Cr(VI) ions adsorption using CNM adsorbent best fitted to Freundlich isotherm model and Cr(VI) ions adsorption using S-CNM adsorbent best fitted to Langmuir isotherm model. Again, Cd(II) ions adsorption using CNM and S-CNM adsorbents were best fitted to Langmuir isotherm model. Finally, Pb(II) ions adsorption using CNM and S-CNM adsorbents were best fitted to Freundlich isotherm model.

Table 6. Langmuir and Freundlich isotherm constants for Cr(VI), Cd(II), and Pb(II) ions adsorption by CNMs and S-CNM, MA-CNM, and DACNM adsorbents at 25℃.

Isotherm Models	Langmuir				Freundlich		
	Q_{max} (mg/g)	b	R_L	R^2	K_f	n	R^2
CNM	60.24	0.59	0.027	0.963	1.035	6.32	0.981
S-CNM	156.25	0.592	0.027	0.985	1.035	6.32	0.981
CNM	75.76	0.032	0.167	0.943	1.036	7.78	0.932
MA-CNM	215.52	0.083	0.602	0.977	0.91	1.97	0.936
CNM	91.74	0.18	0.057	0.929	0.94	3.57	0.949
DACNM	384.62	0.011	0.195	0.947	0.899	1.91	0.989

From the adsorption isotherm study, it is possible to determine the equilibrium concentration and equilibrium adsorption capacity. Also, it is important to determine the adsorption mechanisms clearly. Therefore, based on the adsorption isotherm study the heavy metal ions form a monolayer or multilayer interactions of molecules with the actve sites of the adsorbents. The value of Freundlich parameter n confirms the adsorption process is a physisorption and favorable because the value of n is greater than 1.

4.3.8. Thermodynamics study

The thermodynamic study of the Cr(VI), Cd(II) and Pb(II) ions adsorption processes were carried out through calculating the standard thermodynamic parameter, such as, Gibbs free energy (ΔG), change in enthalpy (ΔH) and change in entropy (ΔS) values at optimum temperature as given in Table 7. The Gibbs free energy (ΔG°) values for the adsorption of Cr (VI), Cd(II) and Pb(II) ions on CNM and S-CNM, CNM and MA-CNM and DACNM, respectively, were calculated using Equation 10. The entire obtained ΔG° values were negative suggesting spontaneous adsorbing mechanism. Different temperatures (25-45°C) were used to determine the thermodynamic parameter and reported at optimum temperature value. For the Cr(VI) and Pb(II) ions adsorption process, the highest values of ΔG° occurs at optimum temperature of 25 °C and for Cd(II) ions adsorption process, the highest negative

values of ΔG° occurs at optimum temperature of 25 °C suggesting that adsorption efficiency increase by decreasing the temperature. Furthermore, the negative values of ΔG° confirms the spontaneity and feasibility of Cr(VI), Cd(II) and Pb(II) ions adsorption onto their respective adsorbent surfaces [252].

Table 7. Thermodynamic parameters for Cr(VI), Cd(II) and Pb(II) ions adsorption by CNM and S-CNM, CNM and MA-CNM and DACNM, respectively, at optimum temperature.

Adsorbents	**Thermodynamic Parameters**		
	ΔG (KJ/mol)	**ΔH (KJ/mol)**	**ΔS (J/mol k)**
CNM	-2.8	+33.65	-103.6
S-CNM	-5.3	+43.59	-128.6
CNM	-1.5	+39.90	-126.9
MA-CNM	-2.7	+30.91	-94.36
CNM	-2.2	+33.11	-104.4
DACNM	-4.4	+43.60	-127.6

4.3.9. Adsorption kinetics:

The adsorption kinetics of Cr(VI), Cd(II), and Pb(II) ions by CNM and S-CNM, CNM and MA-CNM and DACNM, respectively, were tested using linearized pseudo-first order and pseudo second order (PSO) equations (Equation 7 & 8), respectively. The plot of $\log(q_e-q_t)$ vs. t and the plot of qe/qt versus log t are given in Appendix Figure 2 (a,c&e) & (b,d&f), respectively.

The R^2 determination of the experimental data using pseudo-first order (PFO) kinetics model was too poor both at initial concentration and final adsorption processes because the experimental qe value was much different than from the calculated qe value for both sorbents. This specifies that the adsorption kinetics does not follow this model. Therefore, results from the Appendix Figure 2 (a-f) indicates a representative fitness of the data corresponding to pseudo second order (PSO) model for Cr(VI), Cd(II), and Pb(II) ions adsorption on CNM and S-CNM, CNM and MA-CNM and DACNM adsorbents, respectively. These results were in agreement with the research reported by Mohammad & Rana [253] on mechanistic

understanding of the adsorption and thermodynamic aspects of cationic methylene blue dye onto cellulosic olive stones biomass from wastewater.

The calculated kinetic data are presented in Table 8. This model provides the maximum correlation coefficient value for CNM and S-CNM, CNM and MA-CNM and DACNM adsorbents of R^2= (0.992 & 0.987), for Cr(VI) removal), (0.998 & 0.995) for Cd(II) removal, and (0.965 & 0.970) for Pb(II) removal, respectively, using PSO model and very low correlation coefficient values were obtained using PFO model. In conclusion, the results have indicated PSO model better represents the Cr(VI), Cd(II), and Pb(II) ions adsorption kinetics, suggesting that more of the adsorption processes are chemisorption.

Table 8. The values of parameters and correlation coefficients of Pseudo first order (PFO) and Pseudo second order (PSO) kinetics.

Kinetics	**PFO**				**PSO**			
	$q_{e.}$ cal. (mg/g)	$q_{e.}$ exp. (mg/g)	k_1	R^2	$q_{e.}$ cal. (mg/g)	$q_{e.}$ exp. (mg/g)	k_2	R^2
CNM (Cr)	31.09	8.25	0.534	0.765	11.83	11.78	0.898	0.992
S-CNM	5.69	5.54	0.273	0.976	23.23	23.20	0.387	0.987
CNM (Cd)	1.04	2.06	0.16	0.578	9.93	9.37	0.074	0.998
MA-CNM	1.29	3.23	0.340	0.830	14.68	14.96	0.030	0.995
CNM (Pb)	1.220	9.47	0.173	0.576	9.880	9.78	0.095	0.965
DACNM	1.315	10.23	0.380	0.837	14.99	15.06	0.021	0.970

4.4. Adsorption of Methylene Blue (MB) Dye

4.4. 1. Effects of initial MB concentration

Figure 26(a) indicates the effects of initial MB solution concentrations (10−40 mg/L) for the removal of cationic MB using DACNM adsorbent. Findings indicated that on varying the pollutant MB concentration from 10 to 40 mg/L, the %R is increased from 39.25 to 78.21% using DACNM adsorbent. These results are in agreement with researches reported by Munir

et al. and Gupta et al. [254,255] on MB dye removal. The adsorption process can be both very rapid and slow. At low initial concentration, the dye removal process was very fast due to the presence of more available active sites on the surface of the DACNM adsorbent. Conversely, the slow adsorption process may be attributed to the external diffusion of MB into a hydrodynamic boundary layer of the DACNM adsorbent surfaces [256,257]. At increased initial concentrations (C_i), the removal capability progressively increases and approached to reach the equilibrium value at C_i = 30 mg/L. At this point, the adsorbent evidently displayed maximum dye percent removal (%R) capacity of 78.1%. Beyond this point, the % R becomes constant. The constant %R of MB dye was observed due to the presence of greater number of cationic MB dye in solution than the number of active sites in the adsorbent surface [253].

4.4.2. Effect of contact time

The time necessary for achieving equilibrium is one of the greatest significant aspects which decide the effectiveness of the progress possibility, and the wastewater treatment cost [258]. The effect of contact time on the MB dye removal was conducted by using experimental procedures at optimum DACNM dose of 1 g, temperature of 25 °C, and initial MB concentration of 30 mg L^{-1} (Figure 26 (b). These optimum values of the parameters are the values at which the higher adsorption efficiency was detected. As seen from Figure 26b, the color removal by using DACNM was increased with increasing the contact time up to the equilibrium and the optimum time of 60 min, due to the presence of highly active sites on the surfaces of the adsorbent [259]. The maximum percent color removal (%R) of 78.1% was observed at the equilibrium contact time of 60 min. After this time, the %R processes proceed in a fixed manner. This is because, the adsorbent has limited active sites and steric hindrance on its surface, which makes the adsorption process to slow down and reaches equilibrium. Therefore, this equilibrium contact time is a significant parameter as a contact time more than needed would result in higher energy stresses and economically costly [238].

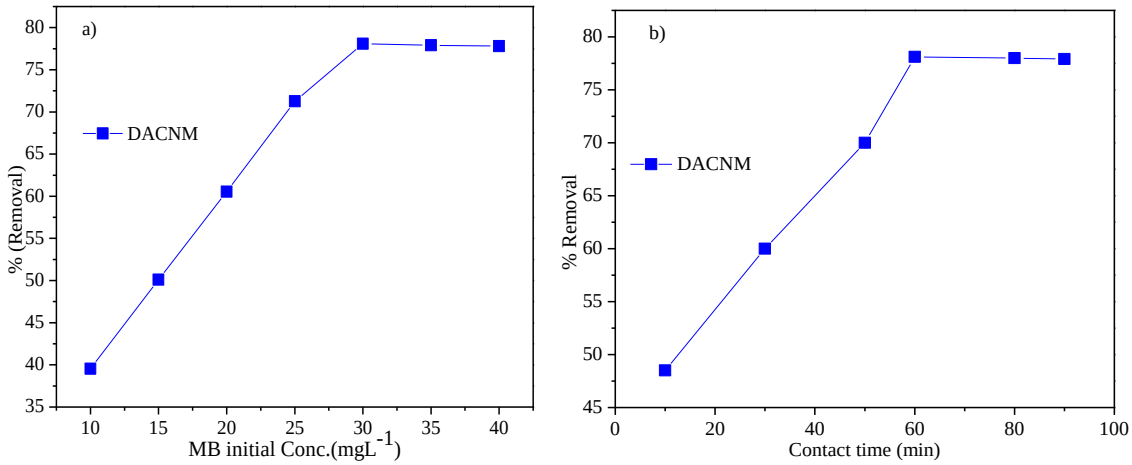

Figure 26. The effect of MB initial concentration (a) and contact time (b) for the color removal at optimum temperature of 25 ℃, adsorbent dosage of 1 g and solution pH of 8.

4.4.3. Effect of adsorbent dose

Figure 27a indicates the effect of adsorbent dose on adsorption ability and degree of color removal at the optimum temperature of 25℃, MB initial concentration of 30 mg L^{-1}, the contact time of 60 min. and solution pH of 8. Different doses of DACNM adsorbent ranged from 0.4 to 2 g were used in the experiments. Results exhibited that the increase of the adsorbent dosage from 0.4 to 1 g increases the %R from 35.51% to 78.50%. Conversely, the increased %R and efficiency were reported by Tan et al. [260] for MB dye removal using cellulose-based nanomaterials as an adsorbent from synthetic wastewater. The relatively low efficiency and %R was observed in this study due to the competition of other contaminants to the active site of the adsorbent since this study was focused on the removal of cationic dye from real textile industrial wastewater. Beyond the optimum value of 1 g, the color removal remains constant due to the quantity of ions bonded to the adsorbent and the number of mobile ions in the wastewater becomes constant even with additional increase of the adsorbents dose [261].

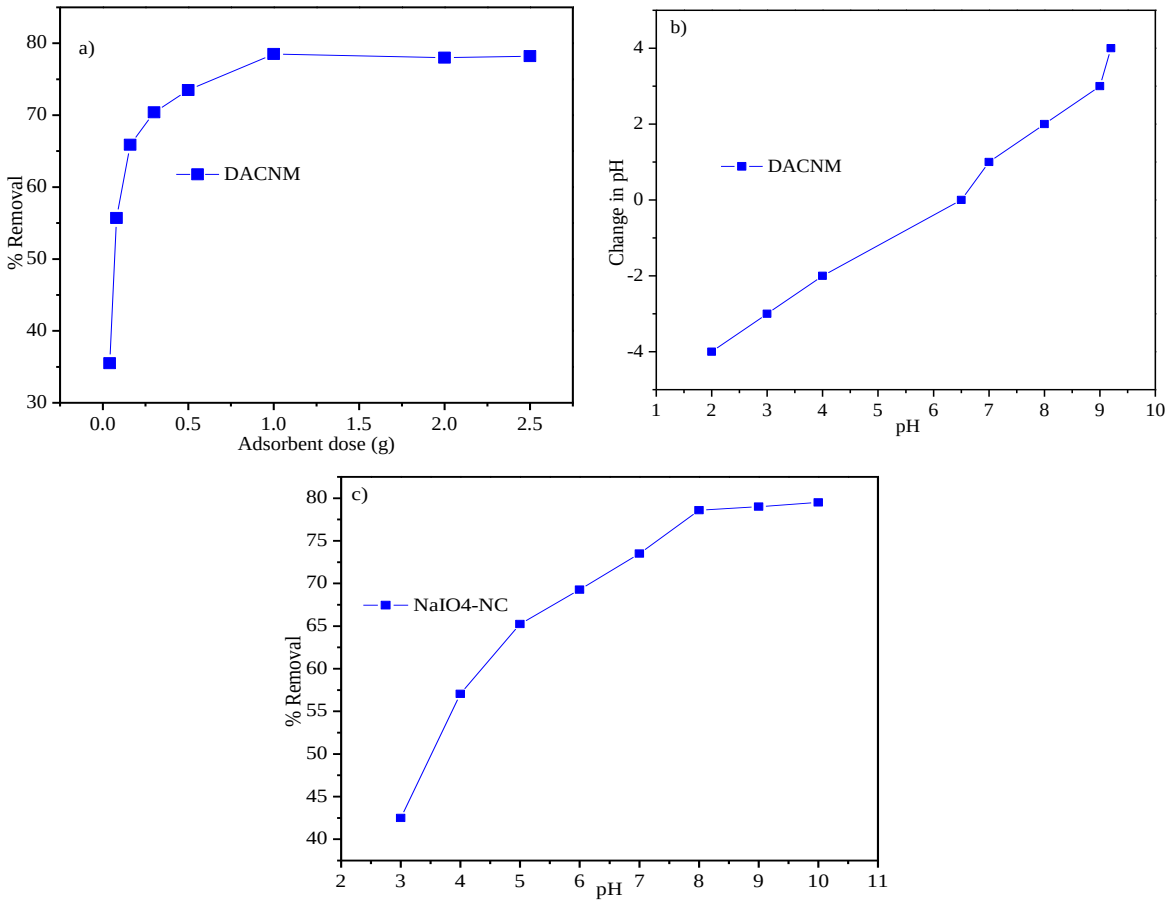

Figure 27. Effect of adsorbent dosage (a), PZC (b), and solution pH (c) for color removal using DACNM adsorbent at optimum contact time of 60 min., optimum temperature of 25 ℃ and initial MB concentration of 30 mgL^{-1}.

4.4.4. Effect of solution pH

The solution pH circumstance in which the surface charge density equals zero is termed as the pH point of zero charges (pHPZC). Figure 27b indicated the pHPZC of the material and its value was 6.5. From the plot, it is possible to deduce that, the adsorbent surface is positively charged at pH < 6.5 and becomes negatively charged at pH > 6.5. Thus, the high uptake capacity was observed at pH > 6.5 which is a pH of 8. For pH < 6.5 uptake process is decreased by the repulsive electrostatic force of attractions between the MB dye ions and positively charged functional groups of the DACNM adsorbent [262].

The effect of solution pH on MB cation removal is presented (Figure 27c). The DACNM adsorbent used in this study has shown that high color removal abilities in the solution pH range of 3–8. These are a result of the presence of hydrogen ions (H^+) on the adsorption site of MB cations to the surface of the adsorbent active sites. At low pH values, the interaction of MB cations with sorbents is decreased owing to the H^+ ions competes with the MB cations on the active sites of the adsorbent. And, as the pH of WW increases (i.e. less H^+ ions), MB cations adsorption onto the DACNM adsorbent surfaces increases leading to higher color removal towards the optimum pH value of 8. At alkaline medium (high pH value), the adsorbent becomes negatively charged and MB cations effectively adsorbed onto the surfaces of the adsorbent. This result was in agreement with the study reported by Salama et al. [244] on the removal of methylene blue on oxidized cellulose reinforced silica gel.

4.4.5. Adsorption Isotherms

Here, adsorption isotherm models describe the distribution of the cationic MB among the liquid and solid states according to expectations related to the heterogeneity or homogeneity of the DACNM adsorbent surface, the category of coverage, and the prospect of contact between the cationic MB. This study was performed by mixing 1 g of DACNM adsorbent in different concentrations of MB, 10, 15, 20, 25, 30, 35, and 40 mg L^{-1}, at a pH of 8 for 60 min. of contact time. Langmuir and Freundlich isotherms were tested to investigate the removal of MB by using DACNM adsorbent and their equation was presented in Equation 2 and Equation 5, respectively. Langmuir isotherm model describes the information for the adsorption of MB dye onto the outer surface of DACNM adsorbent homogeneously and the dye molecules will form a monolayer onto the adsorption sites [252]. The Freundlich isotherm model predicts that multilayer adsorption occurs on the uneven surface of the DACNM adsorbent [263].

Figure 28 (a, b & c) indicates Langmuir and Freundlich isotherms for MB dye removal using DACNM sorbents. Table 9 describes the MB dye uptake by the adsorbent fits more beter with Freundlich isotherms because the R^2 value was higher compared to R^2 value resulted from Langmuir isotherm model. The maximum MB removal ability (q_{max}) of the DACNM sorbent

per unit mass was 90.91 mg/g from real textile industrial wastewater. This result showed relatively low removal efficiency than the results reported by Salama et al. [244] the removal of methylene blue on oxidized cellulose reinforced silica gel, maybe due to the presence of different matrix in real wastewater. If there is no computing matrix other than the target adsorbate, then all the active sites of the adsorbent were occupied by the target element. This indicates that when an active site of adsorbent was occupied by a molecule, no other molecules could be adsorbed onto the surface [263]. This result was in agreement with the study reported by Qian et al [252] for the adsorption of MB on modified bamboo hydrochar adsorbent. The calculated value for b and a dimensionless equilibrium parameter (R_L) of DACNM sorbent was 0.075 L mg^{-1} and 0.308, respectively.

Table 9. Langmuir and Freundlich isotherm constants for cationic MB dye uptake by DACNM adsorbent at 25℃.

Isotherm	**Langmuir**				**Freundlich**		
Models	Q_{max} (mg/g)	b	R_L	R^2	K_f	n	R^2
DACNM	90.91	0.075	0.308	0.925	1.02	2.22	0.959

A dimensionless equilibrium parameter (RL) value calculated using Equation 5 for MB was found in the range of $0 < R_L < 1$, representing the removal process by DACNM adsorbent was favorable. Typically, the degree of favorability is linked to the irreversibility of the adsorption system, and this may afford the identification of the interactions between DACNM adsorbent and the MB dye adsorbate [264]. Also, the magnitude for K_f and n of DACNM sorbent for MB removal was 1.02 and 2.22, respectively, which was found between 1 & 10. This has shown that the results indicated an easy MB removal from wastewater and clearly describes the proposed removal mechanism. Therefore, DACNM adsorbent is a highly efficient adsorbent for the removal of cationic MB dye.

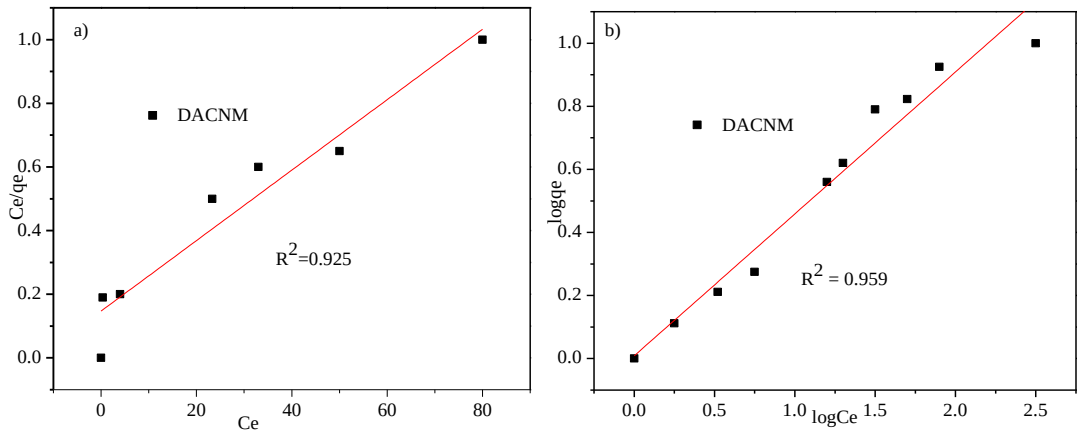

Figure 28. Langmuir (a) and Freundlich adsorption isotherm for the MB dye removal, respectively, at C_i = 30 mgL^{-1}, pH = 8, adsorbent dose = 1 g and contact time=60 min.

4.4.6. Thermodynamics study

The thermodynamic study of the cationic MB dye adsorption processes were performed calculating the standard thermodynamic parameter, such as, Gibbs free energy (ΔG), change in enthalpy (ΔH) and change in entropy (ΔS) values at optimum temperature and given in Table 10. The Gibbs free energy (ΔG°) value for the adsorption of cationic MB dye on DACNM was calculated using Equation 10. Table 10 presents the calculated Gibbs free energy value for the studied cationic MB dye. The obtained ΔG° was negative suggesting the adsorbing mechanism was spontaneous and feasible [264]. The highest value of ΔG° occurs at optimum temperature of 20 °C suggesting that adsorption efficiency increase by decreasing the temperature.

Table 10. Thermodynamic parameters for cationic MB dye adsorption by DACNM at optimum temperature.

Adsorbents	**Thermodynamic Parameters**		
	ΔG (KJ/mol)	**ΔH (KJ/mol)**	**ΔS (J/mol k)**
DACNM	-1.40	+31.7	-103.9

4.4.7. Adsorption kinetics:

The adsorption kinetics of cationic MB dye by DACNM adsorbent was conducted by using pseudo-first order (PFO) and pseudo second order (PSO) given in Equation 7 and Equation 8, respectively. The parameters in relation to each kinetic uptake model were established considering their linear best fits (Figure 31). Table 11 indicates the correlation coefficient, R^2, values of 0.887, 0.998, and 0.542 obtained by PFO, PSO, and intraparticle diffusion kinetic models, respectively. The resultant R^2 of PSO kinetic model value approaches to unity.

Table 11. The values of parameters and correlation coefficients of Pseudo first order (PFO) and Pseudo second order (PSO) for DACNM adsorbent.

Kinetics	**PFO**				**PSO**			
	$q_{e.}$ cal. (mg/g)	$q_{e.}$ exp. (mg/g)	k_1	R^2	$q_{e.}$ cal. (mg/g)	$q_{e.}$ exp. (mg/g)	k_2	R^2
DACNM	4.099	19.45	0.297	0.887	20.83	20.58	5.78	0.998

This model offers the greater value of qe (20.83 mgg^{-1}), compared to the PFO qe (4.099 mgg^{-1}), which is in disagreement with the value obtained experimentally qe (19.45 mgg^{-1}). According to R^2 values, the uptake of cationic MB dye on DACNM fits well with the PSO kinetic model. A similar result was previously reported for the uptake of MB on cellulose-based adsorbent by Ma et al. [265].

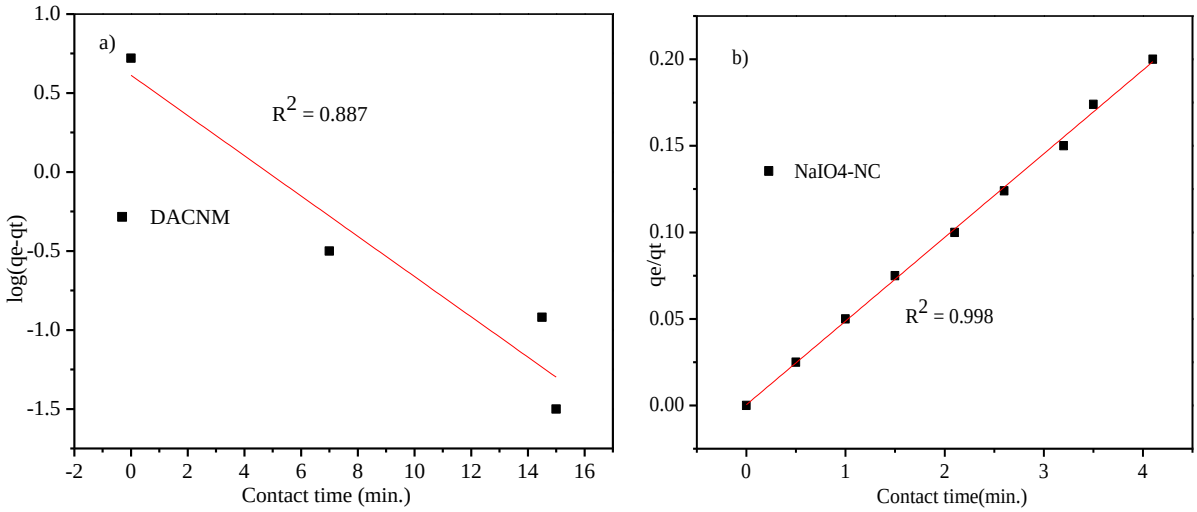

Figure 29. Plot of the PFO (a) PSO (b) and intra-particle diffusion kinetics (c) model at Ci = 30 mgL^{-1}, pH = 8, adsorbent dose = 1 g and contact time=60 min for cationic MB dye removal, respectively.

4.5. Treatment of the Real Textile Wastewater (WW) Relative to Synthetic MB Solution

To assess the effectiveness of the treatment process by the adsorbent, it is possible to investigate the uptake of real textile industrial WW taken from Hawassa textile industry), containing MB as the main dye, relative to synthetic MB solution. The textile industry WW was characterized by determining its pH, EC, Cl^-, Cu^{2+}, $Cr^{6+}$and cationic MB dye before and after adsorption was given in Table 11. The uptake investigations were performed by using 30 mL of WW with 0.08, 0.5, 1, 1.5, and 2 g of DACNM adsorbent dose for 60 min. of reaction time at 20℃. From this optimization process, the optimum value of the adsorbent dose obtained was 1 g, because the maximum uptake value was detected at this value of the adsorbent dose. Figure 30 shows the absorbance spectra of synthetic MB solution (a) and real WW (b), respectively, before and after treatment and the comparison study for the uptake capacity of MB from synthetic MB solution and real textile industrial WW solutions (c). From the UV-Vis absorbance spectra, it is possible to conclude that percent removal (%R) of synthetic MB solution was higher than that of the real WW. This may be because the real WW treatment was hindered by the presence of a different matrix that competes with the MB dye.

Table 12. Physico-chemical properties of the WW sample collected from Hawassa textile effluents used in the study before treatment and after treatment.

Parameter	Before Treatment	After Treatment	Probability(P) value
pH	7.4 ± 0.03	7.05 ± 0.03	$1.0 * 10^{-2}$
Color	Black	Colorless	
EC(µS cm^{-1})	5.08 ± 0.5	1.3 ± 0.5	$4.3 * 10^{-5}$
Cu^{2+} (mg /L)	2.8 ± 0.04	0.2 ± 0.04	$2.15 * 10^{-4}$
Cr^{6+} (mg /L)	4 ± 0.02	3.7 ± 0.02	$5.7 * 10^{-3}$
Cl^- (mg/L)	18.5 ± 0.03	0.2 ± 0.03	$2.8 * 10^{-4}$
Cationic MB dye	35.5 ± 0.05	9.7 ± 0.05	$2.64 * 10^{-5}$

Results are calculated at 95% confidence interval (p=0.05) from the pooled standard deviation for the mean of a triplicate analysis.

Table 12 indicated the statistical data for the physicochemical property measurement of Hawassa textile industrial WW effluents. Results have shown that the obtained probability value is much less than 0.05 and indicated the significant difference between the physicochemical property measurement of WW before and after treatment. Clearly, the concentration values of Cl^- and cationic MB dye decreased by approximately 99% and 78.5%, respectively. In addition to this, the results confirmed that the presence of Cr^{6+} ions in the textile WW had no any negative effect on the %R of cationic MB dye at optimum solution pH values. Furthermore, the %R efficiency comparison study of synthetic cationic MB dye solution and real textile wastewater was conducted and presented in Figure 30c. The findings show that a very high %R (99.99%) of cationic MB was removed from synthetic MB solution and relatively less %R (78.5%) of cationic MB was removed from real WW by using 1 g DACNM adsorbent and 30 mgL^{-1} initial concentration and 60 min. contact time. These great variations of %R observed between two systems were due to presence of competing cations that reduces the %R of cationic MB dye from real WW.

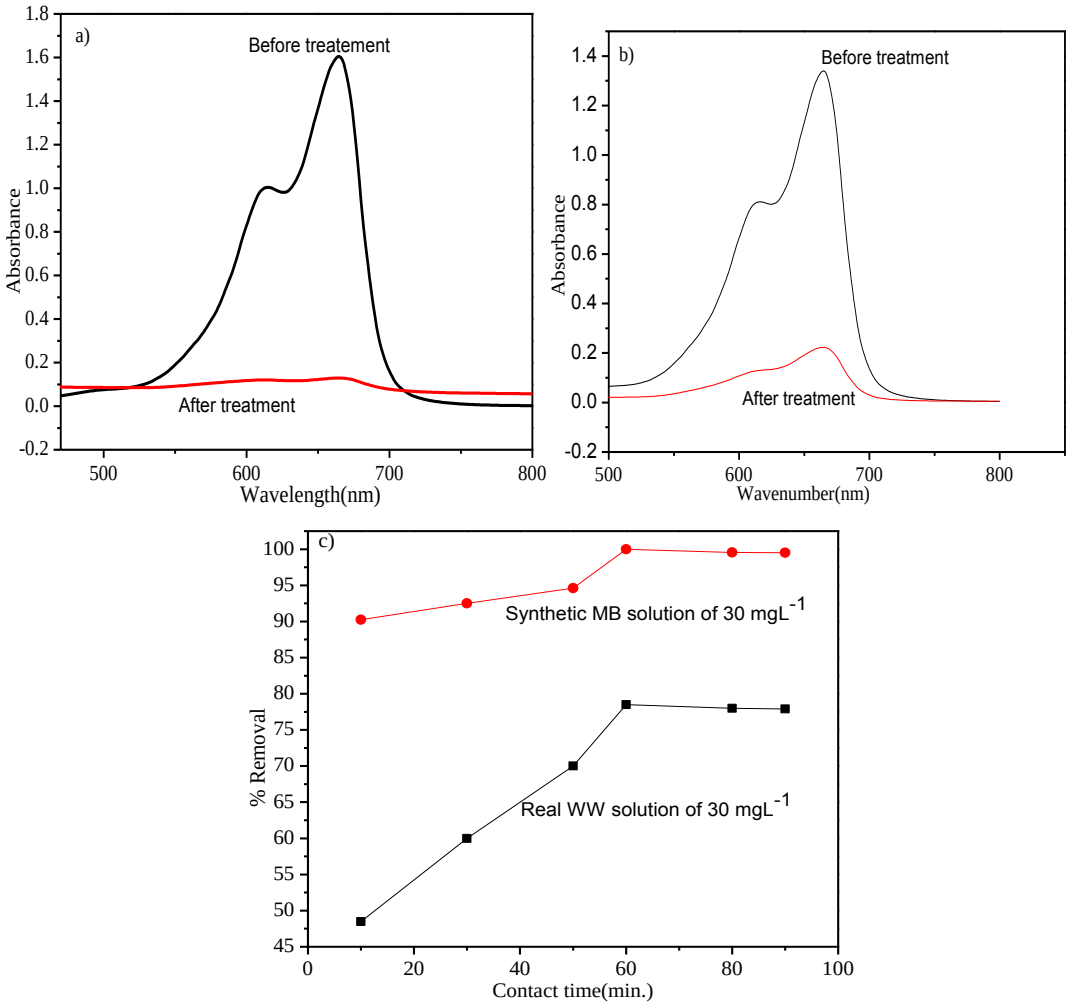

Figure 30. UV–Visible spectra of synthetic MB (a) and real textile wastewater (b) before and after 60 min. of treatment at λmax of 664 and %R trends of synthetic and real wastewater (c) at optimum initial concentration of 30 mgL^{-1}.

4.6. Proposed Adsorption Mechanism

The probable proposed adsorption mechanism of Cr(VI), Cd(II), and Pb(II) ions, respectively, on the surface CNMs adsorbents was presented based on the functional groups of the CNMs adsorbents obtained with the help of FTIR spectrometry. Thus, to understand the adsorption mechanisms of the cations onto the surface of CNMs adsorbent one can possibly identify the nature of cations and the CNMs material. Therefore, heavy metal cations in aqueous solution can be found mainly as $[M(H_2O)_b]^{n+}$, and the inner-sphere or the outer-sphere metal complex formation mechanisms may be the way these heavy metal cations adsorb onto the surface of

CNMs. Where n+ is the number of electrical charge, b is number of water molecules, and M is heavy metals. Accordingly, water molecules surrounding hydrated Cr(VI), Cd(II), and Pb(II) ions are replaced by carboxylate ions present on the surface of CNMs, when inner-sphere mechanism takes place; as a result, a semi-covalent bond between the carboxylate and the Cr(VI), Cd(II), and Pb(II) ions occurs. Obstinately, when outer-sphere complex formation occurs, water molecules that hydrate the Cr(VI), Cd(II), and Pb(II) ions remain when the reaction to form the complex with the corresponding functional group happens. Consequently, the interaction is driven by electrostatic interactions between the carboxylate groups of CNMs and the hydrated cations can be given in Equation 18 &19 [275].

$$R_1OH + M^{n+} + H_2O \rightarrow R_1OMOH + nH^+ \quad (18)$$

$$R_1OH + R_1OH + M^{n+} \rightarrow (R_1O)(R_1O)M + nH^+ \quad (19)$$

Where R_1 is the active site on the CNMs surface and M^{n+} is the heavy metal ions. Again, the possible mechanism of complexation of Cr(VI), Cd(II), and Pb(II) ions with the carbonyl, and carboxyl functional groups of the chemically modified CNMs can be presented in Equation 20 & 21, respectively.

$$R_1CO^- + M^{n+} + H_2O \rightarrow (RCO)(RCO)M \quad (20)$$

$$R_1COO^- + M^{n+} + H_2O \rightarrow (RCOO)(RCOO)M \quad (21)$$

The probable proposed adsorption mechanism of Cr(VI), Cd(II), and Pb(II) ions on S-CNM, MA-CNM, DACNM , respectively, is schematically represented in Figure 33a, and cationic MB dye adsorption onto the surfaces of DACNM was given in Figure 33b. The surface of the sodium periodate solution treated CNMs contains carbonyl aldehyde groups. Also, the surface of the succinic and maleic anhydride treated CNMs contains carboxyl and ester functional groups. Furthermore, in the case of cationic MB dye adsorption mechanisms cationic MB dye was adsorbed electrostatically onto the DACNM at basic pH value. That is why the maximum adsorption efficiency for cationic MB adsorption onto the surfaces of DACNM was observed at pH value of 8.

The comparison between the chemically modified and pristine CNMs, the chemically modified CNMs indicates the radically better chemical contaminant removal efficiency than the pristine CNMs. This is due to the presence of additional carbonyl functional groups

resulted from the functionalization of CNMs with sodium periodate solutions, and additional ester and carboxyl functional groups resulted from esterification reaction.

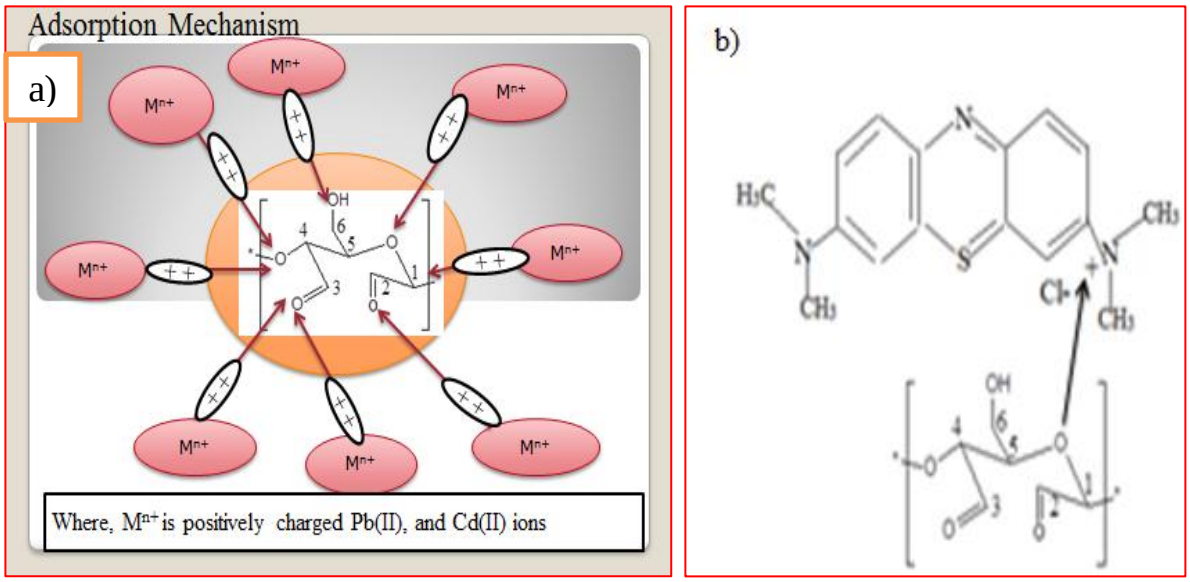

Figure 31. Adsorption mechanism of Cr(VI), Pb(II), Cd(II) (a), and MB ions (b) on both the pristine and chemically modified CNMs.

4.7. Comparison with other Adsorbents

The data in Table (13-16) represents the comparative adsorption efficiency results reported for Cr(VI), Pb(II), Cd(II), and MB cations removal by other researchers using other adsorbents.

Table 13: Comparison of adsorption capacity of Cr(VI) ions by different adsorbents

Adsorbent	Adsorption condition	qm(mg/g)	Isotherms	Kinetics	References
Polyethylenimine Facilitated Ethyl Cellulose	25 °C, pH 3	36.8	Langmuir	PSO	[266]
Carboxymethyl cellulose-ethylenediamine	25 °C, pH 2	177.6	Langmuir	PSO	[267]
Polyvivylimidazole modified cellulose	25 °C, pH 2	134.18	Langmuir	PSO	[268]
Polyethylene imine modified hydrochar	25 °C, pH 3	33.6	Langmuir	PSO	[269]
CNM	25 °C, pH 5	60.24	Langmuir	PSO	This work
S-CNM	25 °C, pH 5	156.25	Langmuir	PSO	This work

The maximum Cr(VI), Pb(II), Cd(II), and MB cations uptake (q_{max}) values of the CNM ,S-CNM, CNM , DACNM, MA-CNM, and DACNM adsorbents were 60.24 156.25, 91.74 384.62, 75.76 ,215. 52, and 90.91 mgg^{-1}, respectively. As can be observed in Table (12-15), the uptake capacity of all used adsorbents in this study is higher than that of the majority of the adsorbents in the reported literatures [266-284]. Furthermore, for example, the uptake capacity of Pb(II) cations by Tannin-nanocellulose (TNCC) at the same pH of 6 has lower uptake capacity of Pb(II) cations than adsorbents in the present study. Therefore, this study approves the possibility of using current adsorbents for their better performance, and environment friendlineess, in comparison to other adsorbents in the reported works.

Table 14: Comparison of adsorption capacity of Pb(II) ions by different adsorbents

Adsorbent	Adsorption condition	qm(mg/g)	Isotherms	Kinetics	References
Chitosan functionalized with xanthate	25 °C, pH 4	322.6	Langmuir	PSO	[270]
Tannin-nanocellulose (TNCC)	25 °C, pH 6	53.37	Langmuir	PSO	[271]
Activated carbon	25 °C, pH 7	47.61	Langmuir	PSO	[272]
Fe_3O_4@TATS@ATA	25 °C, pH 5.7	205.2	Langmuir	PSO	[273]
Co-CYCS/CNC	25 °C, pH 7	334.9	Langmuir	PSO	[274]
Magnetic hydrogel beads (m-CS/PVA/CCNFs)	35 °C, pH 4.5	171	Langmuir	PSO	[275]
Biomass-magnetic hybrid	25 °C, pH 6.8	63.6	Langmuir	PSO	[276]
CNM	25 °C, pH 6.0	91.74	Langmuir	PSO	This work
DACNM	25 °C, pH 6	384.62	Langmuir	PSO	This work

Generally, many researchers have been reported number of adsorbents previously for the removal of contaminates from wastewater such as pharmaceuticals, metal ions, and dyes etc. but previously reported adsorbents were synthesized by using expensive adsorbent materials and much costly methods. The advantage of this work is to develop sustainable and greener materials from completely waste based, biodegradable, non-toxic, cheap adsorbent using cost effective methods for wastewater treatment.

Table 15: Comparison of adsorption capacity of Cd(II) ions by different adsorbents

Adsorbent	Adsorption condition	qm(mg/g)	Isotherms	Kinetics	References
Coffee grounds	20 °C, pH 7	15.65	Langmuir	PSO	[277]
Chitosan/rectorite nano-hybrid composite microspheres	25 °C, pH 5	16.53	Langmuir	PSO	[278]
Chitosan nanofibril	25 °C, pH 5	60.85	Langmuir	PSO	[279]
Chitosan saturated montmorillonite	25 °C	14.33	Langmuir	PSO	[280]
CNM	25 °C, pH 5	75.76	Langmuir	PSO	This work
MA-CNM	25 °C, pH 5	215.52	Langmuir	PSO	This work

The reported adsorbents in the literature were costly, time consuming, need inert atmospheric condition, and high temperature for synthesis. But, compared with the reported once, the prepared CNM and S-CNM, CNM and DACNM, MA-CNM, and DACNM adsorbents were less expensive, less time consuming and needed low and room temperature of working range for synthesis and gave reasonably good adsorption efficiency as indicated in Table (13-16). Within the framework of a sustainable, greener and scalable process it should be implemented in current industrial wastewater applications in large scale; which were explained under application of CNM and S-CNM, CNM and MA-CNM, CNM and DACNM, and DACNM adsorbents for the removal of Cr(VI), Pb(II), Cd(II), and MB cations from real industrial effluents wastewater samples.

Table 16: Comparison of adsorption capacity of cationic MB by different adsorbents

Adsorbent	Adsorption condition	qm(mg/g)	Isotherms	Kinetics	References
Moroccan pozzolana	25 °C, pH 9	43.86	Langmuir	PSO	[281]
UiO-66/nanocellulose aerogels	25 °C, pH 7	51.8	Langmuir	PSO	[282]
Carbon sheet@sea sand composite (CS@SSC)	25 °C, pH 2	83.33	Langmuir	PSO	[283]
ZnO/cellulose nanocrystal hybrids	25 °C	33.6	-	PSO	[284]
DACNM	25 °C, pH 8	90.91	Langmuir	PSO	This work

4.8. Desorption of Cr(VI), Cd(II), Pb(II), and MB cations

Desorption studies help in understanding the reusability of the adsorbents without any loss of effectiveness of the adsorbent. Therefore, different eluents were engaged to desorb adsorbates (Cr(VI), Cd(II), Pb(II), and cationic MB dyes) from adsorbents (S-CNM, MA-CNM, and DACNM), respectively [26]. Thus, desorption of Cr(VI), Cd(II), Pb(II), and cationic MB dyes are performed using 10 mL of 0.1 M HCl and presented in Figure 32. The obtained results indicate that the maximum percent desorption of Pb(II) ions is found to be 94.5% from DACNM adsorbent with a low solution pH of 2. Similarly, the maximum percent desorption of Cd(II) ions is found to be 74.2% from MA-CNM with a low solution pH of 2. Also, the maximum percent desorption of Cr(VI) ions and cationic MB dye is found to be 70.6% and 71.5% from S-CNM and DACNM, respectively, with a low solution pH of 2. From these results, it is possible to confirm that adsorbates were possibly desorbed under low pH values to that of the maximum adsorption of adsorbate took place [285]. After the adsorbates desorption, the adsorbents were separated, carefully washed with distilled water, and dried.

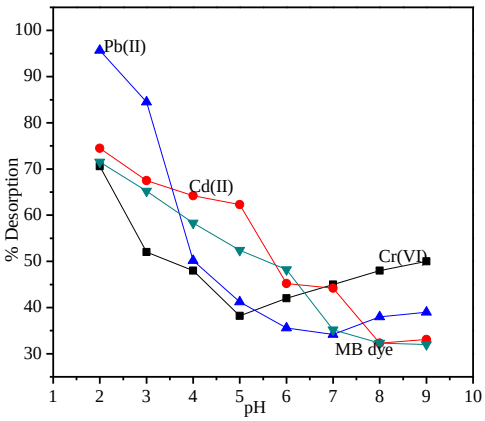

Figure 32. Effect of pH on desorption of Cr(VI), Cd(II), Pb(II) ions and MB dyes using S-CNM, MA-CNM, and DACNM adsorbents, respectively, at varied pH values.

4.9. Regeneration Test

To make the adsorption processes cost-effective and appropriate at commercial scale, the regeneration of the used adsorbents are essential. The regenerated and dried adsorbents were subsequently re-used as adsorbent for at least 13^{th} cycles. The results found that the adsorption capabilities of the contaminants for adsorbents were progressively decreased with increasing cycles of reusable trial (Figure 33). The decrease in uptake capability of the adsorbents with increased reusable times is ordinarily because of the loss of active sites on the surfaces of adsorbents. The pleased reusability with conserving basically high uptake abilities for the adsorbents postulates the adsorbents were effective for operating the uptake process of the stated contaminants. Generally, it was found that the pollutant removal ability of the adsorbents did not suggestively change after 13^{th} cycle of procedure as the %R until high. The %R for each successive cycle was less than 6%. In the whole, this confirms that adsorbents could be used for contaminant uptake for long time with good possibility. The results of regeneration studies for all of the studied adsorbents are summarized in Table 17.

Table 17. The results of regeneration studies for all of the studied adsorbents.

Adsorbents	Adsorbates	Regenerants	Cycles	Regeneration efficiency (%)
			1^{st}	90.2
S-CNM	Cr(VI)	HCl (0.1M)	4^{th}	75
			13^{th}	50
			1^{st}	88
MA-CNC	Cd(II)	HCl (0.1M)	4^{th}	67
			13^{th}	50
			1^{st}	96
DACNM	Pb(II)	HCl (0.1M)	4^{th}	85
			13^{th}	80
			1^{st}	76
DACNM	MB dye	HCl (0.1M)	4^{th}	60
			13^{th}	50

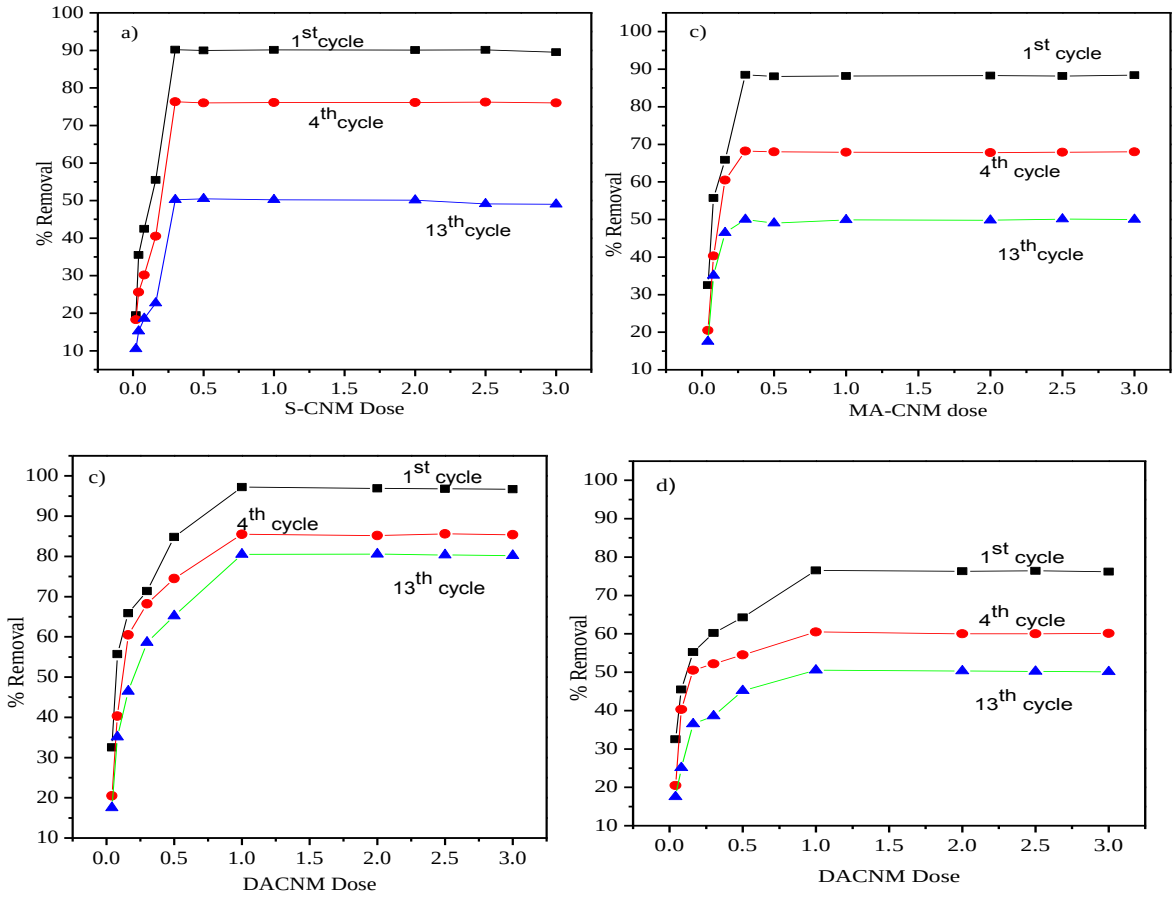

Figure 33. Percentage of Cr(VI) ions (a), Cd(II) ions (b) and (Pb(II) ions & cationic MB dyes) (c & d) removal after different cycles (1^{st}, 4^{th} and 13^{th}) by S-CNM, MA-CNM, and DACNM adsorbents, respectively at optimum pH of (5, 8, & 6), room temperature, C_i of (2, 20, & 30 mgL^{-1}), contact time of (90,120,&120 min.), and agitation speed of (300, 250, & 250 rpm).

5. CONCLUSION AND RECOMMENDATIONS

5.1. Conclusion

Recently, Wastewater (WW) treatment technologies were the most crucial issues all over the world. Thus, biodegradable, nontoxic, cost-effective and easily available pristine (CNM) and chemically functionalized (S-CNM, MA-CNM and DACNM) adsorbents were prepared from easily available and cheap lignocellulosic biomass by sulfuric acid hydrolysis methods. The prepared adsorbents were characterized using TGA-DTA, FTIR, XRD, SEM and EDX characterization techniques. Next, the prepared adsorbents were applied to the removal of Cr(VI) Cd(II) and (Pb(II) ions & cationic MB dyes from real wastewater. The WW samples were collected from the selected sites by using EPA guide line protocols. The collected WW physicochemical analyses were performed within 24 hours after collection. All the adsorption studies were performed by using batch experiments.

The optimization of different parameters that affects the adsorption processes was performed. The adsorption processes of Cr(VI), Cd(II), and Pb(II) ions were well fitted with Langmuir and Freundlich isotherm models with maximum uptake capacity of (60.24 & 156.25) mgg^{-1} for (CNM & S-CNM), respectively, (75.76 & 215.52) mgg^{-1} for (CNM & MA-CNM), and (91.74 & 384.62) mgg^{-1} for (CNM & DACNM), respectively. This mechanism suggests the adsorption occur at both monolayer and multilayer the adsorbents active sites. The rate of the interaction between the Cr(VI), Cd(II), and Pb(II) ions by (CNM & S-CNM), (CNM & MA-CNM), and (CNM & DACNM) adsorbents, respectively were described by PSO model. The adsorption processes was carried out by the force of electrostatic attraction between the negatively charged adsorbent surfaces and positively charged metal ions.

The adsorption process of cationic MB dyes was well fitted with Langmuir and Freundlich isotherm models with maximum uptake capacity of 90.91 mgg^{-1} by DACNM adsorbent. PSO kinetics model was well suited for the uptake of cationic MB by the force of electrostatic attraction between the negatively charged adsorbent surfaces and cationic MB dye. In addition to the color removal, uptake by DACNM adsorbent was decreased with the presence of

different physicochemical parameters of the WW. This recommends that the MB uptake processes occur both in monolayer and multilayer of adsorbents active sites.

Generally, the results obtained from adsorption study have shown that the adsorption efficiencies of the adsorbents for the %R of cations were affected by the presence of cations and %R of Cr(VI) ions affected by presence of anions in the WW sample. Furthermore, the higher adsorption capacity observed by the chemically modified adsorbents than pristine adsorbents. Finally, the desorption study of Cr(VI), Cd(II), Pb(II) ions, and cationic MB dyes from their respective adsorbents was done in accordance with the solution pH values. After the desorption study, the recycled adsorbents were re-applied as adsorbents for 13^{th} successive cycles with less than 6% in each successive cycles. Results have shown that, the adsorbents were recyclable and economically friendly re-used at least 13^{th} successive cycles for contaminant removals. In the whole, the obtained results suggested that both pristine and chemically modified (CNM & S-CNM, CNM & MA-CNM, and DACNM) adsorbents were an effective adsorbents for the removal of Cr(II), Cd(II), Pb(II) ions, and cationic MB dyes in particular and contaminants in general from the real WW.

5.2. Recommendations

From the findings it is possible to conclude that the adsorbent shows that it is capable of removing Cr(VI), Cd(II), Pb(II), MB cations from WW. Therefore, arising from the outcome of the study the following recommendations are made:

- Carry out the research on the removal of anionic pollutants using these adsorbents from WW.
- Future studies will focus on optimization of CNMs chemical modifications specified for specific industrial effluents and understanding how other charged and uncharged pollutants affect the adsorption.
- The research results of this dissertation will be used as a foundation for future research in which modified CNMs adsorbents can be employed in pilot/full-scale applications.
- In the long run, the goal is to produce commercially competitive cellullulose nanomaterial adsorbents to immobilize pollutant ions for wastewater treatement.
- Also, a study considering the effect of ionic strength and CNMs adsorbents characterization by BET, AFM, TEM, and XPS is required for further study.
- Greener approach in modifying nanocellulose should be encouraged

6. REFERENCES

[1]. Berger, E., Haase, P., Kuemmerlen, M., Leps, M., Bernhard, R., & Sundermann A. (2017), 'Water quality variables and pollution sources shaping stream macroinvertebrate communities,' *Water Res*earch, 5: pp. 881–10.

[2]. Brandes, R., Belosinschi, D., Brouillette, F., & Chabot, B. (2019), 'A new electrospun chitosan / phosphorylated nanocellulose biosorbent for the removal of cadmium ions from aqueous solutions,' *Journal of Environmental Chemical Engineering,* 7: pp. 103477.

[3]. Haji, M., Melesse, A.M., & Reddi, L. (2016), 'Water quality assessment and apportionment of pollution sources using APCS-MLR and PMF receptor modeling techniques in three major rivers of South Florida,' *Science of the Total Environment,* 567: pp. 1552–1567.

[4]. Anush, S.M., Chandan, H., & Vishalakshi, R. (2019), 'Synthesis and metal ion adsorption characteristics of graphene oxide incorporated chitosan Schiff base,' *International Journal of Biological Macromolecules,* 126: pp. 908–916.

[5]. Stobel, J., Christy, E., Gopi, S., Rajeswari, A., Sudharsan, G., & Pius, A. (2019), 'Highly crosslinked 3-D hydrogels based on graphene oxide for enhanced remediation of multi contaminant wastewater,' *Journal of Water Processing Engineering,* 31: pp.100850.

[6]. Tofighy, M.A., & Mohammadi, T. (2020), 'Divalent heavy metal ions removal from contaminated water using positively charged membrane prepared from a new carbon nanomaterial and HPEI,' *Chemical Engineering Journal,* 388: pp. 124192.

[7] Singh, N.B., Nagpal, G., & Agrawal, S. (2018), 'Water purification by using adsorbents: a review, *Environmental Technology Innovation,* 11: pp. 187–240.

[8] Jehan, S., Khan, S., Anjum, S., Muhammad, S., & Rashid, A. (2019), 'Hydrochemical properties of drinking water and their sources apportionment of pollution in Bajaur agency, Pakistan,' *Measurement,* 139: pp. 249–257.

[9]. Abdelrahman M., Awad, Rem, Jalab, Abdelbaki, Benamor, Mustafa S., Nasser, Muneer M., Ba-Abbad, Muftah, El-Naas, & Abdul Wahab, Mohammad (2020), 'Adsorption of organic pollutants by nanomaterial-based adsorbents: An overview,' *Journal of Molecular Liquids,* 301: pp. 112335.

[10]. Shu, Y., Fanyong, Z., Lu W., Yedong, R., Peigang, H., Dechang, J., & Jinlong Y. (2019), 'A green and low-cost hollow gangue microsphere/geopolymer adsorbent for the effective removal of heavy metals from wastewaters', *Journal of Environmental Management,* 246: pp. 174–183.

[11]. Guo, S., Dan, Z., Duan, N., Chen, G., Gao, W. & Zhao, W. (2018), Zn (II), Pb (II), and Cd (II) adsorption from aqueous solution by magnetic silica gel: preparation, characterization, and adsorption,' *Environmental Science and Pollution Research*, 25: pp. 30938–30948.

[12]. Zhao, X., Liu, S., Tang, Z., Niu, H., Cai Y., & Meng, W. (2015), 'Synthesis of magnetic metal-organic framework (MOF) for efficient removal of organic dyes from water,' *Scientific Reports*, 5: pp. 11849 | doi: 10.1038/srep11849.

[13]. Amanda, A., Rifathin, A., Arum, A., Sampora, Y. (2020), 'Oil palm empty fruit bunch-based nanocellulose as a super-adsorbent for water remediation,' *Carbohydrate Polymer*, 229: pp. 115433.

[14]. Islam, M. A., Morton, D. W., Johnson, B. B., Pramanik, B. K., Mainali, B.and Angove, M. J. (2018), 'Opportunities and constraints of using the innovative adsorbents for the removal of cobalt(II) from wastewater: A review,' *Environmental Nanotechnology, Monitoring and Management*, 10: pp. 435–456.

[15]. Shahnaz, T., Sharma, V., Subbiah, S., & Narayanasamy, S. (2020), 'Multivariate optimisation of Cr (VI), Co (III) and Cu (II) adsorption onto nanobentonite incorporated nanocellulose / chitosan aerogel using response surface methodology,' *Journal of Water Processing Engineering*, 36: pp.101283.

[16]. Tshikovhi, A., Mishra, S.B., & Mishra, A.K. (2020), 'Nanocellulose-based composites for the removal of contaminants from wastewater,' *International Journal of Biological Macromolecules*, 152: pp. 616–632.

[17]. Bhanjana, G., Dilbaghi, N., Kim, K., Kumar, S. (2017), 'Carbon nanotubes as sorbent material for removal of cadmium,' *Journal of Molecular Liquids*, 242: pp. 966–970.

[18]. Atkovska, K., Lisichkov, K., Ruseska, G., & Dimitrov, A.T. (2018), 'A Removal of heavy metal ions from wastewater using conventional and nanosorbents: A review,' *Journal of Chemical Technology Metallargy*, 53(2): pp. 202-219.

[19]. Nguyen, K.M., Nguyen, B.Q., Nguyen, H.T., & Nguyen, H.T.H. (2019), 'Adsorption of Arsenic and Heavy Metals from Solutions by Unmodified Iron-Ore Sludge,' *Applied Science*, 9: pp. 619.

[20]. Xu, Q., Wang, Y., Jin, L., Wang, Y., & Qin, M. (2017), 'Modified cellulose membrane with good durability for effective oil-in- water emulsion treatment,' *Journal of Hazardious Matererials*, 339: pp. 91–99.

[21]. Gaurav, B., Neeraj, D., Ki-Hyun, K. & Sandeep, K. (2017), 'Carbon nanotubes as sorbent material for removal of cadmium,' *Journal of Molecular Liquids*, 242: pp. 966–970.

[22]. Rathnasekara, R. A. S. D., Botheju, W. S. M., Liyanage, J. A., Weragoda, S. K., & Kularathne K. A. M. (2021), 'Risk Assessment of Trace Element Contamination in Drinking

Water and Agricultural Soil: A Study in Selected Chronic Kidney Disease of Unknown Etiology (CKDu) Endemic Areas in Sri Lanka,' *Journal of Chemistry,* 1: pp. 1-10.

[23]. Ayangbenro, A.S. & Babalola, O.O. (2017), 'A New Strategy for Heavy Metal Polluted Environments: A Review of Microbial Biosorbents,' *International Journal of Environmental Research and Public Health,* 14: PP. 94.

[24]. Wu, Z., Zhong, H., Yuan, X., Wang, H., Wang, L., Chen, X., Zeng, G., Wu, Y. (2014), 'Adsorptive removal of methylene blue by rhamnolipid-functionalized grapheme oxide from wastewater,' *Water Research,* 67: pp. 330–344.

[25]. Mohd Nor, F. N., Noor Azilah, M. K., Victor, F. K., and Wan Md, Z. W. Y. et al. (2021), 'Nanocellulose: a bioadsorbent for chemical contaminant remediation,' *RSC Advances,* 11: pp. 7347–7368.

[26]. Agnes, P., Eliazer, B. N., and Augustine, E. O. (2020), 'Batch and continuous flow studies of Cr(VI) adsorption from synthetic and real wastewater by magnetic pine cone composite,' *Chemical Engineering Research and Design*, 153: pp. 806–818.

[27]. Anjum, M., Miandad, R., Waqas, M., Gehany, F., & Barakat, M.A. (2019), 'Remediation of wastewater using various nano-materials,' *Arabian Journal of Chemistry,* 12: pp. 4897–4919.

[28]. Mohib, U., Ruqia, N., Muslim, K., Waliullah, K., Mohib, S., Sahib, G. A., and Amir, Z. (2020), 'The effective removal of heavy metals from water by activated carbon adsorbents of Albizia lebbeck and Melia azedarach seed shells,' *Soil and Water Research*, 15: pp. 30–37.

[29]. Matsis V. M. and Grigoropoulou H. P. (2008), 'Kinetics and equilibrium of dissolved oxygen adsorption on activated carbon," *Chemical Engineering Science*, 63: pp. 609–621.

[30]. Nur Syahirah, Kamarudin, Rohayu, Jusoh, Herma Dina, Setiabudi, Nuramira Fateha, Sukor, & Jun Haslinda, Shariffuddin, (2020), 'Potential nanomaterials application in wastewater treatment: Physical, chemical and biological approaches,' *Materials Today: Proceedings xxx (xxxx) xxx*, Article in press.

[31]. Biming, L., Zhenxue, L., Haixia, W., Shunlong, P., Xing, C., Yongjun, S., Yanhua, X., (2020), 'Effective and simultaneous removal of organic/inorganic arsenic using polymer-based hydrated iron oxide adsorbent: Capacity evaluation and mechanism,' *Science of the Total Environment*, 742: pp. 140508.

[32]. Jianhua, Q., Xue, T., Zhao, J., Bo, C., Modupe, S. A., Qi, H., Chengcheng, F., Yan, F., Xianlin, M., Ying, Z. (2020), 'Multi-component adsorption of Pb(II), Cd(II) and Ni(II) onto microwavefunctionalized cellulose: Kinetics, isotherms, thermodynamics, mechanisms and application for electroplating wastewater purification', *Journal of Hazardous Materials,* 387: pp. 121718.

[33]. Yeit, H. T., Siti, N. A., & Kah, C. H., (2020), 'Sustainable approach to the synthesis of cellulose membrane from oil palm empty fruit bunch for dye wastewater treatment,' *Journal of Water Process Engineering*, 34: pp. 101182.

[34]. Khalil, H. P. S. A., Khalil, H., Davoudpour, Y., Mustapha, A., Islam, M. N., Sudesh, K., … Jawaid, M. (2014), 'Production and modification of nanofibrillated cellulose using various mechanical processes: A review,' *Carbohydrate Polymers*, *99*: pp. 649–665.

[35]. Nilanjal, M., Swarnima, R., Narender, K. G., Shubhangi, A. S., & Virendra, K., (2020), 'Radiation grafted cellulose fabric as reusable anionic adsorbent: A novel strategy for potential large-scale dye wastewater remediation,' *Carbohydrate Polymers*, 249: pp. 116902.

[36]. Chen, X., Liu, L., Luo, Z., Shen, J., Ni, Q., & Yao, J. (2018), 'Facile preparation of a cellulose based bioadsorbent modified by hPEI in heterogeneous system for high-efficiency removal of multiple types of dyes,' *Reactive and Functional Polymers*, 77: pp. 83-125.

[37]. Kim, J. H., Shim, B. S., Kim, H. S., Lee, Y. J., Min, S. K., Jang, D., … Kim, J. (2015), 'Review of nanocellulose for sustainable future materials,' *International Journal of Precision Engineering and Manufacturing Green Technology*, 2(2): pp. 197–213.

[38]. Ahankari, S., George, T., Subhedar, A., and Kar, K. K. (2020), 'Nanocellulose as a sustainable material for water purification,' *SPE Polymers*, 1: 69–80.

[39]. Hokkanen, S., Bhatnagar, A., & Sillanpaa, M. (2016) 'A review on modification methods to cellulose-based adsorbents to improve adsorption capacity,' *Water Research*, 91: pp. 156–173.

[40]. Anirudhan, T. S. & Deepa, J. R. (2015), 'Synthesis and characterization of multi-carboxyl-functionalized nanocellulose/nanobentonite composite for the adsorption of uranium (VI) from aqueous solutions : Kinetic and equilibrium profiles,' *Chemical Engineering Journal*, 273: pp. 390–400.

[41]. Iyabode, A., Felicia, L., Okunola, A., Ajao, J., and Victor, T. (2021), 'Isolation and characterization of nanocrystalline cellulose from cocoa pod husk (CPH) biomass wastes,' *Heliyon*, *7*: pp e06680.

[42]. Pyrzynska, K. 'Removal of cadmium from wastewaters with low-cost adsorbents,' *Journal of Environmental Chemical Engineering*, vol. 7, No. 1, pp. 102795, 2019. 127

[43]. Kumagai, A., Endo, T., & Adachi, M. (2019), 'Evaluation of Cellulose Nanofibers by Using Sedimentation Method,' *JAPAN TAPPI Journal*, 73: pp. 461–469.

[44]. Quim, T., Oliver-Ortega, H., Manel, A., Xavier Espinach, F., Pere, M., & Delgado-Aguilar, M. (2020), 'Research on the Strengthening Advantages on Using Cellulose Nanofibers as Polyvinyl Alcohol Reinforcement,' *Polymers*, 12: pp. 974.

[45]. Khatri, Z., Mayakrishnan, G., Hirata, Y., Wei, K. & Kim, I. S. (2013), 'Cationic-cellulose nanofibers: Preparation and dyeability with anionic reactive dyes for apparel application,' *Carbohydrate Polymers*, 91(1): pp. 434–443.

[46]. Deepa, B., Abraham, E., Cordeiro, N., Mozetic, M., Mathew, A. P., Oksman, K., … Pothan, L. A. (2015), 'Utilization of various lignocellulosic biomass for the production of nanocellulose,' a comparative study. *Cellulose*, 22(2): pp. 1075–1090.

[47]. Hang, Z., Hongxiang, Z., Fei, X., Hui, H., & Shuangfei, W. (2019), 'Cellulose-based amphoteric adsorbent for the complete removal of low-level heavy metal ions via a specialization and cooperation mechanism,' *Chemical Engineering Journal*, 385: pp. 123879.

[48]. Jian, Wang, Min, Liu, Chao, Duan, Jianpeng, Sun, & Yaowei, Xu, (2019), 'Preparation and characterization of cellulose-based adsorbent and its application in heavy metal ions removal,' *Carbohydrate Polymers*, 206: pp. 837–843.

[49]. Cheng, J., Zhan, C., Wu, J., Cui, Z., Si, J., Wang, Q., Peng, X., & Lih-Sheng T. (2020), 'Highly Efficient Removal of Methylene Blue Dye from an Aqueous Solution Using Cellulose Acetate Nanofibrous Membranes Modified by Polydopamine,' *ACS Omega* 5: pp. 5389−5400.

[50]. Qi, Wu, Hui, He, Hang, Zhou, Fei, Xue, Hongxiang, Zhu, Shile, Zhou, Lei, Wang, & Shuangfei, Wang, (2020), 'Multiple active sites cellulose-based adsorbent for the removal of low-level Cu(II), Pb(II) and Cr(VI) via multiple cooperative mechanisms,' *Carbohydrate Polymers*, 233: pp. 115860.

[51]. Jing, Liu, Tai-Wen, Chen, Ya-Li, Yang, Zong-Chun, Bai, Li-Ru, Xia, Min, Wang, Xiao-Lan, Lv, & Li, L. (2020), 'Removal of heavy metal ions and anionic dyes from aqueous solutions using amide-functionalized cellulose-based adsorbents,' *Carbohydrate Polymers*, 230: pp. 115619.

[52]. Shan, Lu, Wenbin, Liu, Yabo, Wang, Yongkui, Zhang, Panyu, Li, Diyong, Jiang, Cuiting, Fang, & Yonghong, Li, (2019), 'An adsorbent based on humic acid and carboxymethyl cellulose for efficient dye removal from aqueous solution,' *International Journal of Biological Macromolecules*, 135: pp. 790–797.

[53]. Martin, A., H., Keith, R., B., W. Gilbert, O. & Yogesh, Ch., S. (2012), 'Cellulosic Substrates for Removal of Pollutants From Aqueous Systems: a Review,' *Bioresources*, 7(2): pp. 2592–2687.

[54]. Parisa, Moharrami, & Elaheh, Motamedi, (2020), Application of cellulose nanocrystals prepared from agricultural wastes for synthesis of starch-based hydrogel nanocomposites: Efficient and selective nanoadsorbent for removal of cationic dyes from water,' *Bioresource Technology*, 313: pp. 123661.

[55]. Bassyouni, M., Zoromba, M. S. & Drioli, E. (2019), 'A review of polymeric nanocomposite membranes for water purification,' *Journal of Industrial and Engineering Chemistry*, 73: pp. 19–46.

[56]. Adel, A., El-Shafei, A., Ibrahim, A. and Al-Shemy, M. (2018), 'Extraction of oxidized nanocellulose from date palm (Phoenix Dactylifera L.) sheath fibers: Influence of CI and CII polymorphs on the properties of chitosan/bionanocomposite films,' *Industrial Crops and Products*, *124*: pp. 155–165.

[57]. Do Nascimento, J. H. O., Luz, R. F., Galvao, F. M. F., Melo, J. D. D., Oliveira, F. R., Ladchumananandasivam R. & Zille, A. (2015), 'Extraction and Characterization of Cellulosic Nanowhisker Obtained from Discarded Cotton Fibers,' *Materials Today: Proceedings*, *2*(1): pp. 1–7.

[58]. Harini, K., Ramya, K. & Sukumar, M. (2018), 'Extraction of nano cellulose fibers from the banana peel and bract for production of acetyl and lauroyl cellulose,' *Carbohydrate Polymers*, *201*: pp. 329–339.

[59]. Yang, X., Han, F., Xu, C., Jiang, S., Huang, L., Liu, L. & Xia, Z. (2017), 'Effects of preparation methods on the morphology and properties of nanocellulose (NC) extracted from corn husk,' *Industrial Crops and Products*, 109: pp. 241–247.

[60]. WHO, (2017), 'WHO Joint Monitoring Program for Water Supply, Sanitation and Hygiene (JMP),' *Annual report*.

[61]. Islam, M.A., Ali I., Karim, S.M.A., Hossain Firoz, M.S., Chowdhury, A.-N., Morton D.W., Angove M.J., (2019), ' Removal of dye from polluted water using novel nano manganese oxide-based materials,' *Journal of Water Process Engineering*, 32: pp. 100911.

[62]. Lee, L.Y., Chin, D.Z.B., Lee, X.J., Chemmangattuvalappil, N., & Gan, S., (2015a), 'Evaluation of Abelmoschus esculentus (lady's finger) seed as a novel biosorbent for the removal of Acid Blue 113 dye from aqueous solutions,' *Process Safety and Environmental Protection*, 94: pp. 329-338.

[63]. Coppeaux, Z., Corral-Colliere, C., Ilhami, A., Laigle, R., Savu, N., & Soudan, M. (2016), Does Ethiopia have a comparative advantage in the leather industry? (February, 2016). Retrieved from *http://www.cerna.mines-paristech.fr/Donnees/data12/1259*- Mines-ParisTech-Working-Paper-Ethiopia-2016.pdf. 40 pp.

[64]. Tesfaye, Admassu, Abate, Adey, Desta, F., & Nancy, G. Love, (2020), 'Evaluating tannery wastewater treatment performance based on physicochemical and microbiological characteristics: An Ethiopian case study,' *Water Environment Research*, pp. 1–12.

[65]. UNIDO (2010), 'Enhancing the Ethiopian leather industry and its market competitiveness,' Organized By Leather Industry Development Institute (LIdI) In

Collaboration With United Nations Industrial Development, *Proceeding of National Workshop,* July 2010, Adama, Ethiopia.

[66]. Jan G. and Werner R. (2019), 'The Ethiopian Leather and Leather Products Sector: An Assessment of Export Potentials to Europe and Austria,' Vienna, Austrian Foundation for Development Research, pp. 77.

[67]. Simoes, A. J. G. & Hidalgo, C. A.. (2011), 'The economic complexity observatory: An analytical tool for understanding the dynamics of economic development,' Scalable Integration of Analytics and Visualization*: Papers from the 2011 AAAI Workshop* (WS-11-17). pp. 39-40.

[68]. Dierig, S. (1999), 'Urban environmental management in Addis Ababa: problems, perspectives, and the role of NGOs.(unpublished).

[69]. LIDI, (2018), 'Leather Industry Development Institute held discussion with stakeholders on 2017/18 performance review and 2018/19 fiscal year planning,' *http://www.elidi.org/images/discussionwithstakeholders*.pdf (11/3/2019).

[70]. Sarma, G.K., (2015),'Adsorptive removal of cationic and anionic dyes from water: a case study with kaolinite and acid-treated kaolinite,' *Journal of Applied and Fundamental Sciences,* 1: pp. 32.

[71]. Alderin, C. (2014), 'Challenges and Opportunities in Emerging Textile Industry in Ethiopia, Department of Social and Economic Geography, Uppsala Universitet, Uppsala, Sweden, pp. 32.

[72]. Hundessa, D. D., Tatek, T., Hanna, B. L. (2020), 'Assessment on technology utilization of Ethiopian selected manufacturing industries,' Assessment Report: Ministry of Innovation and Technology, Ethipia., *Ethiopian Society of Chemical Engineers,* pp. 47.

[73]. Chandanshive, V., Kadam, S., Rane, N., Jeon, B., Jadhav, J., & Govindwar, S. (2020), 'Chemosphere In situ textile wastewater treatment in high rate transpiration system furrows planted with aquatic macrophytes and fl oating phytobeds,' *Chemosphere,* 252: pp. 126513.

[74]. Suvendu, M., Debasis, R., Prosenjit, S., Deepu, G., & Sabu T. (2017), 'Rapid methylene blue adsorption using modified lignocellulosic materials,' *Process Safety and Environmental Protection,* 107: pp. 346–356.

[75]. Kishor, R., Purchase, D., Dattatraya, G., Ganesh, R., Fernando, L., Ferreira, R., … Naresh, R. (2021), 'Ecotoxicological and health concerns of persistent coloring pollutants of textile industry wastewater and treatment approaches for environmental safety,' *Journal of Environmental Chemical Engineering,* 9: pp. 105012.

[76]. Rahil, Kiani, Fatemeh, Mirzaei, Farshid, Ghanbari, Rouzhan, Feizi, & Fayyaz, Mehdipour, (2020), 'Real textile wastewater treatment by a sulfate radicals-Advanced Oxidation Process: Peroxydisulfate decomposition using copper oxide (CuO) supported onto activated carbon,' *Journal of Water Process Engineering* , 38: pp. 101623.

[77]. Jindrayani Nyoo, Putro, Alfin, Kurniawan, Suryadi, Ismadji, & Yi-Hsu, Ju, (2017), 'Nanocellulose based biosorbents for wastewater treatment: Study of isotherm, kinetic, thermodynamic and reusability,' *Environmental Nanotechnology, Monitoring & Management* 8: pp. 134–149.

[78]. Yashvi, Sheth, Swapnil, Dharaskar, Mohammad, Khalid, Shriram, Sonawane, (2021), 'An environment friendly approach for heavy metal removal from industrial wastewater using chitosan based biosorbent: A review,' *Sustainable Energy Technologies and Assessments*, 43: pp. 100951.

[79]. Jun, Liua, Stefan, Willfor, & Albert, Mihranyan, (2017), 'On importance of impurities, potential leachables and extractables in algal nanocellulose for biomedical use,' *Carbohydrate Polymers*, 172: pp. 11–19.

[80]. Adel, A., El-Shafei, A., Ibrahim, A. & Al-Shemy, M. (2018), 'Extraction of oxidized nanocellulose from date palm (Phoenix Dactylifera L.) sheath fibers: Influence of CI and CII polymorphs on the properties of chitosan/bionanocomposite films,' *Industrial Crops and Products*, 124: pp. 155–165.

[81]. Suman, K. A., Gera, M. & Jain, V. K. (2015), 'A novel reusable nanocomposite for complete removal of dyes, heavy metals and microbial load from water based on nanocellulose and silver nano-embedded pebbles,' *Environmental Technology, (United Kingdom)*, 36: pp. 706–714.

[82]. Fu, F. & Wang, Q. (2011), 'Removal of heavy metal ions from wastewaters: a review,' *Journal of Environmental Management*, 92(3): pp. 407–418.

[83]. Mandeep, Kaura, Praveen, Sharma, & Santosh, Kumari, (2019), 'Response surface methodology approach for optimization of Cu^{2+} and Pb^{2+} removal using nanoadsorbent developed from rice husk, *Materials Today Communications*, 21: pp. 100623.

[84]. Tan, H., Ooi, B.S. and Leo, C.P. 'Future perspectives of nanocellulose-based membrane for water treatment," *Journal of Water Process Engineering*, 37: pp. 101502, 2020.

[85]. Subrata M. (2017), "Preparation, properties and applications of nanocellulosic materials," *Carbohydrate Polymers*, 163: pp. 301–316.

[86]. Maschal Tarekegn, M. (2018), 'Causes and impacts of shankila river water pollution in Addis Ababa, Ethiopia,' *Environmental Risk Assessessment and Remediat*ion, 2: pp. 21–30.

[87]. Kiani, R., Mirzaei, F., Ghanbari, F., Feizi, R., & Mehdipour, F. (2020), 'Real textile

wastewater treatment by a sulfate radicals-Advanced Oxidation Process : Peroxydisulfate decomposition using copper oxide (CuO) supported onto activated carbon,' *Journal of Water Process Engineering,* 38: pp. 1–8.

[88]. Khandaker, N.R., Afreen, I., Diba, D.S., Huq, F.B., Akter, T. (2020), 'Treatment of textile wastewater using calcium hypochlorite oxidation followed by waste iron rust aided rapid filtration for color and COD removal for application in resources challenged Bangladesh,' *Groundwater Sustainable Development*, 10: pp. 100342.

[89]. Hokkanen, S., Bhatnagar, A. & Sillanpaa, M. (2016), 'A review on modification methods to cellulose-based adsorbents to improve adsorption capacity,' *Water Research*, *91*: pp. 156–173.

[90]. Klaus-J Appenroth (2010), 'What are ''heavy metals'' in Plant Sciences?,' *Acta Physiol Plant* 32: pp. 615–619.

[91]. Bawuro, A. A., Voegborlo, R. B. and Adimado, A. A. (2018), 'Bioaccumulation of Heavy Metals in Some Tissues of Fish in Lake Geriyo,' *Journal of Environmental and Public Health*, 2018: pp. 7. https://doi.org/10.1155/2018/1854892.

[92]. Carolin, C. F., Kumar, P. S., Saravanan, A., Joshiba, G. J., & Naushad, M. (2017), 'Efficient techniques for the removal of toxic heavy metals from aquatic environment : A review,' *Journal of Environmental Chemical Engineering, 5*: pp. 2782–2799.

[93]. Verma, R., Vijayalakshmy, K., and Chaudhiry, V. (2019), 'Detrimental impacts of heavy metals on animal reproduction : A review: Detrimental impacts of heavy metals on animal reproduction : A review,' *Journal of Entomology and Zoology Studies,* 6: pp. 27-30.

[94] S. Chowdhury, M.A.J., Mazumder, O., & Al-Attas, T. H. (2016), 'Heavy metals in drinking water: Occurrences, implications, and future needs in developing countries,' *Science of the Total Environment*, 570: pp. 476–488.

[95] Amir, M., Anwar ul Haq, A. S., and Salma, B. (2020), 'Effective adsorption of hexavalent chromium and divalent nickel ions from water through polyaniline , iron oxide , and their composites,' *Applied Sciences*, 10: pp. 2882.

[96]. Vaiopoulou, E., Gikas, P. (2020), 'Regulations for chromium emissions to the aquatic environment in Europe and elsewhere,' *Chemosphere*, 254: pp. 126876.

[97]. Ab Latif, W., Anjum, A., Jawed, A. U. (2015), 'Lead toxicity: a review,' *Interdisciplinary Toxicology*, 2015; 8: pp. 55–64.

[98]. Mohsen, A., Sara H., and Masoud, A. (2015), 'Removal of lead ions from industrial wastewater: A review of Removal methods,' International Journal of Epidemiologic Research, 2015; 2(2): 105-109.

[99]. Sarai, Ramos-Vargas, Rafael, Huirache-Acuna, J. G., & Cortes-Martínez, R.Q. R. (2020), 'Effective lead removal from aqueous solutions using cellulose nano fibers obtained from water hyacinth,' *Water Supply,* 20: pp. 2715–2736.

[100]. Tinkov, A.A., Filippini, T., Ajsuvakovae, O.P., Skalnaya, M.G., Aasethf, J., Bjørklundh, G., Gatiatulinai, E.R., Popova, E.V., Nemereshinai, O.N., Huangk, P.T., et al. (2018), 'Cadmium and atherosclerosis: A review of toxicological mechanisms and a meta-analysis of epidemiologic studies,' *Environmental Research,* 162: pp. 240–260.

[101]. Sokol, R.Z. & Berman, N. (1991), 'The effect of age of exposure on lead-induced testicular toxicity,' *Toxicology,* 69: pp. 269–78.

[102]. Friberg, L.T., Elinder, G.G., Kjellstrom, T., Nordberg, G.F. ed. (1986), 'Cadmium and Health: A Toxicological and Epidemiological Appraisal, Volume 1: Exposure, Dose, and Metabolism,' 1st Edition, *Taylor and Frances eBooks*, USA, pp. 222.

[103]. Rahimzadeh, M.R., Rahimzadeh, M.R., Kazemi, S., & Moghadamnia, A.A. (2017), 'Cadmium toxicity and treatment: An update,' *Caspian Journal of International Medicine*, 8: pp. 135–145.

[104]. Genchi, G., Carocci, A., Lauria, G., Sinicropi, M.S., & Catalano, A. (2020), 'Nickel: Human health and environmental toxicology,' *International Journal of Environmental Research and Public Health*, 17: pp. 679.

[105]. Hogervost, J., Plusquin, M., Vangronsvel, J., Nawrot, T., Cuypers, A., Van Hecke, E., Roels, H.A., Carleer, R., & Staessen, J.A. (2007), 'House dust as possible route of environmental exposure to cadmium and lead in the adult general population,' *Environmental Research,* 103: pp. 30–37.

[106]. Casado, M., Anawar, H.M., Garcia-Sanchez, A., & Santa Regina, I. (2008), 'Cadmium and zinc in polluted mining soils and uptake by plants (El Losar mine, Spain),' *International journal of Environtal Pollution,* 33: pp. 146–159.

[107]. Satarug, S. (2018), Dietary Cadmium intake and its effects on kidneys. Review,' *Toxics,* 6: pp. 1-23.

[108]. Tinkov, A.A., Gritsenko, V.A., Skalnaya, M.G., Cherkasov, S.V., Aaseth, J., Skalny, A.V. (2018), 'Gut as a target for cadmium toxicity,' *Environmental Research,* 235: pp. 429–434.

[109]. IARC (1993), 'Monographs on the Evaluation of the Carcinogenic Risks to Humans Beryllium, Cadmium, Mercury and Exposures in the Glass Manufacturing Industry,' *IARC Scientific Publications*, Lyon, France, pp. 119–238.

[110]. IARC (1997), IARC Monographs on the Evaluation of Carcinogenic Risks to Humans-Beryllium, Cadmium, Mercury, and Exposures in the Glass Manufacturing Industry. In

Summary of Data Reported and Evaluation; *International Agency for Cancer Research-World Health Organization,* Geneva, Switzerland, 58: pp. 453.

[111]. Mezynska, M. & Brzóska, M.M. (2018), 'Environmental exposure to cadmium: A risk for health of the general population in industrialized countries and preventive strategies,' *Environmental Science and Pollution Research,* 25: pp. 3211–3232.

[112]. Tamas, M.J., Fauvet, B., Christen, P., & Goloubinoff, P. (2018), 'Misfolding and aggregation of nascent proteins: A novel mode of toxic cadmium action in vivo. Review:,' *Current Genetics* 64: pp. 177–181.

[113]. Buha, A., Jugdaohsingh, R., Matovic, V., Bulat, Z., Antonijevic, B., Kerns, J.G., Goodship, A., Hart, A., & Powell, J.J. (2019), 'Bone mineral health is sensitively related to environmental cadmium exposure-experimental and human data,' *Environmental Research*, 176: pp. 108539.

[114]. Jacobo-Estrada, T., Cardenas-Gonzalez, M., Santoyo-Sánchez, M.P., Thevenod, F., Barbier, O. (2018), 'Intrauterine exposure to cadmium reduces HIF-1 DNA-binding ability in rat fetal kidneys, *Toxics,* 6: pp. 1-11. doi:10.3390/toxics6030053.

[115]. Liu, Z., Cai, L., Liu, Y., Chen, W., Wan, Q. (2019), 'Association between prenatal cadmium exposure and cognitive development of offspring: A systematic review,' *Environmental Pollution*, 254: pp. 113081.

[116]. Han, Y.L., Sheng, Z., Liu, G.D., Long, L.L., Wang, Y.F., Yang, W.X., & Zhu, J.Q. (2015), 'Cloning, characterization and cadmium inducibility of metallothionein in the testes of the mudskipper Boleophthalmus pectinirostris,' *Ecotoxicology* and *Environmental* Safety, 119: pp. 1–8.

[117]. Prabu, S.M. & Shagirtha, K. (2019), 'Cadmium and Apoptosis: A Molecular Approach,' *Research and Reviews: Journal of Toxicology,* 6: pp. 8–17.

[118]. Somji, S., Garrett, S. H., Sens, M. A., Gurel, V., and Sens, D. A. (2004), 'Expression of Metallothionein Isoform 3 (MT-3) Determines the Choice between Apoptotic or Necrotic Cell Death in Cd^{+2} -Exposed Human Proximal Tubule Cells,' *Toxicological Sciences*, 80: pp. 358–366.

[119]. Muneko, N., Hideaki, N., Yasushi, S., Kazuhiro, N. and Teruhiko, K. (2017), 'Causes of death in patients with Itai-itai disease suffering from severe chronic cadmium poisoning: a nested case control analysis of a follow-up study in Japan,' *Biomedical Journal*, 7: pp. 015694. http://dx.doi. org/10.1136/bmjopen-2016- 015694.

[120]. WHO, (2006), 'A Compendium of Standards for Wastewater Reuse in the Eastern Mediterranean Region,' Regional Office for the Eastern Mediterranean Regional Centre for Environmental Health Activities CEHA: Los Angeles, CA, USA, pp. 1–19.

[121]. Saba, T., Minhas, F., Malik, M. I., Talpur, F. N., Jabbar, A., & Bhanger, M. I. (2018), 'Efficient Removal of Reactive Orange 107 Dye from Aqueous Media by Shrimp Shell Derived Chitosan Functionalized Magnetic Nanoparticles,' *American Journal of Analytical Chemistry*, 9: pp. 633–653.

[122]. Gholivand, M. B., Yamini, Y., Dayeni, M., & Seidi, S. (2015), 'Removal of methylene blue and neutral red from aqueous solutions by surfactant-modified magnetic nanoparticles as highly efficient adsorbent,' *Environmental Progress & Sustainable Energy*, 34: pp. 1683–1693.

[123]. Lee, L.Y., Chin, D.Z.B., Lee, X.J., Chemmangattuvalappil, N., & Gan, S., (2015a), 'Evaluation of Abelmoschus esculentus (lady's finger) seed as a novel biosorbent for the removal of Acid Blue 113 dye from aqueous solutions,' *Process Safety and Environmental Protect*ion, 94: pp. 329-338.

[124]. Garg, V.K., Amita, M.; Kumar, R., & Gupta, R. (2004), 'Basic dye (methylene blue) removal from simulated wastewater by adsorption using Indian Rosewood sawdust: A timber industry waste,' *Dye Pigment*,' 63: pp. 243–250.

[125]. Zhou, Y., Lu, J., Zhou, Y., & Liu, Y. (2019), 'Recent advances for dyes removal using novel adsorbents: a review,' *Environmental Pollution,* 252: pp. 352-365.

[126]. Es-sahbany, H., Berradi, M., Nkhili, S., Hsissou, R., Allaoui, M., & Loutfi, M. (2019), 'Removal of heavy metals (nickel) contained in wastewater-models by the adsorption technique on natural clay,' *Materials Today: Proceedings,* 13: 866–875.

[127]. Gholivand, M. B., Yamini, Y., Dayeni, M., & Seidi, S. (2015), 'Removal of methylene blue and neutral red from aqueous solutions by surfactant-modified magnetic nanoparticles as highly efficient adsorbent,' *Environmental Progress & Sustainable Energy,* 34(6): pp. 1683–1693.

[128]. Ji Z. (2017), 'Electrochemical degradation of diclofenac for pharmaceutical wastewater treatment,' *International Journal of Electrochemical Science,* pp. 7807-7816.

[129]. Abdullah, N., Yusof N., Lau W.J., Jaafar J. & Ismail A.F. (2019), 'Recent trends of heavy metal removal from water/wastewater by membrane technologies,' *Journal of Industrial and Engineering Chemistry,* 76: pp. 17-38.

[130]. Shahedi, A., Darban, A. K., Taghipour F. & Jamshidi-Zanjani, A. (2020), 'A review on industrial wastewater treatment via electrocoagulation processes,' *Current Opinion in Electrochemistry,* 22: pp.154–169.

[131]. Pohl, A. (2020), 'Removal of Heavy Metal Ions from Water and Wastewaters by Sulfur-Containing Precipitation Agents,' *Water, Air,and Soil Pollution,* 231,503: 1–17.

[132]. Chitpong N., Husson S.M. (2017), 'High-capacity, nanofiber-based ion-exchange membranes for the selective recovery of heavy metals from impaired waters,' *Separation and Purification Technology*, 179: pp. 94–103.

[133]. Fomkin, A. A. (2009), 'Nnoporous materials and their adsorption properties,' *Protection of Metals and Physical Chemistry of Surfaces*, 45(2): pp. 121–136.

[134]. Langmuir, I. (1918), 'The adsorption of gases on plane surfaces of glass, mica and platinum,' *Journal of American Chemical Society,* 40(9): pp. 1361–1403.

[135]. Hall K.R., Eagleton L.C., Acrivos A., Vermeulen, T. (1966), 'Pore- and solid-diffusion kinetics in fixed-bed adsorption under constant-pattern conditions,' *Industrial* and *Engineering Chemistry Fundamentals,* 5: pp. 212-223.

[136]. Freundlich, H. (1906), 'Uber die Adsorption in Losungen,' *Zeitschrift für Physikalische Chemie*, 57:pp. 385-470.

[137]. Hamdaoui, O. and M. Chiha, 2007. Removal of Methylene Blue from Aqueous Solutions by Wheat Bran, *Acta Chimica Slovenica* 54, 407–418.

[138]. Ho, Y.S. McKay, G. (1998), 'Kinetic models for the sorption of from aqueous solution by wood,' *Journal of Environmental Science and Health,* 76:183–191.

[139]. Rodrigues, L.A. & Silva, M.C.P. (2009), 'An investigation of phosphate adsorption from aqueous solution onto hydrous niobium oxide prepared by co-precipitation method,' *Colloids and Surfaces,* 334: pp. 191–196.

[140]. Laura García, Juan Carlos Leyva-Díaz, Eva Díaz, Salvador Ordóñez, (2021), 'A review of the adsorption-biological hybrid processes for the abatement of emerging pollutants: Removal efficiencies, physicochemical analysis, and economic evaluation,' *Science of the Total Environment,* 780: pp. 146554.

[141]. Aryee, A. A., Mpatani, F. M., Kani, A. N., Dovi, E., Han, R., Li, Z., and Qu, L. (2021), 'A review on functionalized adsorbents based on peanut husk for the sequestration of pollutants in wastewater : Modification methods and adsorption study,' *Journal of Cleaner Production* , 310: pp. 127502.

[142]. Weber Jr., W.J. (1985) Adsorption theory, concepts, and models. In: Slejko, F.L. (Ed.), Adsorption Technology: A Step by Step Approach to Process Evaluation and Application. Marcel Dekker, Inc., United States of America, pp. 3–18.

[143]. Ruthven, D.M. (1984), 'Principles of Adsorption & Adsorption Processes,' *Wiley-Interscience Publications*, Canada.

[144]. Ahsan, M.A., Islam, M.T., Imam, M.A., Hyder, A.G., Jabbari, V., Dominguez, N., Noveron, J.C. (2018c) Biosorption of bisphenol A and sulfamethoxazole from water using

sulfonated coffee waste: isotherm, kinetic and thermodynamic studies,' *Journal of Environmental Chemical Enginering,* 6: pp. 6602–6611.

[145]. Iakovleva, E. & Sillanpaa, M. (2013), 'The use of low-cost adsorbents for wastewater purification in mining industries,' *Environmental Science and Pollution Research*, *20*(11): pp. 7878–7899.

[146]. Ibrahim, M.M., Moustafa, H., Rahman, E., Mehanny, S., Hemida, M.H., & El-Kashif, E. (2020), 'Reinforcement of starch based biodegradable composite using Nile rose residues,' *Journal of Material Research Technol*ogy, 9(3): pp. 6160-71.

[147]. Mehanny, S., Darwish, L., Abd El Haleem, M., El-Kashif, E., Farag, M., Ibrahim, H. (2019), 'Effect of glue and temperatures on mechanical properties of starch-based biodegradable composites reinforced with bagasse fibers,' *Internal Journal of Biotechnology Biomaterials Engineering,* 1: pp. 11.

[148]. Vaisanen, T., Haapala, A., Lappalainen, R., Tomppo, L. (2016), 'Utilization of agricultural and forest industry waste and residues in natural fiber-polymer composites: a review,' *Waste Manag*ement, 54: pp. 62-73.

[149]. Yu, S., Sun, J., Shi, Y., Wang, Q., Wu, J., & Liu, J. (2021), 'Nanocellulose from various biomass wastes: Its preparation and potential usages towards the high value-added products,' *Environmental Science and Ecotechnology,* 5: pp. 100077.

[150]. Phanthong, P., Reubroycharoen, P., Hao, X., Xu, G., Abudula, A., & Guan, G. (2018), 'Nanocellulose: Extraction and application,' *Carbon Resources Conversion*, 1: pp. 32–43.

[151]. Abebe, A. (2018), 'Nitrogen release dynamics of Erythrina abyssinica and Erythrina brucei litters as influenced by their biochemical composition,' *African Journal of Plant Science,* 12: pp. 331–340.

[152]. Abebe, A. & Wassie, H. (2017), 'Aerobic mineralization of selected organic nutrient sources for soil fertility improvement in cambisols, Southern Ethiopia,' *African Journal of Environmental Science and Technology*, 11: pp. 79–88.

[153]. Andualem, B. & Gessesse, A. (2014), 'Proximate composition, mineral content and antinutritional factors of Brebra (Millettia ferruginea) seed flour as well as physicochemical characterization of its seed oil,' *SpringerPlus*, 3: pp. 1–10.

[154]. Heyne, K. (1987), 'Useful Plants in Indonesia 2nd edition. Bogor: Forestry Research and Development Agency,' Ministry of Forestry, Republic of Indonesia (in Indonesia). Pp. 68. ISBN: 978-979-8452-60-4.

[155]. Setyaningsih, L., Satria E., Khoironi , H., Dwisari, M., Setyowati, G., Rachmawati, N., Kusuma R. and Anggraeni, J. 'Cellulose extracted from water hyacinth and the application in hydrogel,' *Materials Science and Engineering*, 673: pp. 012017.

[156]. Asrofi, M., Abral, H., Kasim, A., Pratoto, A. Mahardika, M. Park, J.W., & Kim, H. J. (2018), 'Isolation of nanocellulose from water hyacinth fiber (WHF) produced via digester-sonication and its characterization,' *Fibers and Polymers*, 19: pp. 1618–1625.

[157]. Pakutsah, K., & Aht-ong, D. (2020), 'Facile isolation of cellulose nano fibers from water hyacinth using water- based mechanical de fi brillation : Insights into morphological , physical , and rheological properties,' *International Journal of Biological Macromolecules,* 145: pp. 64–76.

[158]. Haziqatulhanis, Ibrahim, Norazlianie, Sazali, Wan, Norharyati, Wan, Salleh, Muhammad, Nizam Zainal, Abidin (2020), 'A short review on recent utilization of nanocellulose for wastewater remediation and gas separation,' *Materials Today:* Proceedings xxx (xxxx) xxx. Article in Press.

[159]. Sarkar, M., Rahman, A.K.M.L., Bhoumik, N.C. (2017), 'Remediation of chromium and copper on water hyacinth (E. crassipes) shoot powder,' *Water Resources and Industry,* 17: pp. 1-6.

[160]. Ghanbarian, M., Nabizadeh, R., Nasseri, S., Shemirani, F., Mahvi, A.H., Beyki, M.H., & Mesdaghinia, A. (2017), 'Potential of amino-riched nano-structured $MnFe_2O_4$@cellulose for biosorption of toxic Cr (VI): modeling, kinetic, equilibrium and comparing studies,' *International Journal of Biological Macromolecules*, 104: pp. 465–480.

[161]. Tshikovhi, A., Shivani Mishra, B., Ajay Mishra, K. (2020), 'Nanocellulose-based composites for the removal of contaminants from wastewater,' *International Journal of Biological Macromolecules*, 152: pp. 616–632.

[162]. Ngah, W.S.W. & Hanafiah, M.A.K.M., (2008), 'Removal of heavy metal ions from wastewater by chemically modified plant wastes as adsorbents: a review,' *Bioresource. Technol*ogy, 99: pp. 3935–3948.

[163]. S. Mondal, (2017), 'Review on nanocellulose polymer nanocomposites,' *Polymer Plastics Technology and Engineering*, 57: pp. 1–15.

[164]. O'Connell, D.W., Birkinshaw, C., O'Dwyer, T.F., (2008), 'Heavy metal adsorbents prepared from the modification of cellulose: a review,' *Bioresource. Technol*ogy 99: pp. 6709–6724.

[165]. Hokkanen, S., Bhatnagar, A., Repo, E., Lou, S., Sillanpaa, M., (2016a), 'Calcium hydroxyapatite microfibrillated cellulose composite as a potential adsorbent for the removal of Cr(VI) from aqueous solution,' *Chem. Eng. J.* 283: pp. 445–452.

[166]. Hokkanen, S., Bhatnagar, A., Sillanpaa, M., (2016b), 'A review on modification methods to cellulose-based adsorbents to improve adsorption capacity,' *Water Resorce*, 91: 156–173.

[167]. Grishkewich, N., Mohammed, N., Tang, J., & Tam, K. C. (2017), 'Recent advances in the application of cellulose nanocrystals,' *Current Opinion in Colloid & Interface Science*,*29*: pp. 32–45.

[168]. Olivera, S., Muralidhara, K., Venkatesh, V.K., Guna, K., Gopalakrishna, Y., & Kumar K. (2016), 'Potential applications of cellulose and chitosan nanoparticles/composites in wastewater treatment: a review,' *Carbohydrate Polymer*, 153: pp. 600–618.

[169]. Mahmoud, M.E., Abdou, A.E.H., Sobhy, M.E. & Fekry, N.A. (2017), 'Solid-solid crosslinking of carboxymethyl cellulose nanolayer on titanium oxide nanoparticles as a novel biocomposite for efficient removal of toxic heavy metals from water,' *International Journal of Biological Macromolecules*, 105: pp. 1269-1278.

[170]. Maiti, S., Jayaramudu, J., Das, K., Reddy, S.M., Sadiku, R., Ray, S.S., & Liu, D. (2013), 'Preparation and characterization of nano-cellulose with new shape from different precursor,'*Carbohydrate Polymer,* 98: pp. 562–567.

[171]. Si, J., Cui, Z.,Wang, Q., Liu, Q., & Liu, C. (2016), 'Biomimetic composite scaffolds based onmineralization of hydroxyapatite on electrospun poly(-caprolactone)/nanocellulose fibers,' *Carbohydrate Polymer*, 143: pp. 270–278.

[172]. Gomez C., Serpa, H. A., Velasquez-Cock, J., Ganan, P., Castro, C., Velez, L., Zuluaga, R. (2016), 'Vegetable nanocellulose in food science: a review, *Food Hydrocolloids*, 57: pp. 178–186.

[173]. Lavoine, N., Desloges, I., Dufresne, A., Bras, J. (2012), 'Microfibrillated cellulose - its barrier properties and applications in cellulosic materials: A review,' *Carbohydrate Polymer* 90: pp.735–764.

[174]. Faruk, O., Bledzki, A. K., Fink, H. and Sain, M. (2012), 'Progress in Polymer Science Biocomposites reinforced with natural fibers,' *Progress in Polymer Science*, 37: pp. 1552–1596.

[175]. Zugenmaier, P. (1999), 'Analytical Methods in Wood Chemistry,' *Pulping, and Papermaking* , (E. Sjöström & R. Alén, eds.). pp. 9783540631026.

[176]. Khalil, H. P. S. A., Khalil, H., Davoudpour, Y., Mustapha, A., Islam, M. N., Sudesh, K., … Jawaid, M. (2014), 'Production and modification of nanofibrillated cellulose using various mechanical processes: A review,' *Carbohydrate Polymers*, *99*: pp. 649–665.

[177]. Kim, Jeong Hoon, Kim, J. H., Choi, E. S., Yu, H. K., Kim, J. H., Wu, Q., … Lee, S. Y. (2013), 'Colloidal silica nanoparticle-assisted structural control of cellulose nanofiber paper separators for lithium-ion batteries,' *Journal of Power Sources*, *242*: pp. 533–540.

[178]. Klemm, D., Heublein, B., Fink, H. and Bohn, A. (2005), 'Polymer Science Cellulose :

Fascinating Biopolymer and Sustainable Raw Material Angewandte,' *Journal of the Gesellschaft Deutscher Chemiker*, 36: pp. 3358–3393.

[179]. Donius, A. E., Liu, A., Berglund, L. A. and Wegst, U. G. K. (2014), 'Superior mechanical performance of highly porous, anisotropic nanocellulose-montmorillonite aerogels prepared by freeze casting,' *Journal of the Mechanical Behavior of Biomedical Materials*, 37: pp. 88–99.

[180]. Lin, N. and Dufresne, A. (2014), 'Nanocellulose in biomedicine: Current status and future prospect,' *European Polymer Journal*, *59*: pp. 302–325.

[181]. Jorfi, M. and Foster, E. J. (2015), 'Recent advances in nanocellulose for biomedical applications,' *Journal of Applied Polymer Science*, *132*(14): pp. 1–19.

[182]. Kim, Joo Hyung, Shim, B. S., Kim, H. S., Lee, Y. J., Min, S. K., Jang, D., … Kim, J. (2015), 'Review of nanocellulose for sustainable future materials,' *International Journal of Precision Engineering and Manufacturing - Green Technology*, *2*(2): pp. 197–213.

[183]. Yongvanich, N. and Visuttpitukul, P. (2013), 'Isolation of Nanocellulose from Pomelo Fruit Fibers by Chemical Treatments,' *Advanced Materials Research*, *747*(July 2013): pp. 363–366.

[184]. Lu, Z., Fan, L., Zheng, H., Lu, Q., Liao, Y. and Huang, B. (2013), 'Preparation, characterization and optimization of nanocellulose whiskers by simultaneously ultrasonic wave and microwave assisted,' *Bioresource Technology*, *146*: pp. 82–88.

[185]. Hettrich, K., Pinnow, M., Volkert, B., Passauer, L. and Fischer, S. (2014), 'Novel aspects of nanocellulose,' *Cellulose*, *21*(4): pp. 2479–2488.

[186]. Cherian, B. M., Leão, A. L., de Souza, S. F., Thomas, S., Pothan, L. A., & Kottaisamy, M. (2010),' Isolation of nanocellulose from pineapple leaf fibres by steam explosion,'*Carbohydrate Polymers*, *81*(3): pp. 720–725.

[187]. Qiao, H., Zhou, Y., Yu, F., Wang, E., Min, Y., Huang, Q., & Ma, T. (2015), 'Effective removal of cationic dyes using carboxylate-functionalized cellulose nanocrystals,' *Chemosphere*, 141: pp. 297–303.

[188]. Loof, D., Hiller, M., Oschkinat, H., & Koschek, K. (2016), 'Quantitative and qualitative analysis of surface modified cellulose utilizing TGA-MS,' *Materials*, 9: pp. 1–14.

[189]. Hokkanen, S., Repo, E., & Sillanpaa, M., (2013), 'Removal of heavy metals from aqueous solutions by succinic anhydride modified mercerized nanocellulose,' *Chemical Engineering Journal*, 223: pp. 40–47.

[190]. Gurgel, L.V.A., Junior, O.K., Gil, R.P.d.F., Gil, L.F. (2008), Adsorption of Cu(II), Cd(II), and Pb(II) from aqueous single metal solutions by cellulose and mercerized cellulose chemically modified with succinic anhydride, *Bioresource Technology*, 99: pp. 3077-3083.

[191]. Gurgel, L. V A, Perin de Melo, J. C., de Lena, J. C., & Gil, L. F. (2009), 'Adsorption of chromium (VI) ion from aqueous solution by succinylated mercerized cellulose functionalized with quaternary ammonium groups,' *Bioresource Technology*, 100: pp. 3214–3220.

[192]. Gurgel, L. V. A., and Gil, L. F. (2009), 'Adsorption of Cu(II), Cd(II), and Pb(II) from aqueous single metal solutions by succinylated mercerized cellulose modified with triethylenetetramine,' *Carbohydrate Polymers*, 77: pp. 142-149.

[193]. Zhou, Y., Jin, Q., Hu, X., Zhang, Q., Ma, T. (2012), 'Heavy metal ions and organic dyes removal from water by cellulose modified with maleic anhydride,' *Journal of Material Science*, 47: pp. 5019–5029.

[194]. Hu, X., Zhao, M., Song, G., Huang, H. (2011), 'Modification of pineapple peel fibers with succinic anhydride for Cu(II), Cd(II), Pb(II) removal from aqueous solutions,' *Environmental Technology,* 32: pp. 739-746.

[195]. Melo, J. C. P., Silva Filho, E. C., Santana, S. A. A., & Airoldi, C. (2011), 'Synthesized cellulose/succinic anhydride as an ion exchanger. Calorimetry of divalent cations in aqueous suspension,' *Thermochimica Acta*, 524: pp. 29–34.

[196]. Pangeni, B., Paudyal, H., Inoue, K., Kawakita, H., Ohto, K., & Alam, S. (2012), 'Selective recovery of gold(III) using cotton cellulose treated with concentrated sulfuric acid,' *Cellulose*, 19: pp. 381–391.

[197]. Georgi, J. V., Sabu, T., Nair, C.P.R.. (2019), 'Maleic acid modified cellulose for scavenging lead from water,' *International Journal of Biological Macromolecules*, 129: pp. 293–304.

[198]. Shin, E. W., Rowell, R.M. (2005), 'Cadmium ion sorption onto lignocellulosic biosorbent modified by sulfonation: the origin of sorption capacity improvement,' *Chemosphere*, 60: pp. 1054-1061.

[199]. Leyva-Ramos, R., Bernal-Jacome, L. A., & Acosta-Rodriguez, I. (2005), 'Adsorption of cadmium(II) from aqueous solution on natural and oxidized corncob,' *Separation and Purification Technology*, 45: pp. 41–49.

[200]. Wartelle, L. H. & Marshall, W. E. (2000), 'Citric acid modified agricultural by-products as copper ion adsorbents,' *Advances in Environmental Research*, 4: pp. 1–7.

[201]. Foglarova, M., Prokop, J., and Milichovsky, M. (2009), 'Oxidized Cellulose: An Application in the Form of Sorption Filter Materials,' *Journal of Applied Polymer Science*, 112: pp. 669-678.

[202]. Fox, S.C., Li, B., Xu, D., and Edgar, K. J. (2011), 'Regioselective esterification and etherification of cellulose: a review,' *Biomacromolecules*, 12 : pp. 1956-1972.

[203]. [234]. Maekawa, E. & Koshijima, T. (1984), 'Properties of 2,3-Dicarboxy Cellulose Combined with Various Metallic Ions,' *Creative Education*, 03(29): pp. 2289–2297.

[204]. Marcela Foglarova, Jiri Prokop, & Miloslav Milichovsky (2009), '*Marcela Foglarova, Jiri Prokop, Miloslav Milichovsky*, 1: pp. 669–678.

[205]. Min, S. H., Han, J. S., Shin, E. W. and Park, J. K. (2004), 'Improvement of cadmium ion removal by base treatment of juniper fiber,' *Water Research*, 38: pp. 1289–1295.

[206]. Bernhard Schrader (1995), 'Infrared and Raman Spectroscopy: Methods and Applications, 1st Edition, B. Schrader, VCH Publishers, Inc, New York, ISBN-13: 978-3527264469.

[207]. French A. D. and Cintron, M. S. (2013), 'Cellulose polymorphy, crystallite size, and the Segal Crystallinity Index," *Cellulose*, 20: pp. 583–588.

[208]. Johan, F., Robert, E., Moon, J. and P. Agarwal et al. **(**2018), "Current characterization methods for cellulose nanomaterials,' *Chemical Society Reviews*, 47: pp. 2609-2679.

[209]. D. E. Newbury, Characterization of Materials, *John Wiley & Sons*, Inc., 2002, DOI: 10.1002/0471266965.

[210]. Jane M-F Johnson and Jack Morgan, (2010), Plant Sampling guidelines in EPA sampling protocols,' R.F. Follett, editor, USDA, U.S., pp. 2-10. www.ars.usda.gov/research/GRACEnet.

[211]. David Duncan & Fiona Harvey, (2007), 'EPA Guidelines: Regulatory monitoring and testing Water and wastewater sampling,' June 2007, EPA, South Australia.

[212]. APHA., (2005), 'Standard methods for the Examination of Water and Wastewater. 21st Edition. *American Public Health Association*, Washington, D.C.

[213]. Abraham, E., Deepa, B., Pothan, L.A., Jacob, M., Thomas, S., Cvelbar, U., & Anandjiwala, R. (2011), 'Extraction of nanocellulose fibrils from lignocellulosic fibres: A novel approach,' *Carbohydrate Polymer*, 86: pp. 1468–1475.

[214]. Asrofi, M., Abral, H., Kasim, A., Pratoto, A., Mahardika, M., Hafizulhaq, F. (2018), 'Characterization of the sonicated yam bean starch bionanocomposites reinforced by nanocellulose water hyacinth fiber (WHF): the effect of various fiber loading,' *Journal of Engineering Science and Technology*, 13: pp. 2700–2715.

[215]. French A. D. and Cintron, M. S. (2013), 'Cellulose polymorphy, crystallite size, and the Segal Crystallinity Index," *Cellulose,* 20: pp. 583–588.

[216]. Anuj, K., Yuvraj, S. N., & Veena, C., Nishi K. B. (2014), 'Characterization of Cellulose Nanocrystals Produced by Acid-Hydrolysis from Sugarcane Bagasse as Agro-Waste,' *Journal of Materials Physics and Chemistry,* 2: pp. 1-8.

[217]. D. E. Newbury, Characterization of Materials, *John Wiley & Sons*, Inc., 2002, DOI: 10.1002/0471266965.

[218]. Kusmono, R., Faiz, Listyanda, Muhammad Waziz, Wildan, & Mochammad, N. I. (2020), 'Preparation and characterization of cellulose nanocrystal extracted from ramie fibers by sulfuric acid hydrolysis.,' *Heliyon* , 6: pp. 5486.

[219]. Lei, W., Fang, C., Zhou, X., Yin, Q., Pan, S., Yang, R., Liu, D., & Ouyang, Y. (2018),' Cellulose nanocrystals obtained from office waste paper and their potential application in PET packing materials,' *Carbohydrate Polym*er, 181: pp. 376–385.

[220]. Lei, Z., Gao W., Zeng, J., Wang, B., & Xu, J., (2020), 'The mechanism of Cu (II) adsorption onto 2,3-dialdehyde nano-fibrillated celluloses,' *Carbohydrate Polymers,* 230: pp. 115631.

[221]. Cristina, K., Carvalho, C., De Jacobus, H., Voorwald, C., Odila, M., Cio, H., … Arantes, V. (2018), 'Preparation of nanocellulose from Imperata brasiliensis grass using Taguchi method,' *Carbohydrate Polymers*, 192: pp. 337–346.

[222]. Xiang, Z., Gao, W., Chen, L.,Lan, W.,& Troy, J. Y. Z. (2016), 'A comparison of cellulose nanofibrils produced from Cladophora glomerata algae and bleached eucalyptus pulp,' *Cellulose,* 23: pp. 493–503.

[223]. Johnston, C.T., Wang, S., & Hem, S.L. (2002), 'Measuring the surface area of aluminum hydroxide adjuvant,' *J. Pharm. Sci.*, 7: pp. 91–1706.

[224]. T., Lu, Q., Li, W., Chen & Yu, H. (2014), 'Composite aerogels based on dialdehyde nanocellulose and collagen for potential applications as wound dressing and tissue engineering scaffold,'*Composites Science and Technology*, 94: pp. 132–138.

[225]. Andreas, B., Maohui, C., Martin, C., Zygmunt, J. J., Tianyang, L. & Linda, J.J. (2016), 'Correlating Cellulose Nanocrystal Particle Size and Surface Area,' *Langmuir,* 32: pp. 6105−6114.

[226]. D., Wei, Q., Liu, Z., Liu, J., Liu, X., Zheng, Y., Pei & Tang, K. (2019), Modified nano micro fibrillated cellulose / carboxymethyl chitosan composite hydrogel with giant network structure and quick gelation formability,' *International Journal of Biological Macromolecules,* 135: pp. 561–568.

[227]. Mendoza, D.J., Browne, C., Raghuwanshi, V.S., Simon, G. P., Garnier, G. (2019), One-shot TEMPO-periodate oxidation of native cellulose,' *Carbohydrate Polymer,* 226: pp. 115292.

[228]. Li, W., Ju, B., Zhang, S. (2020), 'Novel amphiphilic cellulose nanocrystals for pH-responsive Pickering emulsions,' *Carbohydrate Polymer* 229: pp. 115401.

[229]. Tang, Y.J., Yang, S.J., Zhang, N., Zhang, J.H. (2014), 'Preparation and characterization of nanocrystalline cellulose via low-intensity ultrasonic-assisted sulfuric acid hydrolysis,' *Cellulose,* 21: pp. 335–346.

[230]. Lindh, J., Carlsson D.O., Stromme, M., Mihranyan, A. (2014), 'Convenient one-pot formation of 2,3-dialdehyde cellulose beads via periodate oxidation of cellulose in water. *Biomacromole,* 15: pp. 1928–1932.

[231]. Chang-Qing, R., Maria, S., Jonas, L, (2018), 'Preparation of porous 2,3-dialdehyde cellulose beads crosslinked with chitosan and their application in adsorption of Congo red dye, *Carbohydrate Polymer*, 181: pp. 200–207.

[232]. Sun, J., Chen, Y., Yu, H., Yan, L., Du B., & Pei, Z. (2018), 'Removal of Cu^{2+}, Cd^{2+} and Pb^{2+} from aqueous solutions by magnetic alginate microsphere based on Fe_3O_4 / MgAl-layered double hydroxide, *Journal of Colloid and Interface Science,* 532: pp. 474–484.

[233]. Sherif, A. Y., Hubdar, A. M., Jechan, L., & Ki-Hyun, K. (2020), Nanotechnology-based sorption and membrane technologies for the treatment of petroleum-based pollutants in natural ecosystems and wastewater streams,' *Advances in Colloid and Interface Science*, 275: 102071.

[234]. Madivoli, E. S., Kareru, P. G., Gachanja, A. N., Mugo, S., & Murigi, M. K. (2016), 'Adsorption of Selected Heavy Metals on Modified Nano Cellulose,' *International Research Journal of Pure & Applied Chemistry,* 12: pp. 1–9.

[235]. Chand, P., Shil, A.K., Sharma, M., & Pakade, Y.B. (2014), 'Improved adsorption of cadmium ions from aqueous solution using chemically modified apple pomace: mechanism, kinetics, and thermodynamics,' *International Journal of Biodeterior and Biodegradable,* 90: pp. 8-16.

[236]. Tang , L. R., Huang , B., Yang , N. T., Li. , T., Lu , Q.L., Lin, W. Y., & X. R. (2013), 'Organic solvent-free and efficient manufacture of functionalized cellulose nanocrystals *via* one-pot tandem reactions, *Green Chemistry*, 15: pp. 2369 -2373.

[237]. Chen, H., Sharma, S. K., Sharma, P. R.,Yeh, H., Johnson K., & Hsiao, B. S. (2019), 'Arsenic(III) Removal by Nanostructured Dialdehyde Cellulose−Cysteine Microscale and Nanoscale Fibers,' *American Chemical Society Omega*, 4: pp. 22008−22020.

[238]. Hameed, B.H., Akpan, U.G., & Wee, K.P. (2011), 'Photocatalytic degradation of Acid

Red 1 dye using ZnO catalyst in the presence and absence of silver,' *Desalina Water Treatment*, 27: pp. 204-209.

[239]. Radhakrishnan, A., Nahi, J., & Beena, B. (2017), 'Synthesis and characterization of multi-carboxyl functionalized nanocellulose / graphene oxide-zinc oxide composite for the adsorption of uranium (VI) from aqueous solutions : Kinetic and equilibrium profiles,' *International Journal of Biological Macromolecules,* 105: pp. 111–120.

[240]. Alipour, A., Zarinabadi, S., Azimi A. and Mirzaei, M. (2020), 'Adsorptive removal of Pb (II) ions from aqueous solutions by thiourea-functionalized magnetic ZnO/nanocellulose composite: Optimization by response surface methodology (RSM),' *International Journal of Biological Macromolecules,* 151: pp. 124–135.

[241]. L., Dai, Y., Wang, Z., Li, X., Wang, C., Duan, W., Zhao, … Ni, Y. (2020), 'A multifunctional self-crosslinked chitosan / cationic guar gum composite hydrogel and its versatile uses in phosphate-containing water treatment and energy storage,' *Carbohydrate Polymers*, 244: pp. 116472.

[242]. Saravanan, R. & Ravikumar, L. (2015), 'The use of new chemically modified cellulose for heavy metal ion adsorption and antimicrobial activities,' *Journal of Water Resource and Protection*, 7: pp. 530.

[243]. Almomani, F., Bhosale, R., Khraisheh, M., & Almomani, T. (2019), 'Heavy metal ions removal from industrial wastewater using magnetic nanoparticles (MNP), *Applied Surface Science,* 506: pp. 144924.

[244]. Salama, A., Abdullah, H., Rizq, K., & Almomani, T. (2018), 'Oxidized cellulose reinforced silica gel : New hybrid for dye adsorption,' *Matterials Lett*ers, 230: pp. 293–296.

[245]. Liu, Y., Liu, Y., Hu, X., & Guo, Y. (2013), 'Adsorption of Cr(VI) by modified chitosan from heavy-metal polluted water of Xiangjiang River , China,' *Nonferrous Metals Society* of *China* 23: pp. 3095−3103.

[246]. Tsade, H., Abebe, B., Ananda Murthy, H.C. (2019), 'Nano sized Fe–Al oxide mixed with natural maize cob sorbent for lead remediation, *Matereial Research Express,* 6: pp. 085043.

[247]. Qinghua, X., Yulu, W., Liqiang, J., Yu, W., Menghua, Q. (2017), Adsorption of Cu(II), Pb(II) and Cr(VI) from aqueous solutions using black wattle tannin-immobilized nanocellulose, *Journal of Hazardious Materials,* 339: pp. 91–99.

[248]. Yeol, H., Hyuk, J., Hasegawa, Y., An, S., Soo, I., Lee, H., Kim, M. (2020), 'Thiol-functionalized cellulose nano fi ber membranes for the e ff ective adsorption of heavy metal ions in water,' *Carbohydrate Polymers,* 234: pp. 115881.

[249]. Elboughdiri, N. (2020), 'The use of natural zeolite to remove heavy metals Cu(II),

Pb(II) and Cd(II), from indus - trial wastewater The use of natural zeolite to remove heavy, *Cogent Engineering,* 7: pp. 1782623.

[250]. Mahmood, Z. Zahra, S.Iqbal M.& Aamir, M. (2017), 'Comparative study of natural and modified biomass of Sargassum for removal of Cd^{2+} and Zn^{2+} from wastewater,' *Applied Water Sci*ence, 7: pp. 3469–3481.

[251]. Rangabhashiyam, S., Giri, M.S., Nandagopal E., & Selvaraju, N. (2016), 'Adsorption of hexavalent chromium from synthetic and electroplating effluent on chemically modified Swietenia mahagoni shell in a packed bed column,' *Environmental Monitoring Assessessement,* 188: pp. 411.

[252]. Qian, W.C., Luo, X.P., Wang, X., Guo, M., Li, B., (2018), 'Removal of methylene blue from aqueous solution by modified bamboo hydrochar,' *Ecotoxicology, Environment, and Safety*, 157: pp. 300-306.

[253]. Mohammad, A. A. and Rana, S. A. (2020), 'Mechanistic understanding of the adsorption and thermodynamic aspects of cationic methylene blue dye onto cellulosic olive stones biomass from wastewater,' *Scientific Reports,* 10: pp.15928.

[254]. Munir, D., Nazar, M., Zafar, M. F., Zubair, M. N., Ashfaq, M., … Ahmad, A. (2020), 'Effective Adsorptive Removal of Methylene Blue from Water by Didodecyldimethylammonium Bromide-Modified Brown Clay,' *American Chemical Society Omega*, 5: pp. 16711−16721.

[255]. Gupta, V. K., Jain, R., Mittal, A., Saleh, T. A., Nayak, A., Agarwal, S., & Sikarwar, S. (2012), 'Photo-catalytic degradation of toxic dye amaranth on TiO_2/UV in aqueous suspensions,' *Matererials Science and Eng*ineering, 32: pp. 12−17.

[256]. Hsini, A., Essekri, A., Aarab, N., Laabd, M., Ait Addi, A., Lakhmiri, R., Albourine, A., (2020), 'Elaboration of novel polyaniline@Almond shell biocomposite for effective removal of hexavalent chromium ions and Orange G dye from aqueous solutions. *Environmental Science and Pollution Research,* 27: pp. 1-4.

[257]. Titchou, F. E., Akbour, R. A., Assabbane, A., & Hamdani, M. (2020), 'Removal of cationic dye from aqueous solution using Moroccan pozzolana as adsorbent : Isotherms , kinetic studies, and application on real textile wastewater treatment. *Groundwater for Sustainable Development,* 11: pp. 100405.

[258]. Gopal Reddi, M. R., Gomathi, T., Saranya, M., & Sudha, P. N. (2017), 'Adsorption and kinetic studies on the removal of chromium and copper onto Chitosan-g-maliec anhydride-g-ethylene dimethacrylate,' *International Journal of Biological Macromolecules*, 104: pp. 1578–1585.

[259]. Li, D., Li, J., Gu, Q., Song, S., & Peng, C. (2016), 'Co-influence of the pore size of adsorbents and the structure of adsorbates on adsorption of dyes,' *Desalination and Water Treatment*, 57: pp. 14686-14695.

[260]. Tana, K. B., Reza, A. K., Abdullah, A. Z., Horri, B. A., & Salamatinia, B. 'Development of self-assembled nanocrystalline cellulose as a promising practical adsorbent for methylene blue removal," *Carbohydrate Polymers*, 199: pp. 92–101, 2018.

[261]. Ali, I., Alharbi, O.M., Alothman, Z.A., Badjah, A.Y., Alwarthan, A., (2018) 'Artificial neural network modelling of amido black dye sorption on iron composite nanomaterial: kinetics and thermodynamics studies,' *Journal of Molecular Liquid*, 250: pp. 1-8.

[262]. Sakr, F., Alahiane, S., Sennaoui, A., Dinne, M., Bakas, I., Ali A. (2020), 'Removal of cationic dye (Methylene Blue) from aqueous solution by adsorption on two type of biomaterial of South Morocco,' *Materials Today: Proceedings*, 22: pp. 93–96.

[263]. Ezzati, R. (2020), 'Derivation of pseudo-first-order, pseudo-second-order and modified pseudo-first-order rate equations from Langmuir and Freundlich isotherms for adsorption. *Chemical Engineering Journal*, 392: pp. 123705.

[264]. Dbik, A., Bentahar, S., El Khomri, M., El Messaoudi, N., Lacherai, A. (2020), 'Adsorption of Congo red dye from aqueous solutions using tunics of the corm of the saffron,' *Materials Today: Proceedings* 22: pp. 134-139.

[265]. Ma, M., Chen, Y., Zhao, X., Tan, F., Wang, Y., Cao, Y., & Cai, W. 'Effective removal of cation dyes from aqueous solution using robust cellulose sponge," *Journal of Saudi Chemical Society*, 24: pp. 915–924, 2020.

[266]. Qiu, B., Guo, J., Zhang, X., Sun, D., Gu, H., Wang, Q., … Wei, S. (2014), 'Polyethylenimine Facilitated Ethyl Cellulose for Hexavalent Chromium Removal with a Wide pH Range,' *American Chemical Society Applied Materials Interfaces*, 6: pp. 19816−19824.

[267]. Velempini, T., Pillay, K., Mbianda, X.Y., & Arotiba, O.A. (2017), 'Epichlorohydrin crosslinked carboxymethyl cellulose-ethylenediamine imprinted polymer for the selective uptake of Cr(VI),' *International Journal of Biological Macromolecules*,101: pp. 837–844.

[268]. Peng, X., Yan, Z., Hu, L., Zhang, R., Liu, S., Wang, A., … Chen, L. (2020), Adsorption behavior of hexavalent chromium in aqueous solution by polyvinylimidazole modified cellulose,' *International Journal of Biological Macromolecules*, 155: pp. 1184–1193.

[269]. Shi, Y., Zhang, T., Ren, H., Kruse, A., Cui, R. (2018), 'Polyethylene imine modified hydrochar adsorption for chromium (VI) and nickel (II) removal from aqueous solution,' *Bioresource Technol*ogy, 247: pp. 370–379.

[270]. D., Chauhan & Sankararamakrishnan, N. (2008), 'Highly enhanced adsorption for decontamination of lead ions from battery wastewaters using chitosan functionalized with xanthate,' *Bioresource Technol*ogy, 99: pp. 9021–9024.

[271]. Xu, Q., Wang, Y., Jin, L., Wang, Y., & Qin, M. (2017), 'Adsorption of Cu (II), Pb (II) and Cr (VI) from aqueous solutions using black wattle tannin-immobilized nanocellulose,' *Journal of Hazardous Materials*, 339, pp. 91–99.

[272]. Cechinel, M.A.P., Ulson de Souza, S.M.A.G., Ulson de Souza, A.A. (2014), 'Study of lead (II) adsorption onto activated carbon originating from cow bone,' *Journal of Cleaner Prod*uction, 65: pp. 342–349.

[273]. Abdullah, A., Naushad, M.,Alothman, Z. A.,& Alsuhybani, M. (2020), 'Excellent adsorptive performance of a new nanocomposite for removal of toxic Pb (II) from aqueous environment : Adsorption mechanism and modeling analysis,' *Journal of Hazardous Materials*, 389: pp. 121896.

[274]. Xu, X., Ouyang, X., & Yang, L. (2021), 'Adsorption of Pb (II) from aqueous solutions using crosslinked carboxylated chitosan/carboxylated nanocellulose hydrogel beads," *Journal of Molecular Liquids*, 322: pp. 114523.

[275]. Sarai, R.V., Rafael, H. A., Jose, G., Rutiaga, Q., and Raul, C. M. (2020), Effective lead removal from aqueous solutions using cellulose nanofibers obtained from water hyacinth,' *water supply*, 20: pp. 2715-2736.

[276]. Mohubedu, R.P., Diagboya, P.N.E., Abasi, C.Y., Dikio, E.D., & Mtunzi, F. (2019), 'Magnetic valorization of biomass and biochar of a typical plant nuisance for toxic metals contaminated water treatment,' *Journal of Cleaner Production*, 209: pp. 1016–1024.

[277]. Azouaou, N., Sadaoui, Z., Djaafri, A., & Mokaddem, H. (2010), 'Adsorption of cadmium from aqueous solution onto untreated coffee grounds : Equilibrium , kinetics and thermodynamics,' *Journal of Hazardous Materials*, 184: pp. 126–134.

[278]. Zeng, L., Chen, Y., Zhang, Q., Guo, X., Peng, Y., Xiao, H., … Luo, J. (2015), 'Adsorption of Cd (II), Cu (II) and Ni (II) ions by cross-linking chitosan / rectorite nano-hybrid composite microspheres,' *Carbohydrate Polymers*, 130: pp. 333–343.

[279]. Liu, D., Li, Z., Zhu, Y., Li, Z., & Kumar, R. (2014), 'Recycled chitosan nanofibril as an effective Cu(II), Pb(II) and Cd(II) ionic chelating agent : Adsorption and desorption performance,' *Carbohydrate Polymers*, 111: pp. 469–476.

[280]. Hu, C., Zhu, P., Cai, M., Hu, H., & Fu, Q. (2017), 'Comparative adsorption of Pb(II), Cu(II) and Cd(II) on chitosan saturated montmorillonite : Kinetic , thermodynamic and equilibrium studies,' *Applied Clay Science*, 143: pp. 320–326.

[281]. Fatima, E., Titchou, R. A., Akbour, A. A., and Mohamed, H. (2020), 'Removal of cationic dye from aqueous solution using Moroccan pozzolana as adsorbent: Isotherms, kinetic studies, and application on real textile wastewater treatment,' *Groundwater for Sustainable Development*, 11: pp. 100405.

[282]. Wang, Z., Song, L.,Wang, Y., Zhang, X.F., Hao, D., Feng, Y.,Yao, J. (2019), 'Lightweight UiO-66/ cellulose aerogels constructed through self-crosslinking strategy for adsorption applications,' *Chemical Engineering Journal*, 371: pp. 138–144.

[283]. Patil, C. S., Kadam, A. N., Gunjal, D. B., & Naik, V. M. (2020), 'Sugarcane molasses derived carbon sheet @ sea sand composite for direct removal of methylene blue from textile wastewater : Industrial wastewater remediation through sustainable , greener , and scalable methodology,' *Separation and Purification Technology,* 247: pp. 116997.

[284]. Ying, G., Hou-Yong, Y., Somia, Y., Hussain, A., Chuang, W., Feng, T., Jaromir, M.,W., Chen, J., and Ju-Ming, Y. (2019), 'Green one-step synthesis of ZnO/cellulose nanocrystal hybrids with modulated morphologies and superfast absorption of cationic dyes, *International Journal of Biological Macromolecules*, 132: pp. 51–62.

[285]. Safa, H. N., Yakout, Y., Shair, S. M., Iqbal, O. H., & Nazir, A. (2020), 'Efficient removal of dyes using carboxymethyl cellulose / alginate / polyvinyl alcohol / rice husk composite : Adsorption / desorption , kinetics and recycling studies,' *International Journal of Biological Macromolecules,* 150: pp. 861–870.

7. APPENDIX

Appendix Table 1. Effect of initial Pb (II) ion concentration on adsorption capacity of the CNM and DACNM adsorbents for Pb(II) ions removal.

Adsorbents	CNM			DACNM		
Initial Pb (II) ion conc.(mg/L)	Ce (ppm)	%R	q_e(mg/g)	Ce (ppm)	%R	q_e(mg/g)
5	23.85	20.50	74.50	18.0±0.6	40.0	63.60
10	20.26	32.47	72.10	14.97± 1.0	50.1	54.44
20	14.92± 0.09	50.25	66.90	8.62± 0.9	71.25	33.41
30	9.81± 0.04	67.3	58.74	1.05± 0.004	96.5	4.37
40	9.84± 1.5	67.2	58.75	1.14± 1.0	96.21	4.38

Appendix Table 2. Effect of contact time on adsorption capacity of the CNM and DACNM adsorbents for Pb(II) ions removal.

Adsorbents	CNM			DACNM		
Contact time (min.)	Ce (ppm)	%R	q_e(mg/g)	Ce (ppm)	%R	q_e(mg/g)
30	15.45±0.60	48.5	67.76	8.3±0.6	72.42	32.80
60	12.00± 1.5	60	63.16	5.10± 1.0	83.12	20.48
90	10.35± 0.09	65.5	59.80	2.85± 0.9	90.5	11.73
120	8.34± 0.04	72.2	55.6	0.96± 0.004	96.8	4.03

Appendix Table 3. Effect of adsorbent dose on adsorption capacity of the CNM and DACNM adsorbents for Pb(II) ions removal.

Adsorbents	CNM			DACNM		
Adsorbent dose (g)	Ce (ppm)	%R	q_e(mg/g)	Ce (ppm)	%R	q_e(mg/g)
0.3	11.76	60.80	62.55	8.58	71.40	33.26
1	8.25	72.50	55.04	0.66	97.80	2.78
2	8.43	71.90	55.46	0.93	96.9	3.90
2.5	8.37	72.1	55.43	0.99	96.7	4.15

Appendix Table 4. Effect of solution pH on adsorption capacity of the CNM and DACNM adsorbents for Pb(II) ions removal.

Adsorbents	CNM			DACNM		
Solution pH	Ce (ppm)	%R	q_e(mg/g)	Ce (ppm)	%R	q_e(mg/g)
2	17.25	42.5	70.40	8.25	72.50	32.10
4	10.43	65.23	59.94	2.04	93.21	8.46
6	8.62	71.25	55.97	1.09	96.35	4.56
8	8.76	70.8	56.51	1.26	95.8	5.27

Appendix Table 5. Effect of initial Cr(VI) ion concentration on adsorption capacity of the CNM and S-CNM adsorbents for Cr(VI) ions removal.

Adsorbents	CNM			S-CNM		
Initial Pb (II) ion conc.(mg/L)	Ce (ppm)	%R	q_e(mg/g)	Ce (ppm)	%R	q_e(mg/g)
0.5	1.27	36.50	19.61	0.990	50.5	4.85
2	0.64	68.25	24.39	0.155	92.25	4.97
3	0.643	67.86	24.63	0.156	92.2	4.97
4	0.655	67.24	24.51	0.170	91.5	4.98

Appendix Table 6. Effect of contact time on adsorption capacity of the CNM and S-CNM adsorbents for Cr(VI) ions removal.

Adsorbents	CNM			S-CNM		
Contact time (min.)	Ce (ppm)	%R	q_e(mg/g)	Ce (ppm)	%R	q_e(mg/g)
30	1.09	45.50	20.83	0.79	60.50	4.87
60	0.87	56.50	22.52	0.39	80.50	4.95
90	0.715	64.25	23.81	0.182	90.9	4.97
150	0.74	63.01	23.64	0.218	89.08	4.96

Appendix Table 7. Effect of adsorbent dose on adsorption capacity of the CNM and S-CNM adsorbents for Cr(VI) ions removal.

Adsorbents	CNM			S-CNM		
Adsorbent dose (g)	Ce (ppm)	%R	q_e(mg/g)	Ce (ppm)	%R	q_e(mg/g)
0.08	1.30	35.20	19.42	0.80	60.12	4.87
0.16	0.99	50.25	21.55	0.49	75.26	4.92
0.3	0.77	61.30	23.42	0.18	90.80	4.97
2	0.78	61.00	23.31	0.20	90.00	4.92

Appendix Table 8. Effect of solution pH on adsorption capacity of the CNM and S-CNM adsorbents for Cr(VI) ions removal.

Adsorbents	CNM			S-CNM		
Solution pH	Ce (ppm)	%R	q_e(mg/g)	Ce (ppm)	%R	q_e(mg/g)
2	1.59	20.50	17.85	1.15	42.50	4.83
4	1.35	32.40	19.23	0.79	60.24	4.87
5	0.795	60.25	23.26	0.195	90.24	4.97
8	1.35	32.50	19.23	0.60	70.12	4.90

Appendix Table 9. Effect of initial Cd (II) ion concentration on adsorption capacity of the CNM and MA-CNM adsorbents for Cd(II) removal.

Adsorbents	CNM			MA-CNM		
Initial Pb (II) ion conc.(mg/L)	Ce (ppm)	%R	q_e(mg/g)	Ce (ppm)	%R	q_e(mg/g)
10	13.7	31.5	4.73	11.98	40.1	8.99
20	6.96	65.2	8.20	2.3	88.5	14.92
30	7.0	65.00	8.17	2.4	88	14.90
40	6.98	65.10	8.19	2.38	88.1	14.91

Appendix Table 10. Effect of contact time on on adsorption capacity of the CNM and MA-CNM adsorbents for Cd(II) removal

Adsorbents	CNM			MA-CNM		
Contact time (min.)	Ce (ppm)	%R	q_e(mg/g)	Ce (ppm)	%R	q_e(mg/g)
30	15.98	20.12	4.15	13.0	35.02	8.62
60	12.67	36.65	5.07	10.3	48.56	9.61
120	6.50	67.5	8.65	6.50	89.5	11.73
180	6.52	67.4	8.62	0.96	89.2	11.63

Appendix Table 11. Effect of adsorbent dose on on adsorption capacity of the CNM and MA-CNM adsorbents for Cd(II) removal.

Adsorbents	CNM			MA-CNM		
Adsorbent dose (g)	Ce (ppm)	%R	q_e(mg/g)	Ce (ppm)	%R	q_e(mg/g)
0.16	11.7	41.5	5.43	9.75	51.23	9.91
0.3	9.36	53.2	6.89	6.95	65.24	11.36
0.5	5.94	70.3	9.30	1.92	90.40	15.38
2	6.0	70.0	9.17	2.0	90.00	15.33

Appendix Table 12. Effect of solution pH on on adsorption capacity of the CNM and MA-CNM adsorbents for Cd(II) removal.

Adsorbents	CNM			MA-CNM		
Solution pH	Ce (ppm)	%R	q_e(mg/g)	Ce (ppm)	%R	q_e(mg/g)
2	15.5	22.50	4.34	13.98	30.12	8.26
5	11.7	41.50	5.43	9.75	51.23	9.91
8	5.94	70.3	9.30	2.02	89.9	15.38
12	7.30	63.5	7.90	3.26	83.7	14.08

Appendix Table 13. Effect of initial MB cation concentration on adsorption capacity of the DACNM adsorbent for MB removal.

Adsorbents	DACNM		
Initial Pb (II) ion conc.(mg/L)	Ce (ppm)	%R	q_e(mg/g)
10	18.14	39.55	3.19
20	11.84	60.55	4.09
30	6.57	78.1	5.37
40	6.63	77.9	5.36

Appendix Table 14. Effect of contact time on the adsorption capacity of the DACNM adsorbent for MB removal.

Adsorbents	DACNM		
Contact time (min.)	Ce (ppm)	%R	q_e(mg/g)
10	15.45	48.50	3.53
30	12.0	60	4.12
60	6.56	78.12	5.40
90	6.63	77.9	5.36

Appendix Table 15. Effect of adsorbent dose on on the adsorption capacity of the DACNM adsorbent for MB removal.

Adsorbents	DACNM		
Adsorbent dose (g)	Ce (ppm)	%R	q_e(mg/g)
0.3	8.88	70.4	4.74
0.5	7.95	73.5	5.00
1	6.45	78.5	5.43
2	6.6	78	5.38

Appendix Table 16. Effect of solution pH on on the adsorption capacity of the DACNM adsorbent for MB removal.

Adsorbents	DACNM		
Solution pH	Ce (ppm)	%R	q_e(mg/g)
3	17.25	42.5	3.30
5	10.43	65.23	4.38
8	6.15	79.5	5.53
10	6.24	79.2	5.52

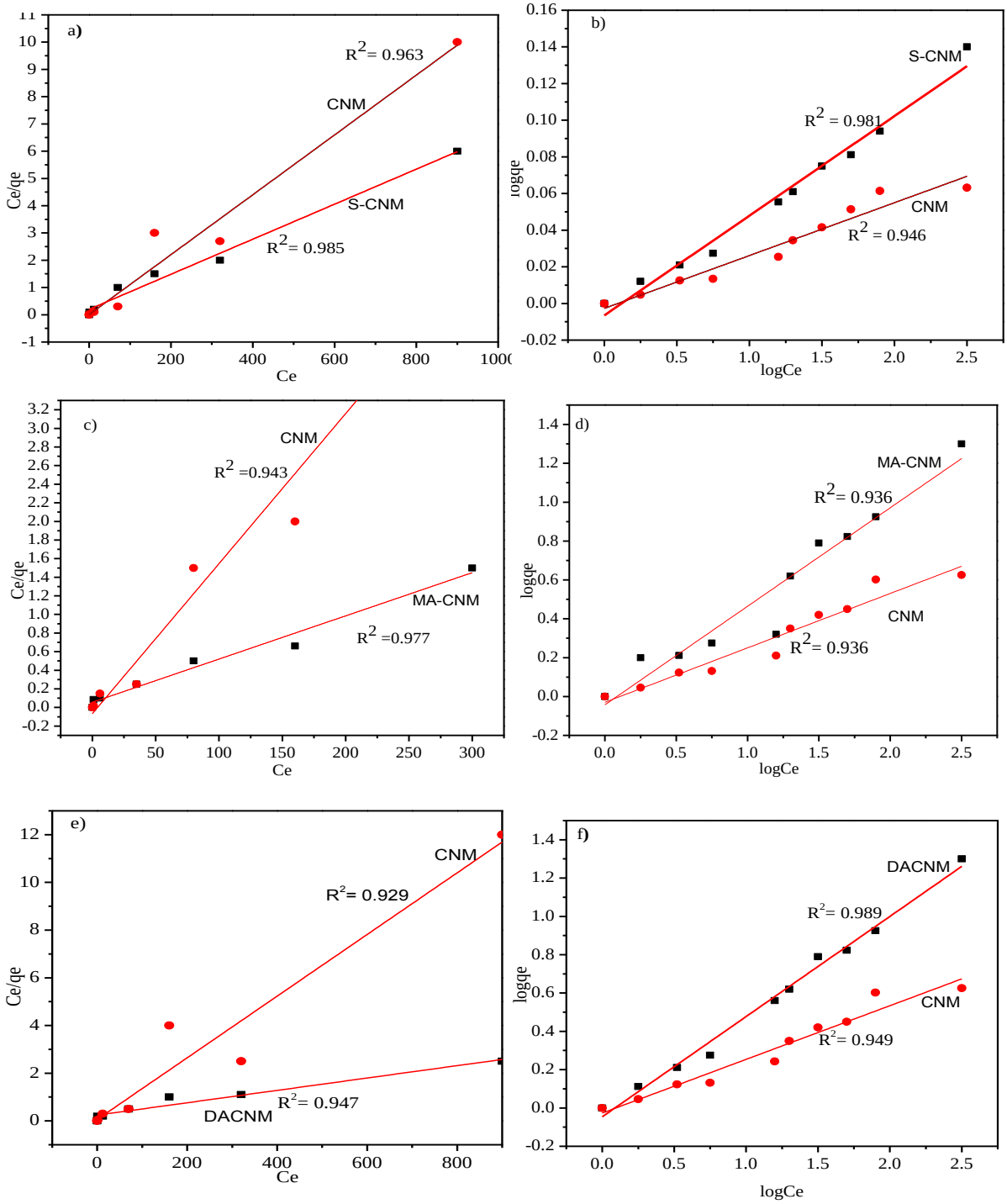

Appendix Figure 1. Langmuir (a, c & e) and Freundlich (b, d & f) adsorption isotherm for the removal of Cr(VI), Cd(II) and Pb(II) ions, at optimum pH of (5, 8, & 6), room temperature, Ci of (2, 20, & 30 mgL^{-1}), dose of (0.3, 0.5, & 1 g), Contact time of (90, 120, & 120 min.), and agitation speed of (300, 250, & 250 rpm), by using S-CNM, MA-CNM, DACNM, respectively.

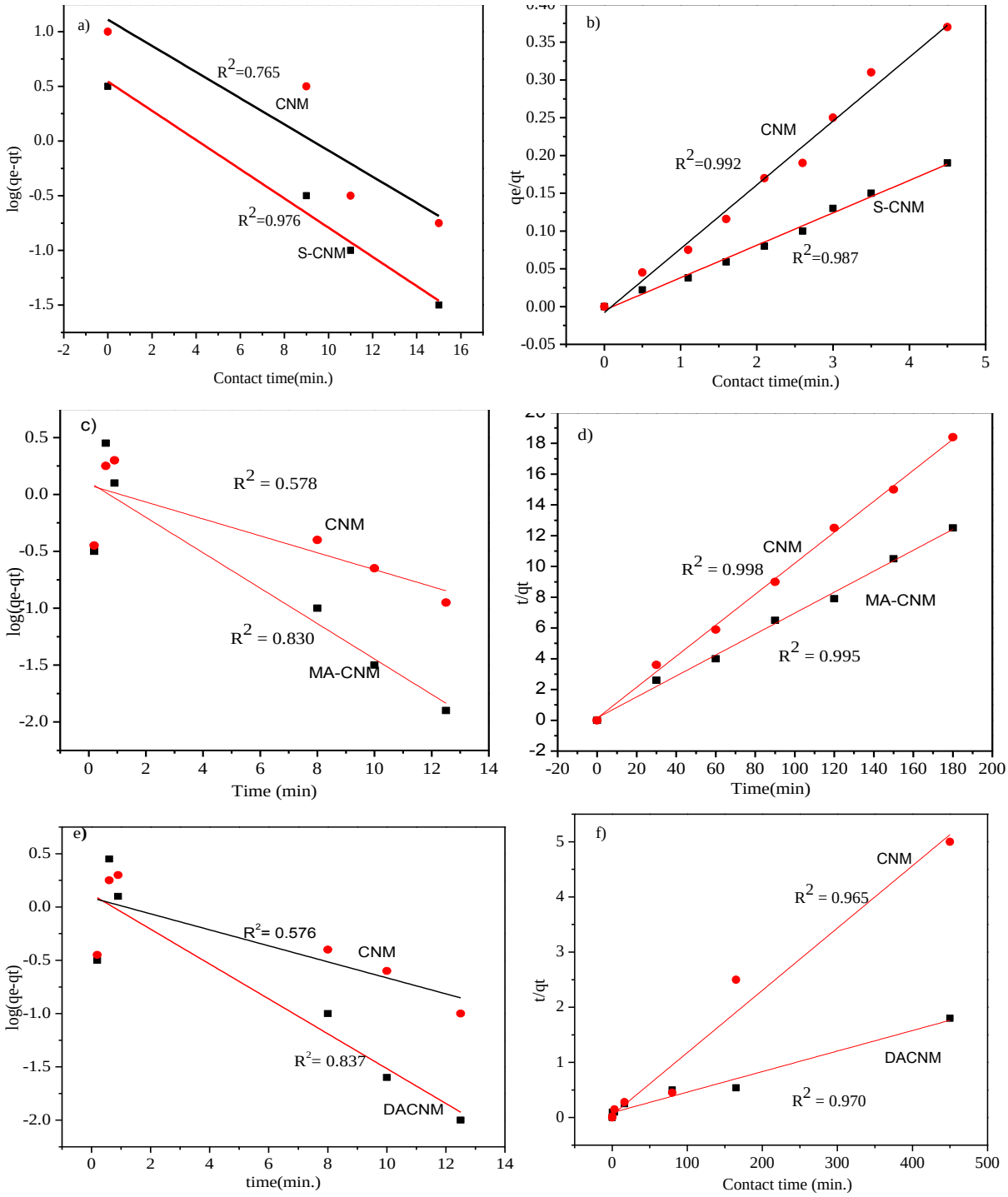

Appendix Figure 2. Plot of the PFO (a, c & e) and PSO (b, d & f) model for Cr(VI), Cd(II) and Pb(II) ions removal at optimum pH of (5, 8, & 6), room temperature, C_i of (2, 20, & 30 mgL^{-1}), dose of (0.3, 0.5, & 1 g), and agitation speed of (300, 250, & 250 rpm), by using CNMs, S-CNM, MA-CNM, DACNM, respectively.

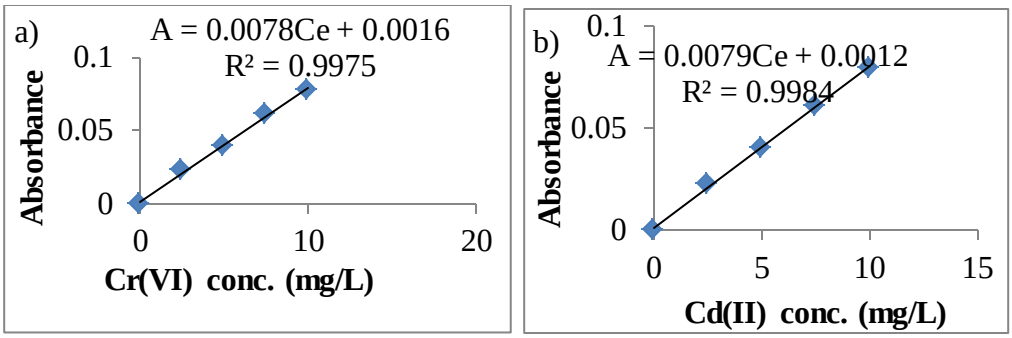

Appendix Figure 3. Calibration curve of (a) Cr(VI) and (b) Cd(II) ions solution, respectively for adsorption study.

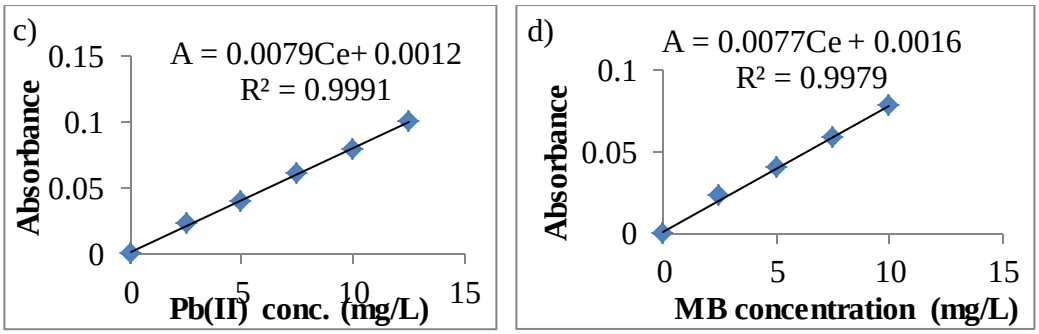

Appendix Figure 4. Calibration curve of (c) Pb(II) and (d) MB solution, respectively for adsorption study.

Abstract of Published Artices

A Novel Modified Cellulose Nanomaterials (CNMs) for Remediation of Chromium (VI) ions from Wastewater

Hizkeal Tsade Kara*[1], Sisay Tadesse Anshebo[2], Fedlu Kedir Sabir[1]

[1]Department of Applied Chemistry, School of Applied Natural Science, Adama Science and Technology University, P.O.Box 1888, Adama, Ethiopia
[2]Department of Chemistry, College of Computational and Natural Science, Hawassa University, Hawassa, P.O. Box 05, Ethiopia

E-mail: hizts4@gmail.com
IOP Publishing, Materials Research Express vol. 7: pp. 115008, (2020).
https://doi.org/10.1088/2053-1591/abcb3c

ABSTRACT

Wastewater (WW) remediation technologies were the most crucial issues all over the world at present time. Thus, the remediation of Cr (VI) ions from real WW was conducted using green biocompatible and biodegradable pristine (CNM) and succinic anhydride functionalized cellulose nanomaterial (S-CNM) adsorbents. Both CNM and S-CNM adsorbents were prepared by using sulfuric acid hydrolysis method and characterized for particle sizes, functional groups, and surface morphologies by using XRD, FT-IR, and SEM instruments, respectively. The physicochemical properties of the collected WW were investigated. Next, both the prepared adsorbents were applied for the remediation of Cr (VI) ions from WW. The remediation processes is spontaneous and have higher remediation efficiencies of Cr (VI) ions from WW. The Cr (VI) ions remediation mechanism was evaluated from both the Cr (VI) ions adsorption isotherms and kinetic concepts. Both Langmuir and Freundlich Cr (VI) ions adsorption isotherm models were certainly fixed to a maximum Cr (VI) ions uptake capability (q_{max}) of 60.24 and 156.25 mg g^{-1} by CNM and S-CNM sorbents, respectively, and it follows pseudo-second-order (PSO) kinetics model through chemisorption processes. The Cr (VI) ions uptake capabilities were hindered by the presence of organic matter and any other competing pollutants in the WW. The S-CNM sorbent was selected for the regeneration study due to its higher efficiencies of remediation relative to CNM sorbent and the study was conducted through desorption of Cr (VI) ions by using HCl. Findings have shown that the sorbent was easily recyclable and applicable for the remediation of pollutants from real WW after consecutive 13th cycles.

Keywords: Cellulose nanomaterials; Wastewater; Cr(VI) ions; Surface modification; Remediation.

Preparation and Characterization of Functionalized Cellulose Nanomaterials (CNMs) for Pb(II) ions Removal from Wastewater

Hizkeal Tsade Kara*[1], Sisay Tadesse Anshebo[2], Fedlu Kedir Sabir[1]

[1]Department of Applied Chemistry, School of Applied Natural Science, Adama Science and Technology University, P.O.Box 1888, Adama, Ethiopia
[2]Department of Chemistry, College of Natural and Computational Science, Hawassa University, Hawassa, P.O. Box 05, Ethiopia

E-mail: hizts4@gmail.com

Hindawi, Journal of Chemistry, Volume 2021, Article ID 5514853, 18 pages
https://doi.org/10.1155/2021/5514853

ABSTRACT

Due to their remarkable properties, cellulose nanomaterials are emerging materials for wastewater treatment (WW). In this study, both pristine cellulose nanomaterial (CNM) and sodium periodate modified cellulose nanomaterial ($NaIO_4$-CNM) were prepared from the stem of the Erythrina Brucei plant for the removal of Pb(II) ions from WW. As-prepared CNMs were characterized by x-ray diffraction (XRD), Fourier transform infrared (FT-IR), scanning electron microscope (SEM), and thermogravimetric with differential thermogravimetric (TGA-DTG) analysis. The as-prepared and characterized CNMs were tested for the removal of Pb(II) ions from secondary run-off wastewater (SERWW). Langmuir and Freundlich adsorption isotherms were certainly fixed to a maximum Pb(II) ions uptake capability (qmax) of 91.74 and 384.62 mg g^{-1} by CNM and $NaIO_4$-CNM adsorbents, respectively. The pseudo-second-order (PSO) kinetics model was well fitted to the uptake process. Results revealed that the % removal (%R) of Pb(II) ions was decreased by the presence of nitrogen and organic matter, but, not affected by the presence of phosphorous in SERWW. Due to its high efficiency, $NaIO_4$-CNM was selected for the regeneration study. The regeneration study was conducted after desorption of Pb(II) ions from the adsorbent by the addition of HCl and reused as an adsorbent for at least 13^{th} successive cycles. Results indicated that excellent recycling capabilities and the adsorbent was used as adsorbing material for the removal of Pb(II) ions from SERWW after 13^{th} successive cycles without significant efficient loss.

Keywords: Cellulose nanomaterials; Wastewater; Pb(II) ions; Surface functionalization; Uptake ability.

Removal of Methylene Blue Dye from Wastewater using Periodiated Modified Nanocellulose

Hizkeal Tsade *[1], Sisay Tadesse Anshebo[2], Fedlu Kedir Sabir[1], Getachew Adam Workneh[3]

[1]*Department of Applied Chemistry, School of Applied Natural Science, Adama Science and Technology University, P.O.Box 1888, Adama, Ethiopia*
[2]*Department of Chemistry, Collage of Natural and Computational Sciences, Hawassa University, Hawassa, P.O. Box 05, Ethiopia*
[3] *Department of Industrial Chemistry, College of Applied Science, Addis Ababa Science and Technology University, P.O. Box 16417, Addis Ababa, Ethiopia*

E-mail: hizts4@gmail.com

Hindawi, International Journal of Chemical Engineering, Volume 2021, Article ID 9965452, 16 pages. https://doi.org/10.1155/2021/9965452

ABSTRACT

The study was focused on the preparation and characterizations of sodium periodate modified nanocellulose ($NaIO_4$-NC) prepared from Eichhornia crssipes for the removal of cationic methylene blue (MB) dye from wastewater (WW). A chemical method was used for the preparation of $NaIO_4$-NC. The prepared $NaIO_4$-NC adsorbent was characterized by using x-ray diffraction (XRD), Fourier transforms infrared (FT-IR), scanning electron microscope (SEM), energy-dispersive x-ray (EDX), and Brunauer–Emmett–Teller (BET) instruments. Next, it was tested to the adsorption of MB dye from WW using batch experiments. The adsorption process was performed using Langmuir and Freundlich isotherm models with maximum adsorption efficiency (q_{max}) of 90.91 mgg^{-1} and percent color removal of 78.1% at optimum 30 mgL^{-1}, 60 min., 1 g, and 8 values of initial concentration, contact time, adsorbent dose and solution pH, respectively. Pseudo-second-order (PSO) kinetic model was well fitted for the adsorption of MB dye through the chemisorption process. The adsorption process was spontaneous and feasible from the thermodynamic study because the Gibbs free energy value was negative. After adsorption, the decreased values for physicochemical parameters of WW were observed in addition to the color removal. From the regeneration study it is possible to conclude that, $NaIO_4$-NC adsorbent was recyclable and re-used as MB dye adsorption for 13^{th} successive cycles without significant efficient loss.

Keywords: Nanocelluloce, Wastewater, Cationic MB, Surface modification, Adsorption

Adsorptive Removal of Cd(II) ions from Wastewater using Maleic Anhydride Nanocellulose

Hizkeal Tsade Kara*[1], Sisay Tadesse Anshebo[2], Fedlu Kedir Sabir[1]

[1]Department of Applied Chemistry, School of Applied Natural Science, Adama Science and Technology University, P.O.Box 1888, Adama, Ethiopia
[2]Department of Chemistry, College of Natural and Computational Science, Hawassa University, Hawassa, P.O. Box 05, Ethiopia

E-mail: hizts4@gmail.com

Hindawi,Journal of Nanotechnology Volume 2021, Article ID 9966811, 15 pages
https://doi.org/10.1155/2021/9966811

ABSTRACT

In this study, both pristine cellulose nanocrystalline (CNC) and maleic anhydride functionalized cellulose nanocrystalline (MA-CNC) were prepared from the stems of Eichhornia crssipes weed by sulfuric acid hydrolysis method. The as-prepared adsorbents were characterized by using x-ray diffraction (XRD), Fourier-transform infrared (FT-IR) spectroscopy, and scanning electron microscopy (SEM), and energy-dispersive X-ray (EDX) spectroscopy, respectively. These materials were applied for the removal of Cd(II) ions from WW. The uptake mechanism was fixed to both Langmuir and Freundlich adsorption isotherms with a maximum Cd(II) ions uptake capability (q_{max}) of 75.76 and 215.52 mgg^{-1} by CNC and MA-CNC adsorbents, respectively. Pseudo-second-order (PSO) kinetics model was well fitted to the uptake process. The adsorbent regeneration study was done after desorption of Cd(II) ions from the adsorbent by HCl washing. Results exhibited that the adsorbent was reused for the removal of Cd(II) ions from real WW after successive 13th cycles.

Keywords: Cellulose nanocrystallines; Wastewater; Cd(II) ions Removal; Surface modification.